

STUDY OF DEVULCANIZED NATURAL RUBBER AS
THE GREEN IMPACT MODIFIER FOR
POLYPROPYLENE WITH ELECTRON BEAM
IRRADIATION

LOO KHENG HOOI

MASTER OF ENGINEERING SCIENCE

LEE KONG CHIAN FACULTY OF ENGINEERING
SCIENCE
UNIVERSITI TUNKU ABDUL RAHMAN
SEPTEMBER 2018

ABSTRACT

STUDY OF DEVULCANIZED NATURAL RUBBER AS THE GREEN IMPACT MODIFIER FOR POLYPROPYLENE WITH ELECTRON BEAM IRRADIATION

The effects of DVC composition, EB-irradiation and UV source degradation in relation to the performance of the PP-DVC compound were investigated. Various DVC compositions (0 phr – 20 phr) were compounded with PP and irradiated at several dosages (0 kGy – 200 kGy) under natural weathering condition (0 month – 6 months). It was found that with the addition of 5 phr DVC added in PP irradiated at 50 kGy has the optimum value of the mechanical properties after 6 months outdoor exposure. It could provide better tensile strength, impact strength and hardness value as the DVC particles dispersed better in PP matrix. The gel content increased with longer exposure period due to a more extensive three-dimensional network formation via a substantial reaction with the larger amount of free radicals promotes at low irradiation dosages. There is an expansion of crystallize size caused by the photo-oxidation where the chain arrangement around crystalline structure re-orientated. However, the intensity of the peaks and crystallinity reduced after outdoor exposure due to the photo-oxidation occurs has broken down the crystalline structure in the PP matrix. Furthermore, the fractured surface has changed from tear lines appearance to flake-like appearance because of the UV exposure has caused the polymer degradation and reduced the filler-matrix interaction. Furthermore, the appearance of two new peaks at 1710 cm^{-1} and 3300 cm^{-1} which are C=O stretching vibration and O-H stretching vibration indicated that the photo-oxidation and electron beam irradiation occurs.

APPROVAL SHEET

This dissertation/thesis entitled “**STUDY OF DEVULCANIZED NATURAL RUBBER AS THE GREEN IMPACT MODIFIER FOR POLYPROPYLENE WITH ELECTRON BEAM IRRADIATION**” was prepared by LOO KHENG HOOI and submitted as partial fulfillment of the requirements for the degree of Master of Engineering Science at Universiti Tunku Abdul Rahman.

Approved by:

(Ir. Dr Lee Tin Sin)
Date:.....
Supervisor
Department of Chemical Engineering
Lee Kong Chian Faculty of Engineering Science
Universiti Tunku Abdul Rahman

(Prof. Ir. Dr Tee Tiam Ting)
Date:.....
Co-supervisor
Department of Chemical Engineering
Lee Kong Chian Faculty of Engineering Science
Universiti Tunku Abdul Rahman

FACULTY OF ENGINEERING SCIENCE
UNIVERSITI TUNKU ABDUL RAHMAN

Date: _____

SUBMISSION DISSERTATION

It is hereby certified that **LOO KHENG HOOI** (ID No: **16UEM06096**) has completed this dissertation entitled “STUDY OF DEVULCANIZED NATURAL RUBBER AS THE GREEN IMPACT MODIFIER FOR POLYPROPYLENE WITH ELECTRON BEAM IRRADIATION” under the supervision of Ir. Dr Lee Tin Sin (Supervisor) from the Department of Chemical Engineering, Lee Kong Chian Faculty of Engineering Science, and Prof. Ir. Dr Tee Tiam Ting (Co-Supervisor) from the Department of Chemical Engineering, Lee Kong Chian Faculty of Engineering Science.

I understand that University will upload softcopy of my dissertation in pdf format into UTAR Institutional Repository, which may be made accessible to UTAR community and public.

Yours truly,

(LOO KHENG HOOI)

DECLARATION

I hereby declare that the dissertation is based on my original work except for quotations and citations which have been duly acknowledged. I also declare that it has not been previously or concurrently submitted for any other degree at UTAR or other institutions.

Name _____
(LOO KHENG HOOI)

Date _____

TABLE OF CONTENTS

	Page
ABSTRACT	ii
APPROVAL SHEET	iii
SUBMISSION DISSERTATION	iv
DECLARATION	v
TABLE OF CONTENTS	vi
LIST OF TABLES	viii
LIST OF FIGURES	ix
LIST OF ABBREVIATIONS	xii
CHAPTERS	
I. INTRODUCTION	1
1.1 Background	1
1.2 Problem Statements	2
1.3 Aims and Objectives	4
1.4 Scope of Study	4
II. LITERATURE REVIEW	5
2.1 Introduction	5
2.2 Natural Rubber – Polyethylene (PE) Blend	7
2.3 Natural Rubber – Polypropylene (PP) Blend	10
2.4 Natural Rubber – Polyethylene Terephthalate (PET) Blend	15
2.5 Natural Rubber – Polystyrene (PS) Blend	18
2.6 Natural Rubber – Polyvinyl Chloride (PVC) Blend	21
2.7 Natural Rubber – Ethylene Vinyl Acetate (EVA) Blend	29
2.8 Natural Rubber – Ethylene Propylene Diene Monomer (EPDM) Blend	35
2.9 Natural Rubber – Polyvinylalcohol (PVA) Blend	38
2.10 Natural Rubber – Butadiene Rubber (BR) Blend	39
2.11 Natural Rubber – Arcylate Blend	41
2.12 Natural Rubber – Rubber Waste Blend	46
2.13 Natural Rubber – Carbon Blend	47
2.14 Natural Rubber – Natural Polymer Blend	50
III. METHODOLOGY	55
3.1 Formulation	55
3.2 Sample Preparation	56
3.3 Natural Weathering Test	56
3.4 Gel Content Test	57
3.5 Tensile Test	57
3.6 Impact Test	58

3.7	Hardness Test	59
3.8	X-ray Diffraction (XRD) Analysis	59
3.9	Scanning Electron Microscope (SEM)	60
3.10	Fourier Transform Infrared Spectroscopy (FTIR)	61
IV.	RESULTS AND DISCUSSIONS	62
4.1	Effect of Devulcanized Natural Rubber Composition on the PP-DVC Compound	62
4.1.1	Gel Content Test	62
4.1.2	Tensile Test	63
4.1.3	Impact and Hardness Test	66
4.1.4	XRD Analysis	68
4.1.5	SEM Analysis	71
4.1.6	FTIR Analysis	72
4.2	Effect of Electron Beam Irradiation on the PP-DVC Compound	75
4.2.1	Gel Content Test	75
4.2.2	Tensile Test	78
4.2.3	Impact and Hardness Test	83
4.2.4	XRD Analysis	86
4.2.5	SEM Analysis	90
4.2.6	FTIR Analysis	92
4.3	Effect of Devulcanized Natural Rubber Composition on the PP-DVC Compound after Natural Weathering	96
4.3.1	Gel Content Test	96
4.3.2	Tensile Test	97
4.3.3	Impact and Hardness Test	100
4.3.4	XRD Analysis	103
4.3.5	SEM Analysis	107
4.3.6	FTIR Analysis	109
4.4	Effect of Electron Beam Irradiation on the PP-DVC Compound after Natural Weathering	113
4.4.1	Gel Content Test	113
4.4.2	Tensile Test	114
4.4.3	Impact and Hardness Test	117
4.4.4	XRD Analysis	120
4.4.5	SEM Analysis	124
4.4.6	FTIR Analysis	126
V.	CONCLUSION	130
5.1	Conclusion	130
5.2	Future Works	131
	REFERENCE	132

LIST OF TABLES

Table		Page
2.1	Summary of Mechanical Data for All Blends	12
2.2	XRD Analysis of NR/modified MMT Nanocomposites	54
3.1	Various Content of Devulcanized Natural Rubber Adding to the Fixed Amount of PP	55
4.1	Inter-chain Separation, d-spacing, Crystallize Size and Crystallinity for Different DVC Composition of PP-DVC Compound at Peak A	70
4.2	Inter-chain Separation, d-spacing and Crystallize Size for Different DVC Composition of PP-DVC Compound at Various Irradiation Dosages at Peak A	88
4.3	Crystallinity for Different DVC Composition of PP-DVC Compound before and after EB-Irradiation	90
4.4	Inter-chain Separation, d-spacing and Crystallize Size for Different DVC Composition of PP-DVC Compound before and after Natural Weathering at Peak A	106
4.5	Inter-chain Separation, d-spacing and Crystallize Size for 5 phr DVC added in PP at Various Irradiation Dosages before and after Natural Weathering at Peak A	122

LIST OF FIGURES

Figures		Page
2.1	SEM Micrographs of NR/LLDPE Blend Tensile-fractured Sample: (a) 120 kGy (b) 240 kGy (c) 10% LNR-6 with 200 kGy (d) 25% LNR-6 with 200 kGy	9
2.2	FTIR Spectrum of NR, NR-g-PS and NR-g-PS with n-BA at Radiation Dose of 50 kGy	20
2.3	The Effect of Different Composition of TMPTA on the Gel Fraction of the PVC/ENR Blend at Various Irradiation Doses	28
2.4	SEM Micrographs of Tensile Fractured Surfaces of Control (A) and Irradiated NR/R-EPDM Blends at 50 kGy (B), 100 kGy (C), 150 kGy (D) and 200 kGy (E)	37
2.5	Tensile Strength versus Polyfunctional Monomers Type under Various EB-Irradiation	44
2.6	SEM Images of CBs Irradiated at (A) 0 kGy (B) 200 kGy (C) 600 kGy	50
4.1	Gel Content for Different DVC Composition of PP-DVC Compound	63
4.2	(a) Tensile Strength, (b) Young's Modulus and (c) Elongation at Break for Different DVC Composition of PP-DVC Compound	65
4.3	(a) Impact Strength and (b) Hardness for Different DVC Composition of PP-DVC Compound	67
4.4	XRD Curve ($3^\circ \leq 2\theta \leq 40^\circ$) for Different DVC Composition of PP-DVC Compound	70
4.5	SEM Micrographs of Fractured Surface for Different DVC Composition of PP-DVC Compound under Magnification of 1000x	72
4.6	FTIR Absorption Spectra for Different DVC Composition of PP-DVC Compound	74
4.7	(a) Wavenumber of the Asymmetric C-H Stretching Vibration and (b) CH ₂ Bending	75

Vibration for Different DVC Composition of PP-DVC Compound

4.8	Gel Content for Different DVC Composition of PP-DVC Compound before and after EB-Irradiation	77
4.9	(a) Tensile Strength, (b) Young's Modulus and (c) Elongation at Break for Different DVC Composition of PP-DVC Compound before and after EB-Irradiation	82
4.10	(a) Impact Strength and (b) Hardness for Different DVC Composition of PP-DVC Compound before and after EB-Irradiation	86
4.11	XRD Curve ($3^\circ \leq 2\theta \leq 40^\circ$) for 50 kGy and 200 kGy of Pristine PP and Different DVC Composition added in PP	88
4.12	SEM Micrographs of Fractured Surface for Different PP-DVC Compound with Various Irradiation Dosages under Magnification of 1000x	92
4.13	FTIR Absorption Spectra for Different DVC Composition of PP-DVC Compound before and after EB-Irradiation	94
4.14	(a) Wavenumber of the Asymmetric C-H Stretching Vibration and (b) CH ₂ Bending Vibration for Different DVC Composition of PP-DVC Compound before and after EB-Irradiation	95
4.15	Gel Content for Different DVC Composition of PP-DVC Compound upon Natural Weathering	97
4.16	(a) Tensile Strength, (b) Young's Modulus and (c) Elongation at Break for Different DVC Composition of PP-DVC Compound Subject to Natural Weathering	100
4.17	(a) Impact Strength and (b) Hardness for Different DVC Composition of PP-DVC Compound Subject to Natural Weathering	102
4.18	XRD Curve ($3^\circ \leq 2\theta \leq 40^\circ$) for Different DVC Composition of PP-DVC Compound before and after Natural Weathering	105
4.19	Crystallinity for Different Composition of PP-	107

DVC Compound upon Natural Weathering

4.20	SEM Micrographs of Fractured Surface for Different DVC Composition of PP-DVC Compound after 6 Months Outdoor Exposure under Magnification of 1000x	109
4.21	FTIR Absorption Spectra of PP-DVC Compound with Different Composition of DVC before and after Natural Weathering	112
4.22	(a) Wavenumber of the Asymmetric C-H Stretching Vibration and (b) Carbonyl Index for Different DVC Composition of PP-DVC Compound before and after Natural Weathering	112
4.23	Gel Content for 5 phr DVC added in PP Compound with Various Irradiation Dosages Subject to Natural Weathering	114
4.24	(a) Tensile Strength, (b) Young's Modulus and (c) Elongation at Break for 5 phr DVC added in PP Compound with Various Irradiation Dosages Subject to Natural Weathering	117
4.25	(a) Impact Strength and (b) Hardness for 5 phr DVC added in PP Compound with Various Irradiation Dosages Subject to Natural Weathering	119
4.26	XRD Curve ($3^\circ \leq 2\theta \leq 40^\circ$) for 5 phr DVC added in PP at Various Irradiation Dosages before and after 6 Months Outdoor Exposure	122
4.27	Crystallinity for 5 phr DVC added in PP at Various Irradiation Dosages upon Natural Weathering	123
4.28	SEM Micrographs of Fractured Surface for Different Irradiation Dosages of 5 phr DVC added in PP before and after Natural Weathering under Magnification of 1000x	125
4.29	FTIR Absorption Spectra of 5 phr DVC added in PP at Various Irradiation Dosages before and after Natural Weathering	128
4.30	(a) Wavenumber of the Asymmetric C-H Stretching Vibration and (b) Carbonyl Index for 5 phr DVC added in PP Compound at Various Irradiation Dosages upon Natural Weathering	129

LIST OF ABBREVIATIONS

2G	Diethyleneglycol Dimethacrylate
AMA	Allyl Methacrylate
APTMS	Acryloxypropyltrimethoxysilane
ASTM	American Society for Testing and Materials
A-TMMT	Tetramethylolmethane Tetraacrylate
BR	Butadiene Rubber
C=C	Carbon-Carbon Double Bond
C=O	Carbonyl
C20A	Dimethyl Dihydrogenated Tallow Quarternary Ammonium Montmorillonite
CB	Carbon Black
C-H	Carbon-Hydrogen Bond
CH ₂	Methylene
CH ₃	Methyl
CNR	Chlorinated Natural Rubber
CNTs	Carbon Nanotubes
CSM	Chlorosulfonated Polyethylene Rubber
DDA-MMT	Dodecyl Ammonium Montmorillonite
DPGDA	Dipropylene Glycol Diacrylate
DVC	Devulcanized Natural Rubber
EB	Electron Beam
EB4830	Aliphatic Polyurethane Acrylate
EDMA	Ethylene Glycol Dimethacrylate
EHA	Ethylhexyl Acrylate

ENR	Epoxidized Natural Rubber
EPDM	Ethylene Propylene Diene Monomer
EPTA	Ehtoxylated Pentaerythritol Tetraacrylate
EVA	Ethylene Vinyl Acetate
FTIR	Fourier Transform Infrared
GF	Glass Fiber
HALS	Hindered Amine Light Stabilizer
HATR	Horizontal Attenuated Total Reflection
HDDA	1,6-Hexandiol-Diacrylate
HDPE	High Density Polyethylene
HEMA	2-Hydroxyethyl Methacrylate
HNT	Halloysite Nanotube
HVA-2	m-Phenylenebismaleimide
LLDPE	Low Linear Density Polyethylene
LNR	Liquid Natural Rubber
MAH	Maleic Anhydride
Na-MMT	Sodium Montmorillonite
n-BA	n-Butyl Acrylate
NR	Natural Rubber
O ₂	Oxygen
ODA-MMT	Octadecylamine Modified Montmorillonites
O-H	Hydroxyl
OMMT	Organo Montmorillonite
OPEFB	Oil Palm Empty Fruit Bunch
PE	Polythylene

PEA	Phenoxy Ethyl Acrylate
PET	Polyethylene Terephthalate
PFM	Polyfunctional Monomer
PP	Polypropylene
PPEGA	Phenoxy Polyethylene Glycol Acrylate
PS	Polystyrene
PVA	Polyvinylalcohol
PVC	Polyvinyl Chloride
RRP	Reclaimed Rubber Powder
SBR	Styrene-Butadiene Rubber
SEM	Scanning Electron Microscopy
SN	Styrene Monomer
TAC	Triallylcyanurate
TAIC	Triallylisocyanurate
TBLS	Tribasic Lead Sulfate
THF	Tetrahydrofuran
TiO ₂	Titanium Dioxide
TMPTA	Trimethylolpropane Triacrylate
TMPTMA	Trimethylolpropane Trimethacrylate
TNPP	Tris-nonyl Phenyl Phosphate
TPGDA	Tripropyleneglycol Diacrylate
UV	Ultraviolet
WRP	Waste Rubber Powder
XRD	X-ray Diffraction
ZDA	Zinc Diacrylate

CHAPTER 1

INTRODUCTION

1.1 Background

In the 21st century, one of the major problems is the waste disposal management issue. As knowing that the waste polymers disposal is serious environmental issues because of the polymeric materials are difficult to decompose. In fact, one of the major waste polymers is generated from rubbers used as tires for vehicles. When these tires are no longer serviceable and discarded after a long run, there is only a small amount of rubber (< 1%) are abraded out from the tire (Adhikari and Maiti, 2000). Since then Malaysian rubber scientists B. C. Sekhar has invented a technology to devulcanize the rubber (Sekhar et al., 1998). The technology claimed that the devulcanize rubber able to regains 75 percent of its virgin properties. Sekhar inventions apply the specially formulated activator to break down the cross-linking so that it can return to the virgin quality. There are several studies that have been carried out to devulcanized the rubber. It can be classified into three groups which are physical process, chemical process and biological process. Physical devulcanization process involves with the aids of external energy such as mechanical (Leyden, 1991 and Fukumori et al., 2001), microwave (Novotny, 1978 and Kleps et al., 2000) and ultrasonic (Isayev and Chen, 1994, Levin et al., 1997 and Yun et al., 2001). Chemical devulcanization process uses

devulcanizing agents such as organic solvents (Hunt and Kovalak, 1999), chemicals (De et al., 1997 and Verbruggen et al., 1999) and inorganic compounds (Myers et al., 1997) to devulcanized the waste rubber. The biological process uses bacteria or microorganisms to break the sulfur cross-link in waste rubber (Holst et al., 1998 and Romine and Snowden-Swan, 1997).

1.2 Problem Statements

Most of the polymers are vulnerable to degradation under natural environment in which involved with ultraviolet and atmospheric oxygen and bring about chain scission in polymer chains. It may be accelerated by the elevated temperatures from the sun (White and Turnbull, 1994). Photo-oxidation degradation occurs when the oxygen present by the activation of the polymer macromolecule with the absorption of a photon of light in the polymer (Rabek, 1995). Generally, the important reactions of the photo-oxidation degradation for almost all the polymers occur as the following process steps (Rabek, 1990):

1. Initial step: Free radicals are formed by photon absorption.
2. Chain Propagation step: A free radical reacts with oxygen to produce a polymer peroxy radical (POO•). This reacts with a polymer molecule to generate polymer hydroperoxide (POOH) and a new polymer alkyl radical (P•).

3. Chain Branching: Polymer oxy radicals (PO•) and hydroxy radicals (HO•) are formed by photolysis.
4. Termination step: Cross-linking is a result of the reaction of different free radicals with each other.

On the other hand, polypropylene (PP) is massively used in many applications because of its distinctive properties such as low density, heat resistant, high melting temperature and high chemical resistance. The superior properties of PP are mainly contributed by its high crystallinity structure and stability of the methyl group. Despite that, one of the major drawbacks of PP is poor performance in impact strength which leads to the limitation to several other applications (Mohamad et al., 2013). Furthermore, PP is vulnerable to degradation under natural environment. As for example, it is enough to initiate the degradation with the wavelengths of the sunshine at the earth's surface which is over 290 nm and caused discoloration, chalking and embrittlement of PP (Song et al., 2014). The problem statements for this study are as follows:

1. What is the effect of devulcanized natural rubber on the mechanical properties, physical properties and chemical interaction of the Polypropylene-Devulcanized Natural Rubber (PP-DVC) compound?
2. What is the effect of electron beam irradiation on the mechanical properties, physical properties and chemical interaction of the Polypropylene-Devulcanized Natural Rubber (PP-DVC) compound?
3. What is the extent of degradation by UV source on the PP-DVC compound?

1.3 Aims and Objectives

The objectives of this study are to investigate the performance of the Polypropylene-Devulcanized Natural Rubber (PP-DVC) compound. The aims and objective of the project are further divided as follows:

1. To investigate the effect of devulcanized natural rubber on the mechanical properties, physical properties and chemical interaction of the Polypropylene-Devulcanized Natural Rubber (PP-DVC) compound.
2. To investigate the effect of electron beam irradiation on the mechanical properties, physical properties and chemical interaction of the Polypropylene-Devulcanized Natural Rubber (PP-DVC) compound.
3. To investigate the extent of degradation by UV source on the PP-DVC compound.

1.4 Scope of Study

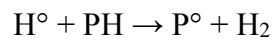
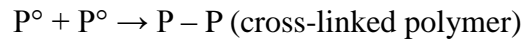
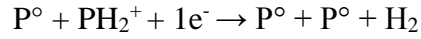
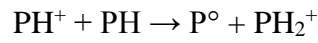
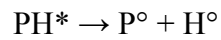
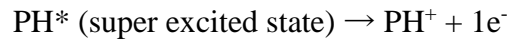
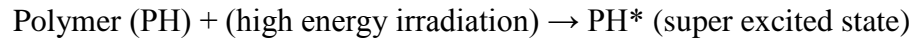
This study mainly focuses on analyzing the characteristic of Polypropylene-Devulcanized Natural Rubber (PP-DVC) compound based on the different composition of DVC and electron beam irradiation dosage while exposed to UV source to determine its durability.

CHAPTER 2

LITERATURE REVIEW

2.1 Introduction

Technology in polymer processing is widely accepted the radiation treatment such as grafting, cross-linking, coating, sterilizing and composite bonding (Chong et al., 2010). Over last few decades, many authors have been investigated the radiation effects on polymers. Therefore, the study of polymer irradiation has become greatly concern due to both reactions of cross-linking and degradation could happen in the polymeric materials at high energy of radiation (Akhtar et al., 1986). One of the important irradiation techniques for the polymer is the utilization of electron beam radiation. It was generated by a heated cathode in a high vacuum condition. Then, the cathode emits electrons will accelerate between cathode and anode in an electrostatic field. As a result, it greatly altered the energy of the accelerated electrons when entering a material (Drobny, 2013). EB technology is well-known to initiates free radicals to induce chemical reactions in polymers or polymer composites. The main advantage of EB technology is the free radicals can be generated with spatial and temporal precise according to the chemical reaction requirement without any use of chemicals as well as independent from the the state of aggregation and temperature (Mondal et al., 2013). The general reaction mechanism of EB irradiation system is shown as below (Hafezi et al., 2007):



Basically, polymers are extensively used in nuclear engineering and technology such as corrosion resistant, desorbing coatings, packing, shock absorbers and biological protection devices. Therefore, the radiation environment is important to the degradation and modification of materials (Bhagawan et al., 1987). The technique of blending polymers is commonly used to develop a product with better physical and chemical properties by using inexpensive polymers. Polymer blending can combine the advantages of the polymers to obtain better material. There is numerous literature published which focus on the natural rubber blend with various types of polymers without EB-irradiation. However, most of the polymers blended with natural rubber are thermodynamically immiscible and exhibit poor properties due to their poor adhesion between the phases and unstable morphology. Thus, the compatibilization on the polymer blends is needed to improve the interfacial properties of the blend and stabilize the morphology. The chemical structure of polymers modified through generated a new reactive chemical groups on the polymer backbone has been widely used in compatibilization of immiscible

polymer blends and functional polymers preparation (Rooj et al., 2011). Over the decades, many researchers had done the improvement on the natural rubber-polymer blend with EB-irradiation to enhance the performance.

2.2 Natural Rubber – Polyethylene (PE) Blend

Ahmad et al. (2005) have examined the mechanical and physical properties of the natural rubber/low linear density polyethylene (NR/LLDPE) blends cross-linked by electron beam (EB) irradiation. They have performed the study on 60/40 NR/LLDPE blends with various dose of EB irradiation. The results indicated that the tensile strength of NR/LLDPE blend increased with higher irradiation dosages up to 250 kGy and then started to decrease with further irradiation dosages increase to 300 kGy. It was concluded that a radiation dose of 200 kGy was needed in order to achieve optimum tensile strength as shown by other researchers (Ahmad et al., 2005, Dahlan et al., 2002 and Muhammad et al., 2011). Several of literatures have reported that mechanical properties can be enhanced with the reinforcing filler added in the natural rubber blends (Chong et al., 2010, Ahmad et al., 2012 and Sam et al., 2012). Muhammad et al. (2011) have reported that by adding m-phenylenebismaleimide (HVA-2) into NR/LLDPE blends can enhance the tensile strength with a lower dosage of EB irradiation. The optimum tensile strength can be achieved at 100 kGy of radiation dose with 0.2 phr of HVA-2 blends while without HVA-2 blends need to increase up to 200 kGy to achieve optimum tensile strength. Generally, with the increasing in radiation dose

could cause the elongation at break of the blends reduced. The blend's rigidity changes to more brittle by the cross-links networks formation caused the elongation at break dropped. Muhammad et al. (2011) reported that the Shore A hardness and impact strength of 60/40 NR/LLDPE blends increasing with higher radiation dose. The presence of HVA-2 in the blends has higher hardness level and impact strength compare to without HVA-2 blends. Similarly, Dahlan et al. (2002) have investigated the hardness of the NR/LLDPE at 200 kGy irradiation dose with incorporation of LNR-6 and LNR-16. Shore A hardness did not affect by the LNR-6 composition increasing in the blends. However, the addition of LNR-16 showed a decreasing trend in Shore A hardness.

Refer to the Figure 2.1, Dahlan et al. (2002) have observed the irradiated tensile fractures of the NR/LLDPE blends. The samples in Figure 2.1 (a) indicate that the cross-link was enough to form in the morphology with the dose of 120 kGy. Besides that, the samples show a great change in topology at 240 kGy doses with the smoother surface as shown in Figure 2.1 (b). The smooth transformation of the morphology corresponds to increase the interaction of the rubber and plastic phase improve the blend compatibility and stability. EB irradiation induces cross-links in rubber and plastic phases (Ahmad et al., 2005). The addition of LNR-6 has further enhanced the fractured surface appearance as it acted as a good compatibiliser in the NR/LLDPE blends. The mixing was not very homogeneous for the sample that contains 10 % LNR-6 with 200 kGy doses as shown in Figure 2.1 (c). However, the tear lines in Figure 2.1 (d) appeared to be more homogeneous

with increased the LNR-6 content from 10 % to 25 %. Chong et al. (2010) have analyzed the functional group on the polyisoprene chains by irradiation for the liquid natural rubber (LNR) coated with rice husk (RH) in NR/HDPE blends. In the $3700 - 3200 \text{ cm}^{-1}$ region has appeared a sharp peak at 3436 cm^{-1} after radiation because of the hydroxyl group (-OH) from the RH and LNR formed. For the modified RH after radiation exposure, the intensity of -C-H vibration peaks was found to be reduced. The =C-H group in the polyisoprene of LNR reduced when irradiated at 20 kGy. The C-H and =C-H groups of the polyisoprene were reduced because of the free radicals generated on the vinyl groups and cross-linking networks formation upon exposure under irradiation.

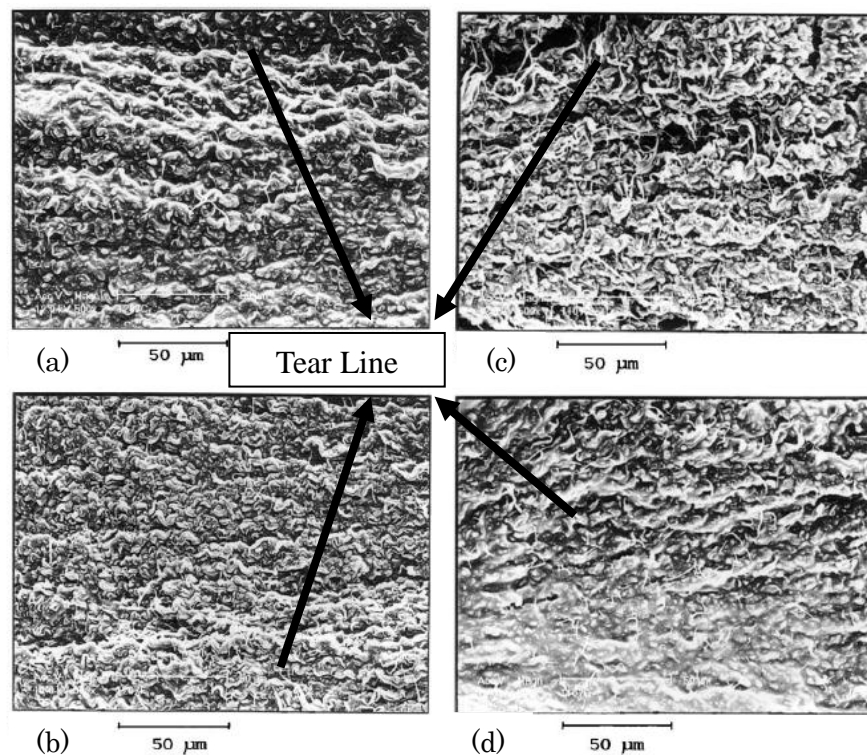


Figure 2.1: SEM Micrographs of NR/LLDPE Blend Tensile-fractured Sample: (a) 120 kGy (b) 240 kGy (c) 10% LNR-6 with 200 kGy (d) 25% LNR-6 with 200 kGy (Ahmad et al., 2005 and Dahlan et al., 2002).

The different irradiation dosages influence on the gel content of NR/LLDPE 60/40 blends was studied by Muhammad et al. (2011) It was found that higher gel content obtained when the radiation dose increasing. A similar phenomenon has reported by other researchers where the gel content of natural rubber blends increase with higher radiation dosage (Ahmad et al., 2005 and Dahlan et al., 2002). The gelation occurs induced strong interactions between rubber and plastic phases. In addition, the gel content was rapidly increases up to 200 kGy and become slow down with further increase in radiation dose. This is due to the predominance of degradation in macromolecular chemical bonds between the cross-linked macromolecular chains at this stage. Also, Muhammad et al. (2011) have reported that by addition of 2.0 phr of HVA-2 in the NR/LLDPE blends can increase the gel content at a lower dosage of 100 kGy. However, further increasing of radiation dose does not increase the gel content in the blends. It shows the effectiveness of HVA-2 as a sensitizer for radiation-induced cross-linking.

2.3 Natural Rubber – Polypropylene (PP) Blend

Senna et al. (2008) have investigated the structural and mechanical properties of polypropylene/epoxidized natural rubber (PP/ENR) blends with the aids of electron beam irradiation. The higher dosages of EB irradiation could cause reduction in tensile strength even though tensile properties of irradiated blends higher than un-irradiated blends. Besides that, higher ratio of ENR to 10 % gives better value of elongation at break whereas it tended to

decrease beyond this ratio due to the rubber added in the PP matrix. The cross-linking of PP occurs by EB-irradiation up to 15 kGy doses and beyond this dose can cause the PP started to degrade while the rubber phase started to cross-link. Additive agents such as compatibilizing agent and cross-linking agent can be added into the blends to further enhance the mechanical properties of the blends (Senna and Monem, 2010 and Oo et al., 2000). Senna and Monem (2010) have studied the applications of compatilizing agents which are polypropylene graft copolymer with maleic anhydride (PP-g-MAH). The multifunctional monomer 1,6-hexandiol-diacrylate (HDDA) was used to improve the mechanical properties of the PP/ENR blends under EB-irradiation. Moreover, it was reported that the HDDA and PP-g-MAH added in the blend matrix enhanced the mechanical properties of the blends. Oo et al. (2000) have used the ethylhexyl acrylate (EHA) as a cross-linking agent in 80/20 PP/NR blends undergone EB irradiation. For the 1.0 pph concentration of EHA irradiated at 100 kGy exhibits the highest tensile strength. However, Mondal et al. (2012) have studied the mechanical properties on the higher dosage of EB irradiation in the PP/NR blends with and without dipropylene glycol diacrylate (DPGDA). The summary of mechanical data for all blends was tabulated in Table 2.1 (Mondal et al., 2012 and Mondal et al., 2013). The 0.6 wt% of DPDGA in blends irradiated at 150 kGy doses obtained the optimum tensile strength while the tensile strength for blend without DPDGA needed 250 kGy to obtain similar value. Elongation at break also exhibited the similar trend. The identical phenomenon was reported by Mondal et al. (2013) by using 2 wt% of TMPTA in the blends. The tensile strength, elongation at break and Young's modulus significantly increase at 150 kGy doses followed by

diminishing at a higher dose. Meanwhile for the hardness, it also sharply increased at the 150 kGy doses but only small improvement with further dose. The tensile strength and elongation at break for the organoclay added in the PP/NR (50/50) blends increased up to 50 kGy and then reduce with further increasing in irradiation dose as the PP matrix degraded (Sharif et al., 2010).

Table 2.1: Summary of Mechanical Data for All Blends (Mondal et al., 2012 and Mondal et al., 2013).

Samples	Tensile Strength [MPa]	Elongation at Break [%]	100% Modulus [MPa]	Young's Modulus [MPa]
Blend_ 0 kGy	7.9 ± 0.3	77 ± 7	-	231 ± 17
Blend_150 kGy	11.8 ± 1.8	250 ± 50	10.0 ± 0.5	209 ± 4
Blend_250 kGy	14.5 ± 0.5	310 ± 10	10.5 ± 0.5	243 ± 15
Blned_350 kGy	13.7 ± 3.4	280 ± 12	11.0 ± 0.5	271 ± 33
Blend_DPGDA_0 kGy	5.5 ± 0.5	46 ± 15	-	204 ± 21
Blend_DPDGA_150 kGy	13.7 ± 2.1	350 ± 10	10.0 ± 0.5	277 ± 2
Blend_DPDGA_250 kGy	6.9 ± 2.0	31 ± 25	-	219 ± 25
Blend_DPDGA_350 kGy	13.7 ± 0.1	220 ± 16	11.0 ± 0.5	251 ± 26
TPE-control	7.0 ± 0.9	113 ± 19	7.0 ± 0.5	141 ± 20
TPV150	13.5 ± 0.5	200 ± 15	12.0 ± 0.4	612 ± 18

TPV250	12.3 ± 0.1	143 ± 10	12.1 ± 0.2	575 ± 16
TPV350	12.0 ± 0.3	140 ± 7	12.0 ± 0.2	534 ± 11

In term of surface morphologies, Senna et al. (2008) have analyzed the fracture surfaces for the irradiated PP/ENR (90/10) blends at 10 kGy, 30 kGy and 50 kGy. The phase separation was found to be reduced compared to the un-irradiated blend. The irradiated blend at 50 kGy has higher roughness and less phase separation due to the free radicals formed with interaction between ENR and PP. The morphology shows a higher NR phase trend for 250 kGy and 350 kGy treated TPVs compared with the 150 kGy dose for the PP/NR (50/50) blends. PP is extremely sensitive to the radiation environment and shear-induced degradation so it might appear to degrade at high level of irradiation dosages. Therefore, it would lower the viscosity of PP matrix and thus the mismatch viscosity of the blends increased. Mondal et al. (2012) have studied the surface morphologies on the PP/NR (50/50) blend with the presence of DPGDA at 150 kGy doses. It showed a well-defined interface as visible through co-continuous pictures indicating the tendency of penetrating network due to the graft-linkage of the region increased during irradiation compared to the bulk volume of NR as the favourable in low viscous DPGDA migrated into the interface. Other than that, Senna et al. (2008) have clarified the crystalline structure change in PP by blending process with the aids of X-ray diffraction (XRD). It was found that the position of (2θ) is shifted to higher values with irradiation dose which means no orientation changes by irradiation and the depredated chains could re-crystallize in both amorphous and crystalline regions with enough mobility. Besides that, Senna and Monem

(2010) have carried out the XRD to clarify the crystalline structure of PP change with the different reactive compatibilizers present in the PP/ENR (90/10) blends upon EB-irradiation at a 30 kGy dose. It showed that the acidic groups of PP-g-MAH and residual monomer (HDDA) have caused the peak intensity and crystallinity increase. However, PP/ENR (90/10) with HDDA irradiated to 30 kGy has reduced the peak intensity due to cross-linking process occurs in the interconnection between ENR phase and PP-ENR phase. Furthermore, Sharif et al. (2010) have studied the XRD pattern on the PP/NR (50/50) blended with organoclay and it showed the intercalated nanocomposites formed with the diffraction peak exists.

Senna and Monem (2010) have carried out the FTIR analysis to investigate the EB irradiation influence on the chemical bonding of PP/ENR blends with the incorporation of the compatibilizing agent PP-g-MAH. As expected, the oxygenated groups to PP were introduced in the blending of ENR undergone EB irradiation. After EB irradiation, there was increasing on the intensity of absorption bands for (-OH), (C=O) and (-C-O-C-) and the incorporation of PP-g-MAH due to the oxygenated groups (-COOH, -OH and C=O) introduce to the PP. On the other hand, Mondal et al. (2012) have investigated the PP/NR (50/50) blends with and without 0.6 wt% of DPGDA. The intensity of C=C stretching reduced at a higher absorbed dose due to cross-linking of NR increased but the C=C content of NR is higher. At about 0.5 % of C=C bonds of NR were utilized at 350 kGy doses. The intensity of absorption band at 1660 cm^{-1} representing the alkene unsaturation (C=C) group are decreased after irradiation due to the cross-link networks formation

and consequently cause the unsaturation in NR reduced (Mondal et al., 2013). The gel content of the PP/NR/clay nanocomposites was found to be increased with irradiation dosages increasing up to 200 kGy due to the cross-linking networks formation increased in the polymer nanocomposites (Sharif et al., 2010). However, EHA did not enhance the cross-linking of the PP/NR blends after irradiation. The presence of TMPTA could enhance the degree of cross-linking with irradiation up to 40 kGy. The gel content dropped after 40 kGy due to the breakdown of the PP at higher irradiation dose. The highest degree of cross-linking is 3.0 pph TMPTA blend (Mondal et al., 2012). Mondal et al. (2013) also have reported the 2.0 wt% of TMPTA in PP/NR (50/50) blend irradiated at 350 kGy doses obtained the maximum gel content value of 32 %. In comparison to the absence of DPGDA in PP/NR blend, there was an increase in gel content value at 150 kGy doses for the PP/NR blend with DPGDA. By comparing to without DPDGA, the gel content percentage was higher than 50 % for the 350 kGy doses with DPDGA (Mondal et al., 2012).

2.4 Natural Rubber – Polyethylene Terephthalate (PET) Blend

High energy of EB-irradiation is effectively to chemically inert polymer such as PET or PE even though it can generate radicals which required for chemical reaction (Kondo et al., 2008). PET appeared to be favourable among all fiber reinforcing materials because of its good mechanical properties with low shrinkage and high modulus but it less likely to adhere with rubbers due to its chemically inert polymer. Therefore, the

adhesion between PET fibers and rubber required to enhance with a lot of additives. EB-irradiation-induced graft polymerization can work effectively with a chemically robust polymer such as PET (Kondo et al., 2008 and Kondo et al., 2009). Kondo et al. (2009) have studied the mechanical properties of the PET fibers-reinforced NR composites under EB-irradiation. The Young's modulus and the breaking strength decrease with higher content of the untreated PET fibers and PET fiber in the NR. The strain was slightly less than pure NR and remains at about 700 % (Kondo et al., 2008). These indicated that the mechanical properties such as breaking strength, strain and Young's modulus do not improve with the untreated-fibers contained in the NR matrix because of the poor interaction between the PET fibers and the NR matrix. Therefore, it caused the slipping in interfacial regions of untreated PET fibers and NR matrix (Kondo et al., 2008 and Kondo et al., 2009). However, grafted-polymerization of PET fibers with EB-irradiation can improve the mechanical properties of the PET fibers-reinforced NR composites. Kondo et al. (2009) have used the Allyl methacrylate (AMA) and Acryloxypropyltrimethoxysilane (APTMS) to graft with PET fibers under 500 kGy of EB-irradiation. The irradiation dosages at 500 kGy utilize the graft polymerization effectively because the tensile strength of the PET fibers hardly damaged by at a high dose of 500 kGy. Although the tensile strength gradually decreases with higher irradiation dosages, it still remains 90 % of the original strength at the 500 kGy doses. Other than that, EB-irradiation hardly influences the modulus and strains which only increases a little bit at 500 kGy. Both grafted PET fibers also reported that have higher strength and modulus compared with untreated PET fibers. This may be due to the interfacial regions enhanced in the grafted

PET fibers and NR matrix (Kondo et al., 2008 and Kondo et al., 2009). The breaking strain of AMA-grafted PET fibers is much less than untreated PET fibers because of the formation of cross-linkage among PET fibers and NR matrix (Kondo et al., 2009).

The grafted PET fibers improve the initial modulus as well as the tensile strength. Some of the chemical reactions were occurred in the interfacial region of PET fibers and NR by cross-linking formed through the sulfuric linkages of NR and grafted side chains of PET fibers (Kondo et al., 2008). AMA-grafted-PET fibers consist of allyl groups in the grafted side chains that act as active sites to cross-link the sulfur atoms in the vulcanization process (Kondo et al., 2009). Kondo et al. (2008) have observed adhesion effect between PET fibers and NR matrix for the fractured surfaces by using scanning electron microscopy (SEM). It was appeared to be weak adhesion in the interfacial region with a crack that occurs between untreated PET fibers and NR matrix. As per contra, the NR matrix was covered by the grafted-PET fibers and this implies a better adhesion effect between grafted-PET fibers and NR matrix. The grafted chains of APTMS or AMA on the fibers surface could give a good quality of the interfacial region between PET fibers and NR matrix. Kondo et al. (2009) also have studied the Fourier transform infrared (FTIR) spectra for the untreated and AMA-grafted PET fibers together with AMA homopolymers. The graft polymerization with AMA occurred on the PET fibers surface under EB-irradiation as the $-CH_2$ group decrease and $-CH_3$ group increase by the graft treatment although the grafting amount appeared to be less at the 500 kGy doses. APTMS-grafted PET fibers also reported same

behavior with AMA-grafted PET fibers as the APTMS-treated PET fibers could observe the C=C double bond in the vinyl group of but not observed in APTMS-grafted PET fibers (Kondo et al., 2008).

2.5 Natural Rubber – Polystyrene (PS) Blend

Muhammad et al. (2002) have conducted the effect of the EB irradiation of mechanical testing included tensile test, hardness test and impact test on the 60/40 natural rubber/polystyrene (NR/PS) blends with and without m-Phenylenebismaleimide (HVA-2). The optimum tensile strength of 2.0 phr of HVA-2 is 10.4 MPa at 50 kGy while the optimum tensile strength of 0 phr of HVA-2 is 7.9 MPa at 200 kGy. This indicated that the presence of the HVA-2 has lowered the optimum dose and also the tensile strength of the NR/PS blends has increased. It is expected that the NR/PS blend become more brittle as the absorbed dose increase. The highest elongation at break for the NR/PS blend with 2.0 phr HVA-2 is 500 % at 100 kGy compared to 528 % for the blend without HVA-2 at 200 kGy. The hardness of the irradiated blends is also reflected in the irradiation-induced cross-linking of polymers. The highest hardness is the blend with 2.0 phr HVA-2 followed by the blend with 1.0 phr. The higher impact strength of the blend can be contributed by the block and copolymer formed during blending of the polymers containing HVA-2 tended to bridge more effectively the NR and PS together. The presence of HVA-2 in NR/PS blend not only gives higher impact strength but also lower the optimum dose. Khamplod et al. (2015) have studied the influence of

irradiation dosages and NR/styrene (NR/St) ratio on the mechanical properties of the NR/PS blend by using EB-irradiation technique to synthesize graft copolymer of NR and PS. The tensile strength of styrene monomer (SN) ratio increased with optimum level of radiation dose (75 kGy). Then, it showed a downward trend due to the molecular chains degraded resulting from the high level of radiation dose. It would cause the graft copolymerization reaction reduced and poor coalescence in cross-linking during latex film formation. While for the 300 % modulus of SN ratio, it increased with higher radiation dose. The elongation at break is inversely proportional to all the factors owing to the restrictions imposed on the flexibility of a molecular chain increased with additional cross-linking formation.

Muhammad et al. (2002) have analyzed the surface morphology of the NR/PS blends. The immiscibility of the NR/PS blend with large and irregular PS domains is dispersed in that continuous NR matrix. Radiation is more effective in imparting better blend homogeneity and firmer structure than HVA-2. The addition of HVA-2 and radiation can further improve the compatibility of the blends which decrease the phase separation and reduce particles size of the dispersed PS domains. The finest structure and the best homogeneity of the blend is 2.0 phr of HVA-2 with 150 kGy irradiation dose. Khamplod et al. (2015) have studied the FTIR spectra of pure NR, NR-g-PS and NR-g-PS with n-BA of the graft polymer of NR and PS are shown in Figure 2.2. The percent transmittance at 1664 and 835 cm^{-1} in all samples corresponding to the C=C stretching of NR and =C-H out of plane bending of NR respectively. The peak at around 1670 - 2000 cm^{-1} and 695 cm^{-1}

represented the -C-H aromatic overtone of PS and the -C-H aromatic out of plane bending of PS which indicated the polystyrene in NR-g-PS occurs. There was C=O conjugation at the peak of 1736.1 cm^{-1} for NR-g-PS with n-BA and it might originated from the over-sensitizing effect of n-BA which may cause the polymerization of n-BA in NR-g-PS system (Khamplod et al., 2014 and Khamplod et al., 2015).

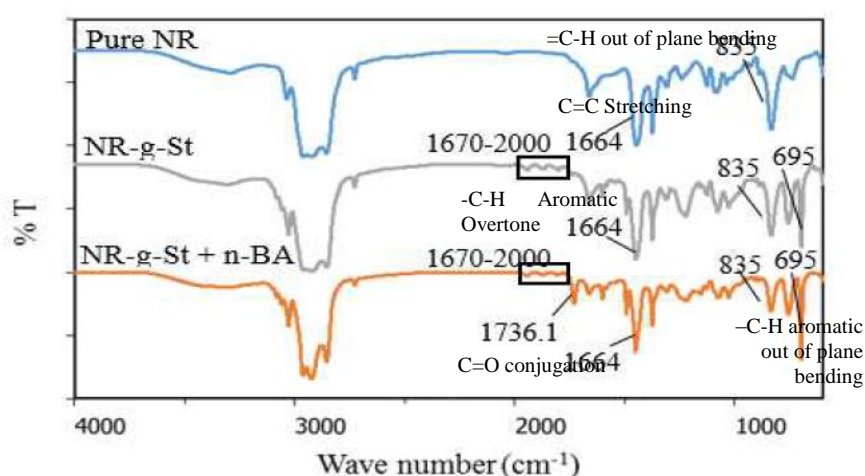


Figure 2.2: FTIR Spectrum of NR, NR-g-PS and NR-g-PS with n-BA at Radiation Dose of 50 kGy (Khamplod et al., 2015).

Muhammad et al. (2002) have studied the gel content of PS and NR for the NR/PS blends. A plateau is observed after the gel content of NR without HVA-2 increases sharply with the irradiation dose up to 150 kGy. A plateau was observed at much lower dose for the NR with 2.0 phr HVA-2 indicated that the blend is more sensitive towards radiation. The gel content of PS without HVA-2 only detectable at 150 kGy and higher doses due to its protective nature towards radiation. However, the gel content of PS with 2.0 phr HVA-2 already detectable at 0 kGy and increasing with higher irradiation

dose. At a lower radiation dose, the gelation is induced when the presence of HVA-2 in the blends as the gel contents of NR and PS exhibit higher values than without HVA-2.

2.6 Natural Rubber – Polyvinyl Chloride (PVC) Blend

Ratnam et al. (2006) have studied the pre-irradiation of epoxidized natural rubber (ENR) 50 influences on the mechanical properties such as tensile test, impact test and hardness test of the 50/50 PVR/ENR blend. The results showed an upward trend with higher radiation dose due to radiation cross-linked rubber phase exists in the blend. It is expected the elongation at break of the blend reduces with the increasing of irradiation dose since the rubber becomes rigid. Ratnam et al. (2006) also have conducted the tensile study on the mixing time and blending temperature influence on polyvinyl chloride/epoxidized natural rubber (PVC/ENR) blend enhanced by electron beam irradiation. The tensile strength has decreased gradually with higher blending temperature above 150 °C. This gradual increase in tensile strength with irradiation dose was caused by the irradiation-induced cross-linking. However, the blend at 150 °C has the best improvement in tensile strength upon irradiation. Mixing time increase could enhance the tensile strength upon irradiation as the blend homogeneity improved. The mixing time and blending temperature on the M100 of the blend is shown an increase with higher irradiation dose. The M100 of the blend enhanced with irradiation dose is reflected by cross-link density increase and the interaction between the

polymers of the homogenous blend increased upon irradiation which longer mixing time to be achieved. The mechanical properties of PVC/ENR blends can be improved by adding additives such as nanofillers, cross-linking agent, antioxidants, stabilizer and natural fibers. Addition of TMPTA gives the best result of tensile strength and hardness value among various cross-linking agents which are 2-ethylhexyl acrylate (EHA), 1,6-hexanediol diacrylate (HDDA) and aliphatic polyurethane acrylate (EB4830) while the HDDA gives the lower tensile strength and hardness value in the 70/30 PVC/ENR blend with various radiation doses. Other than that, elongation at break reduces with the irradiation dose increased for all cross-linking agents (Ratnam and Zaman, 1999). 3.0 phr and 4.0 phr of TMPTA in the 50/50 PVC/ENR blend reach an optimum tensile strength at 70 kGy. Beyond this point, tensile strength reduced with subsequent radiation dose. M100 increased with the level up to 4.0 phr TMPTA upon irradiation and lower M100 is observed with the 5.0 phr TMPTA beyond the 40 kGy dose. A decline in elongation at break with higher radiation dose and TMPTA content was expected and hardness value exhibits the similar trend with modulus (Ratnam et al., 2001). The tensile strength of PVC/ENR 50/50 blend reinforced with grafted oil palm empty fruit bunch (OPEFB) fiber was found to be higher than ungrafted fiber as the grafting the adhesion between the treated fiber and matrix has been enhanced. Addition of tripropyleneglycol diacrylate (TPGDA) enhanced the Young's Modulus of the PVC/ENR blends. A reduction in the elongation at break was observed with higher radiation dosages and the incorporation of TPGDA. A higher elongation at break was observed for the grafted fiber compared to ungrafted fiber (Ratnam et al., 2007). Ratnam (2002) has studied the irradiation dose influence

on the tensile strength of 50/50 PVR/ENR blend with the mixing time of 6 min and 30 min at various tribasic lead sulfate (TBLS) level. The blend with 2.0 phr TBLS was found to yield the highest value in tensile strength and M100 upon irradiation. Further addition of TBLS caused the reduction in tensile strength and M100. The blend is insufficient to have adequate stability with the addition of 1.0 phr TBLS while above 2.0 phr TBLS inhibits the cross-linking reaction by trapping the radical formed in the irradiation process. Elongation at break reduces with increasing the irradiation doses because the segmental mobility of the blend reduced which resulting from the cross-linking of the blend increased. Higher content of TBLS gives lower hardness value at all radiation dose due to cross-link density lower. The use of antioxidants in polymers could help to prevent the polymer degradation from oxidative environment. Ratnam and Zaman (1999) have examined the performance of three antioxidant types which are Irganox 1010, tris-nonyl phenyl phosphate (TNPP) and hindered amine light stabilizer (HALS) for the stabilization and TMPTA as the cross-linking agent in 70/30 PVC/ENR blends. The blend with Irganox 1010 achieved higher optimum dose in tensile strength, hardness and modulus than TNPP and HALS indicated that the radiation-induced cross-link inhibits by the superior radical scavenging ability of Irganox 1010. The blend with Irganox 1010 and TNPP above the optimum dose has drastically dropped in elongation at break due to the excessive of cross-links in addition to severe degradation follow by consumption of the added antioxidant. Ratnam et al. (2001) have studied the tensile strength influenced by different Irganox 1010 level of the irradiated 50/50 PVC/ENR blend. With the addition of beyond 0.5 phr Irganox 1010 show a declining

trend due to the plasticizing effect of additive under irradiation. Ramlee et al. (2015) have studied the TiO₂ nanofillers for various composition ranges influence on the mechanical properties of PVC/ENR blends (30/70, 50/50 and 70/30) under EB-irradiation. The presence of nanofillers in the blend obtained the optimum value in mechanical properties such as tensile strength, impact strength and hardness at all blend composition ranges upon radiation up to 100 kGy. However, the tensile strength starts to drop when exposing to higher than 100 kGy doses. Furthermore, Ratnam et al. (2015) have performed a mechanical test on the effect of carbon nanotubes (CNTs) in the 50/50 PVC/ENR blends upon irradiation. The incorporation of 2.0 phr CNTs has caused a drop in tensile strength and M100 due to the CNTs dispersed poorly in the PVC/ENR matrix. In contrast, the nanocomposites prepared under melt blending method could exhibit higher tensile strength and M100 compared to neat PVC/ENR blend upon EB-irradiation due to the irradiation-induced cross-linking occurred and dispersion of CNTs improve in the matrix. As expected, the elongation at break was reduced with higher irradiation dose due to irradiation-induced cross-linking occurred.

For the surface morphologies, Ratnam et al. (2001) have examined the fracture surface of the PVC/ENR (50/50) blend before and after irradiation at 200 kGy. Irradiated sample appears to be more brittle and rougher compared to the un-irradiated one. On the other hand, the presence of 4.0 phr TMPTA at 200 kGy of irradiated blend showed at the edges of the cracks have more crack branching and irregularities which attributed to the excessive of cross-links exists and microgels formation upon irradiation. While for the irradiated blend

with 3.0 phr TMPTA at 60 kGy, it shows an extensive tearing matrix that deeply penetrates into the bulk sample resulted from the higher cross-linking degree and the blend offer resistance toward crack propagation increased. The fracture surface of the ungrafted and grafted OPEFB/PVC/ENR composites had been studied by Ratnam et al. (2007). Ungrafted fiber reinforced composites show that during the fracture pulls out most of the fibers without breaking as the weak adhesion and poor dispersion between the matrix and fiber. OPEFB-g-PMA-PVC/ENR composites were observed to have gap between the fiber and polymer matrix indicated that the enhancement between the OPEFB fiber and polymer matrix. The surface morphology of the blend with 0.5 phr Irganox 1010 irradiated at 200 kGy appears brittle and non-existence of microgels indicating the lower cross-linking degree is obtained (Ratnam et al., 2001). The morphological of PVC/ENR (50/50 & 70/30) blends with and without TiO₂ at 100 kGy have been studied by Ramlee et al. (2015). The addition of 6.0 phr TiO₂ in the PVC/ENR (50/50) blend is smoother and characterized by a continuous phase and the blend phase was found to be decreased with finer morphology. For the sample of PVC/ENR (70/30) blend at 150 kGy shows the fracture paths are continuous and deeply penetrates into the material indicated that the failure is essentially brittle. Furthermore, the SEM micrographs for the PVC/ENR/CNT nanocomposites irradiated at 200 kGy via solution blending showed smoother than prepared via melting blending. This indicated that the CNTs prepared via melt blending more effective than solution blending as the propagation of microcracks deflect into a tortuous path in the nanocomposites. Voids that are easy to detached with agglomerated particles from the matrix were not detected imply

that the interaction between CNTs particles and PVC/ENR matrix increased and dispersion enhanced upon EB-irradiation (Ratnam et al., 2015).

FTIR analysis has been carried out to study on the irradiation dosages influence on PVC/ENR blends with the Irganox 1010 immediately after irradiation and after 1-day storage at room temperature. The spectra shows different indicated that the occurrence of radiolysis in Irganox 1010 at 60 kGy and the post-irradiation reactions in the blend could induced by the radiolytic products of Irganox 1010 upon irradiation. The epoxy peak at 872 cm^{-1} and the unsaturated ester band at 1252 cm^{-1} disappear followed by new saturated ester band appeared at 1183 cm^{-1} were observed at 60 kGy of the irradiated sample after 1-day storage. This suggests that the saturated ester cross-link formed through the epoxy group from ENR reacted with the unsaturated ester group from TMPTA by ring opening mechanism of ENR. Such changes were absent at 70 kGy indicated that during radiation has consumed the radiolytic products of the phenols (Ratnam and Zaman, 1999). The effect of irradiation at 200 kGy on the fingerprint region of the FTIR spectra for the 50/50 PVC/ENR blend at 0 and 0.5 phr Irganox 1010 have been studied by Ratnam et al. (2001). Irganox 1010 contains ester linkages and remarkable appeared at 1720 cm^{-1} which represented C=O of the conjugated ester. The remarkable reduction in peaks represents the Irganox 1010 was consumed upon irradiation. The radiolytic degradation of PVC reduced with addition of Irganox 1010 due to the absorption at 1630 cm^{-1} for the blend without Irganox 1010 was higher than the blend with 0.5 phr Irganox 1010. The presence of the epoxy characteristic peak at 872.87 cm^{-1} and the absence of the tetrahydrofuran

(THF) band at 1070.78 cm^{-1} in the FTIR spectrum indicates that the ring opening side chain reaction of ENR prevent by the presence of TMPTA and give rise to unfavorable products formed such as THF when irradiated the PVC/ENR blends. The C-O-C group at band around 1100 cm^{-1} implies that TMPTA enhances cross-linking between PVC and ENR (Ratnam and Zaman, 1999).

Pre-irradiation of ENR 50 shows slightly increase with consistent in gel fraction for the 50/50 PVC/ENR blend observed by Ratnam et al. (2006). With the blending temperature increased to above $150\text{ }^{\circ}\text{C}$ would lower the gel fraction of the blends. The gel fraction beyond 100 kGy for blend mixed at $180\text{ }^{\circ}\text{C}$ has reduced due to the occurrence of radiation-induced degradation (Ratnam et al., 2001). Higher TBLS content could reduce the gel fraction at all irradiation doses. The PVC-based formulations with the heat stabilizer added in such as dioctyl tin oxide has decreased the gel amount (Ratnam, 2002). The gel content with the addition of TiO_2 nanofillers loading in the PVC/ENR blends increased with higher irradiation dose. The highest gel content was obtained at 200 kGy for the blends indicated that the irradiation-induced the formation of cross-linking. However, the increment of gel content is less remarkable (Ramlee et al., 2014). Moreover, the gel fraction of PVC/ENR blends significantly increased with the addition of CNTs due to CNTs participates in the composites for the radiation-induced cross-linking (Ratnam et al., 2015). The addition of TPGDA in the PVC/ENR/OPEFB composites could give higher gel amount upon irradiation compared to without TPGDA because acrylates are widely use as reactive additive to forms cross-link

bridges via radiation-induced free radical mechanism (Ratnam et al., 2007). Thus, the incorporation of cross-linking agent has increased the gel amount upon irradiation. The irradiation dose that required achieving the 70 % of gel fraction followed in order: TMPTA<HDDA<EHA (Ratnam and Zaman, 1999). The higher of TMPTA level will increase the cross-linking efficiency as shown in Figure 2.3. However, further increase 40 kGy doses and above have less effect. The increasing rate was relatively high with the addition of TMPTA up to 3.0 phr and the increase was marginal beyond 3.0 phr TMPTA. This could be attributed to the formation of 3-dimensional network structure has reduced chain mobility upon irradiation (Ratnam et al., 2001). Higher gel content obtained with the presence of antioxidants in the blends due to the free radicals deactivated by the irradiation results in chain scission (Ratnam and Zaman, 1999). However, higher level of Irganox 1010 could decrease the gel content in the blends imply the irradiation-induced cross-linking inhibits with the addition of Irganox 1010 (Ratnam et al., 2001).

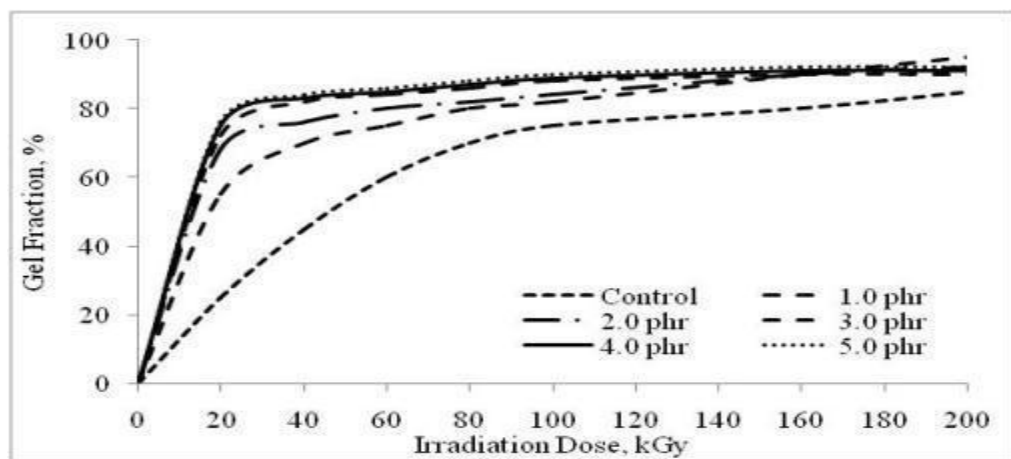


Figure 2.3: The Effect of Different Composition of TMPTA on the Gel Fraction of the PVC/ENR Blend at Various Irradiation Doses (Ratnam et al., 2001).

2.7 Natural Rubber – Ethylene Vinyl Acetate (EVA) Blend

Zurina et al. (2006) have studied the EB-irradiation influence on the mechanical properties of ENR-50/EVA (50/50) blend. Increase in radiation dose will give higher tensile strength and modulus at 200 % strain (M200) but lower the elongation at break. As expected, increase in cross-link density with higher radiation dose enhances the blend's stiffness. The tensile strength and modulus of NR/EVA (60/40) blend using azocarbonamides as the chemical blowing agents are proportional to the irradiation dose (Ghazali et al., 1999). The radiation-induced cross-linking has significantly enhanced the mechanical properties of the NR/EVA (50/50) blend with the addition of TMPTA with the tensile strength and modulus at 100 % elongation (M100) increased but reduction in elongation at break. The hardness found to exhibit same behavior with tensile strength (Ratnam and Abdullah, 2006). The presence of HVA-2 in the NR/EVA (50/50) blend has accelerated the radiation-induced cross-linking in the blend. Furthermore, the tensile strength of the blend increase sharply up to 60 kGy then reduced with further radiation dose owing to the excessive of cross-linking in the blend beyond 60 kGy (Zurina et al., 2008). Many kinds of filler or nanofiller enhanced with polymers such as organoclay and carbon nanotubes. Yatim et al. (2012) have investigated the use of CNTs as nanofiller in NR/EVA (50/50) blend. The tensile strength and M100 have increased almost double compared to the un-irradiated nanocomposites up to 150 kGy and then decrease. Elongation at break reduced with radiation dose increase due to the mobility of polymer chain restricted. The hardness exhibits similar trend with tensile strength and M100 due to the radiation-induced cross-

linking increased in nanocomposites. Different radiation dose influence on the mechanical properties of EVA/ENR-50/Halloysite nanotube (HNT) nanocomposites with cross-linking agent (TMPTA) has investigated by Rudin et al. (2014). Co-existence of HNTs and TMPTA can effectively enhance the properties of nanocomposites. The tensile strength has reduced with higher radiation dose which above the 150 kGy doses due to embrittlement caused by excessive cross-linking in the blend. Moreover, the elongation at break of blend shows increment at lower irradiation dose (50 kGy) owing to the HNTs particles which are capable to interrupting the intermolecular attraction of matrix segment followed by the ENR-50 backbone chains was able to gained additional segmental mobility. Munusamy et al. (2009) have studied the EB-irradiation influence on the mechanical properties of EVA/NR/organoclay with the various composition of organoclay (OMMT). An enhancement of tensile strength and M100 was observed with proportional to higher irradiation dose. The tensile strength was improved to an optimum value with the increasing up to 4.0 phr organoclay loading due to agglomerated are formed at high organoclay loading. Elongation at break increase up to optimum level with 100 kGy then decreased due to radiation-induced cross-linking improved the interaction between EVA and NR phases. 2.0 phr organoclay loading has the optimum value of elongation at break at all irradiation doses. The tensile strength of NR/EVA (40/60) containing dodecyl ammonium montmorillonite (DDA-MMT), dimethyl dihydrogenated tallow quarternary ammonium montmorillonite (C20A) and sodium montmorillonite (Na-MMT) irradiated at 150 kGy decreased with the clay concentration increased due to the nanoparticles cluster in the microstructure and nano to micro-size voids occur

occasionally. The increase of DDA-MMT and Na-MMT concentration has slightly lowered the elongation at break of the composites. In the meanwhile, the elongation at break of NR/EVA/C20A remains unchanged up to 3.0 phr C20A then further increased with up to 10.0 phr C20A content owing to the reduction in radiation-induced cross-linking network formation. The M300 of DDA-MMT and C20A nanocomposites increased with higher clay concentration but the Na-MMT nanocomposites remain unchanged with higher clay content (Sharif et al., 2008). The tensile properties of the irradiated NR/EVA/organoclay with TMPTA are further improved compared to irradiated blend without TMPTA. For the nanocomposites without TMPTA can achieve the optimum tensile strength at 4.0 phr organoclay loading with 200 kGy while for the nanocomposites with TMPTA only needed 4.0 phr organoclay loading with 150 kGy to be achieved. Furthermore, the tensile strength for nanocomposites with TMPTA was found to be decreased at beyond 200 kGy doses. Elongation at break was increased up to 100 kGy at the beginning then reduced for nanocomposites with and without TMPTA (Ismail et al., 2010).

For the surface morphologies, Zurina et al. (2006) have analyzed the fractured surface of non-irradiated and irradiated ENR-50/EVA blends at various radiation dosages. The transformation of co-continuous morphology in non-irradiated blends leads to the dispersed ENR-50 phase in the continuous EVA phase after EB-irradiation. A smaller domain size has produced at higher irradiation dose up to 100 kGy give rise to the better compatibility of the blend. On the other hand, the existence of co-continuous morphology at 40, 60, and

80 kGy for an irradiated blend with HVA-2 indicated that HVA-2 does not promote the interaction between both phases in the blend. One phase morphology exists in the blends at 100 kGy indicated that improved compatibility in ENR-50/EVA blends (Zurina et al., 2008). The irradiated EVA/NR/organoclay nanocomposites have formed the fibril-like structures. A higher resistance towards failure has shown by the stretched and elongated matrix. The elongated fibril-like structures formation is more significant at 200 kGy. Furthermore, blends with 4.0 phr organoclay loading show a ductile fracture surface with finer and longer fibrillar structure at all irradiation dosages. However, the fibrillar structures are thicker and shorter at 8.0 phr organoclay loading. This difference indicating more energy can be absorbed and further deformed the cross-linked before failure thus higher strength at 4.0 phr organoclay loading is exhibited (Munusamy et al., 2009). The phase morphology of NR/EVA nanocomposites with the influence of TMPTA has studied by Munusamy et al. (2013). A phase separation was observed at 50 kGy doses. No phase separation has shown the irradiation dose increasing up to 150 kGy due to cross-link network formation increase in both phases and the interpenetrating network formed. The XRD pattern for NR/EVA/OMMT nanocomposites with 2.0 phr and 8.0 phr organoclay loading are conducted by Munusamy et al. (2009). The diffraction peaks for the irradiated nanocomposites has slightly move to lower angles compared to un-irradiated nanocomposites as the further increasing in the interlayer spacing between the individual silicate layers resulted in the formation of polar groups by EB-irradiation. There is a second diffraction peak showed by 8.0 phr organoclay loading in the nanocomposites indicated that the polymer chains of the blend

did not intercalate into the gallery space of the organoclay's silicate layers during the melt blending resulted in agglomeration of organoclay. Addition of TMPTA in the nanocomposites also has the same behavior as above (Munusamy et al., 2009 and Ismail et al., 2010). A weak peak of NR/EVA/5DDA-MMT was observed indicated that the disturbance on the stack silicate layers of the clay and partially exfoliated the structure of the nanocomposites. The diffraction peak of the DDA-MMT and C20A nanocomposites are slightly shifted to the higher 2θ angle at 150 kGy indicated that the interlayer distance is shrinking due to the cross-linking networks formation (Sharif et al., 2008).

The gel fraction of ENR-50/EVA blends appeared to be sharply increased as the irradiation dose increased from 20 to 60 kGy and then slightly higher with irradiation dose further increased from 60 to 100 kGy (Zurina et al., 2006). The incorporation of Surlyn ionomer and TMPTA in the blends had enhanced the gel content because of these additives were accelerated the radiation-induced cross-linking in the blends. On the contrary, Surlyn ionomer has relatively low extent of cross-linking compared to the TMPTA (Ratnam and Abdullah, 2006). Adding with HVA-2 in the irradiated ENR-50/EVA blends also can enhance the cross-linking density as the gel content is higher than without HVA-2 blends (Zurina et al., 2008). The gel content of blend had improved by adding the HNTS and TMPTA in the blend. In the meanwhile, there is a sharp increase in the gel content of EVA/ENR-50/HNTS with the presence of TMPTA with higher irradiation dose then slight increment with further increased the irradiation dose because TMPTA has more reactive site to

react with EVA and ENR-50 for cross-linking (Rudin et al., 2014). A gradual increase in gel fraction was found in the ENR/EVA/CNTs nanocomposites with increasing of irradiation dosages from 50 to 200 kGy (Yatim et al., 2012). It was remarkably reduced with higher organoclay loading at 50, 100 and 150 kGy doses because of the organoclay could scavenged the NR and EVA radicals thus hindered the radical-radical interaction and reduced the cross-linked network. Furthermore, the sites for polymeric matrix in cross-linking were blocked due to the OMMT nanoparticles exfoliated and intercalated. However, the yielding of gel fraction was slightly affected at 200 kGy by organoclay loading due to a large number of free radicals will be formed to overcome the scavenging and blocking effect of organoclay (Munusamy et al., 2009 and Munusamy et al., 2013). However, the irradiated nanocomposites incorporated with TMPTA can enhance the gel fraction yield as TMPTA is well known in reactive additive which the irradiation-induced free radical mechanism formed cross-link bridges and thus improved the gelation of nanocomposites (Ismail et al., 2010). The gel content of NR/EVA with 5.0 phr of DDA-MMT and C20A increased rapidly with higher irradiation dose up to 150 kGy. In addition, the gel content increased marginally with further increase in irradiation dose. Macromolecular chemical bonds are predominance between the cross-linked macromolecular chains at higher irradiation dose and slowed down the gelation rate. The gel content of NR/EVA/Na-MMT and NR/EVA/DDA-MMT at 150 kGy doses does not significantly change with the presence of 1.0 to 10.0 phr DDA-MMT and Na-MMT. As per contra, the gel content of NR/EVA/C20A nanocomposites continuously decreased with higher C20A concentration (Sharif et al., 2008).

2.8 Natural Rubber – Ethylene Propylene Diene Monomer (EPDM) Blend

In the 1960s, DuPont has developed the Ethylene Propylene Diene Monomer (EPDM) which is a low unsaturated polyolefin. It has attracted much attention compared to other synthetic rubbers due to resistance to heat, aging and oxidation. This resistance results from the presence of double bonds in the side chain in its unsaturated hydrocarbon backbone. The swelling behavior for the NR/R-EPDM blends was investigated by Nabil et al. (2014). The swelling resistance increase with higher irradiation dose indicated that cross-link density increase in the blends. They also have examined the tensile strength and elongation at break of the NR/R-EPDM blends under EB-irradiation. The optimum tensile strength was achieved at 50 kGy doses and then reduced slightly with further irradiation dose. Cross-linking increased with higher irradiation dose result in tensile strength improved. In contrast, more cross-links formed in the sites of blends have restrained the structural rearrangement of the chains during elongation and the mobility of the chains and elongation reduce. In addition, the elongation at break of the irradiated blends was reducing continuously due to the tie-chain molecules break down and entanglements thus the ductility of the polymer reduced. Modulus at 100 % (M100), Modulus at 300 % (M300) and hardness (Shore A) improved with higher irradiation dose due to the irradiation-induced cross-linking occurs. The tensile strength and elongation at break of the blends upon thermal aging were observed reduced compared with un-aged blends due to the polymer oxidation resulted in chain cleavage and lead to a drop in molecular weight or cross-

linking. Generally, a radical termination in which the hydrogen atoms abstract from an allylic position on the rubber molecule occurred after thermal aging of the rubber. However, EB-irradiation already took place in the process and the radical termination in the bulk polymer does no longer exist. Hence, the modulus and tensile strength of the blends was significantly reduced compared to un-aged blends upon thermal aging. However, the hardness result for aged blends is inversely proportional to the tensile strength by exhibiting higher values than the un-aged blends after EB-irradiation because EB-irradiation has no effect on static testing (Nabil and Ismail, 2014).

Nabil et al. (2014) have analyzed the surface morphologies of the NR/R-EPDM blends by using SEM as depicted in Figure 2.4. Figure 2.4 (A) shows surface roughness and tearing lines exist in the blends which mean need more energy to break the sample. The irradiated 50 kGy blend show rougher surfaces and the amount of tear lines were more pronounced and visible as shown in Figure 2.4 (B). The sample has more resistance to crack propagation because had an altered crack path resulted in improved mechanical properties. Moreover, the micro-fractured surface of the irradiated blends was found to be smoother and containing of smaller cracking area when beyond 50 kGy as shown in Figure 2.4 (C) and 2.4 (D). FTIR spectra of the NR/EPDM blends upon EB-irradiation have conducted by Nabil et al. (2014). The bands of C=C groups (1613.48 cm^{-1}) and C=O groups (1727.83 cm^{-1}) increases with higher irradiation dose. There is slight broader C=C peak as well as an increased intensity of the C=O peak in the irradiated blends compare to the un-irradiated blends indicated that formation of irradiation-induced cross-linking. The

coexistence of C=O and O=H groups suggests that the formation of peroxide radicals on the polymer backbone which induced by the presence of oxygen has subsequently converted the adjacent ethylene comonomer unit to hydroperoxides by abstracting the hydrogen.

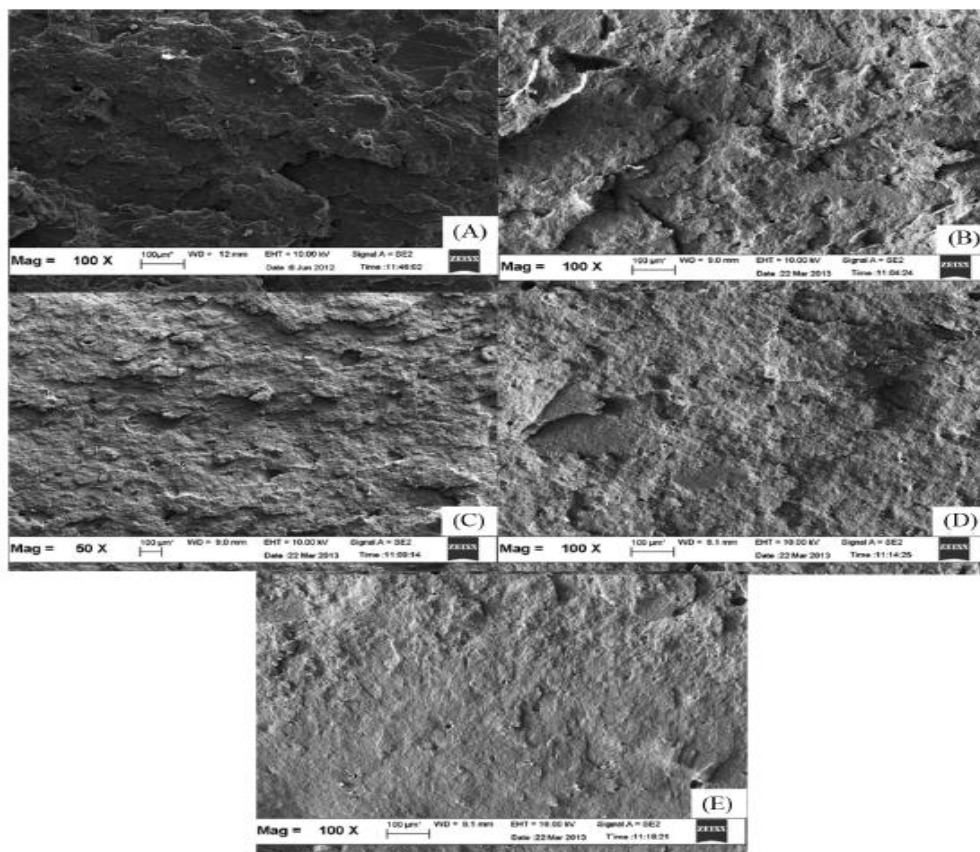


Figure 2.4: SEM Micrographs of Tensile Fractured Surfaces of Control (A) and Irradiated NR/R-EPDM blends at 50 kGy (B), 100 kGy (C), 150 kGy (D) and 200 kGy (E) (Nabil et al., 2014).

2.9 Natural Rubber – Polyvinylalcohol (PVA) Blend

El-Nahas and Magida (2012) have prepared multilayer films by including the polyvinylalcohol (PVA) as a central layer (hydrophilic) and NR as external layers which resistant to water (hydrophobic) in order to protect the inner layer from attack by water when exposure continuously. They have studied the behaviours of tensile strength and elongation at break in the dry and wet condition. As expected, PVA is mainly responsible for improving the tensile strength of multilayer unit in dry condition owing to it exhibits higher tensile properties than NR or NR-PVA blend. In contrast, the behavior becomes different in wet condition due to the water content affected in PVA as well as plasticization of free water result in tensile strength reduced. In the meanwhile, the elongation at break of multilayer film at wet condition gives higher values compared to the dry condition owing to the swelling properties of PVA and the blend. In addition, the mechanical properties of PVA films improved by radiation cross-linking. Other than that, they also have analyzed the fracture surfaces of the NR/PVA multilayer film. The un-irradiated sample with two layers of NR/PVA completely delaminated because of the interfacial adhesion between two layers is extremely poor while the low ratio of adhesion between two layers was recorded at 25 kGy doses. Besides that, the samples of three layers NR/blend/PVA was found to be partially delaminated which have better adhesion. Furthermore, there is no delamination at 25 kGy gives higher interfacial adhesion result in high peel strength. El-Nahas et al. (2010) have analyzed the morphological of PVA as a dry polymer which obtained from radiation, chemical and freeze-thaw gelation. The irradiated PVA dry gel

shows the molecular chains are compacted and oriented each other's in parallel due to the occurrence of irradiation-induced cross-linking while the un-irradiated PVA surface was observed to be smooth and no strains or pores appeared. A cross-linking has apparently appeared for the freeze-thaw process after irradiation where the rods has overlapping in fractured surface and became rougher and more rigid giving insoluble gel in boiled water while un-irradiated for freeze-thaw process was appeared to be a parallel un-cross-linked rods shape due to the freeze-thaw gelation with the fracture was observed to be slightly rough and shallow ridges. The SEM micrographs for the chemical gelation of PVA was observed as alternated muscle shape arranged in succession and in pseudo-homogenous structure with can easily modified the mold dimension by a sensitive hand pressing while there is a large coiled muscle shape due to the irradiation which gave a stable shape in dimension and a rubber-gel phase was observed in chemical process with EB-irradiation.

2.10 Natural Rubber – Butadiene Rubber (BR) Blend

Shen et al. (2013) have investigated the mechanical properties of NR/styrene-butadiene rubber (SBR) (70/30) vulcanizates upon irradiation. The results were found that the tensile strength and elongation at break decrease with higher irradiation dose while the hardness and modulus at 100 % elongation increase with higher irradiation dose due to the carbon black particles are irradiated by EB-irradiation and formed the defects on the

particles surface in order to enhance the interaction between the rubber and carbon black. At a low dosage of irradiation, the tensile strength of the NR/SBR blend increase with SBR content up to 15 kGy and start decrease beyond 15 kGy doses. Elongation at break decreased with higher SBR content in the blend due to the incorporation of rigid SBR chains in the copolymer matrix (Chaudhari et al., 2005). At a high dosage of irradiation, the tensile strength and hardness was observed to be increase while the elongation at break decreases with higher irradiation dose. NR/SBR (30/70) blend has the highest tensile strength at 400 kGy before and after aging due to the higher cross-link density of the blend. The elongation at break decreases while the hardness increases with higher irradiation dose due to a cross-linking degree increase and the network structure formed (Manshaie et al., 2011). The vulcanization dose at 100 kGy decreased with 4 parts of the ethoxylated pentaerythritol tetraacrylate (EPTA) added in the NR-acrylonitrile-butadiene rubber (NBR) (50/50 blend). The optimum tensile strength was increased from 11.5 MPa (0 part EPTA) to 15.5 MPa (4 parts EPTA). In contrast, the tensile strength for the blend decreased at higher dose due to the excessive of cross-links is generated (Chowdhury, 2007).

The IR-horizontal attenuated total reflection (HATR) spectra have taken with NR-NBR blend with containing 4 parts of EPTA. The 1625 cm^{-1} (C=C stretching) / 2223 cm^{-1} (-CN stretching) has sharply decreased while 1450 cm^{-1} (-CH₂-) / 2223 cm^{-1} has sharply increased up to 100 kGy due to the depletion of C=C bonds during grafting and cross-link formation by involving the polyfunctional monomer (PFM) together with partly self-cross-link of the

polymer during radiation. The absorbance values were marginally changed above 100 kGy. The gel content for NR/SBR blend increased with higher radiation dose due to the three-dimensional network structure formed. However, the gel content has marginally increased at relatively higher doses due to less number of sites available for cross-linking. The process of cross-linking predominates over the degradation as the SBR content increase. The effect of adding SBR was similar to the addition of sensitizer in the NR (Manshaie, et al., 2011). The swelling ratio for NR/NBR (50/50) with the addition of EPTA decrease while the gel content increases with higher radiation dose because of the cross-linking promotion by the multifunctional monomer resulted in higher cross-link density (Chowdhury, 2007).

2.11 Natural Rubber – Acrylate Blend

Monofunctional and polyfunctional acrylates act as sensitizer for the radiation vulcanization of natural rubber latex with γ -rays had been investigated by many researchers (Cockbain et al., 1959, Hossain and Chowdhury, 2010, Makuuchi and Hagiwara, 1984, Haque et al., 1996, Peng et al., 1993, Sabharwal et al., 1998 and Rahman et al., 2015). EB-irradiation application for irradiated the NR latex is necessary as the price of the Cobalt-60 source more likely to increase. The cost of irradiation by electron accelerators is expected to be much cheaper than the gamma radiation (Chirinos et al., 2003). Tensile strength and Young's modulus of the 3.0 phr butyl acrylate blend in NR latex was found to be increased while the

elongation at break decreased with higher irradiation dose (Mitra et al., 2008 and Mitra et al., 2010). Besides that, Ratnam et al. (1999) have observed that there are no significant changes in mechanical properties of the 80 % 2-hydroxyethyl methacrylate (HEMA)/20 % n-butyl acrylate (n-BA) coated NR film at various irradiation doses compared to uncoated film. Manaila et al. (2014) have studied the polyfunctional monomers (PFMs) which are triallylcyanurate (TAC), triallysicyanurate (TAIC), trimethylolpropane trimethacrylate (TMPTMA), ethylene glycol dimethacrylate (EDMA) and zinc diacrylate (ZDA) influence on the mechanical properties of natural rubber cross-linked by EB-irradiation. The hardness of PFMs increased slowly with higher radiation dose by following the order in TMPTMA > ZDA > EDMA > TAC > TAIC due to the increasing in cross-link density. TMPT has higher solubility and lower molecular weight in NR than other PFMs. The influence of PFMs in tensile strength for the blends has followed the order as TMPTMA > EDMA > ZDA > TAIC > TAC as shown in Figure 2.5. The optimum value of TMPTMA used as a PFM is 8.3 N/mm² with 100 kGy doses. The elongation at break reduces with radiation dose increase up to 100 kGy due to the network structure for the cross-linked rubbers become inflexible and tighter so the molecular movements are restricted. Stelescu and Manaila (2007) have concluded that the NR blend containing 6.0 phr and 9.0 phr of TMPTMA irradiated at 200 kGy exhibit better mechanical properties than cured by peroxide at 160°C. Furthermore, Jayasuriya et al. (2001) have compared the effect of mechanical properties on different accelerators which are TMPTMA, n-BA, trimethylolpropane triacrylate (TMPTA), phenoxy ethyl acrylate (PEA) and phenoxy polyethylene glycol acrylate (PPEGA) in the NR

latex undergoes EB-irradiation. TMPTMA and PEA have the higher tensile strength compared to PEA and PPEGA with EB-irradiation of NR latex at 5.0 phr concentration of addition. PEA has comparatively higher tensile properties than TMPTMA and imparts around similar properties compared to n-BA. On the other hand, Xu et al. (1997) have investigated the effect of diethyleneglycol dimethacrylate (2G), TMPTA and tetramethylolmethane tetraacrylate (A-TMMT) with EB-irradiation in the cis-1, 4-polyisoprene. It was found that 2G is the best PFMs for EB-irradiation curing among others. Ratnam et al. (2000) have studied the mechanical properties influence on the enhancement of ENR with several additives such as acrylic cross-linking agent (TMPTA), phenolic antioxidant (Irganox 1010) and lead stabilizer (TBLS). Elongation at break reduced with higher irradiation dose because the rubber becomes increasingly brittle and reduces the segmental mobility of the rubber chains. Modulus exhibits similar trend as tensile strength. Hardness for all samples exhibited similar trend as tensile strength at lower 100 doses. TMPTA rendered highest tensile strength followed by stabilizing additives. Presence of Irganox 1010 and TBLS in the ENR exhibit lower tensile strength compared to without additive of ENR because of more chain ends present in the rubber network. The drop in M100, stress at break and elongation at break increase with the addition of Irganox 1010 and TBLS imply that the plasticizing effect by these additives impart to the rubber (Ratnam et al., 2001). Manaila et al. (2008) have reported that by additional use of PFM and microwave energy with EB-irradiation could be obtained good radiation vulcanization degrees at lower doses.

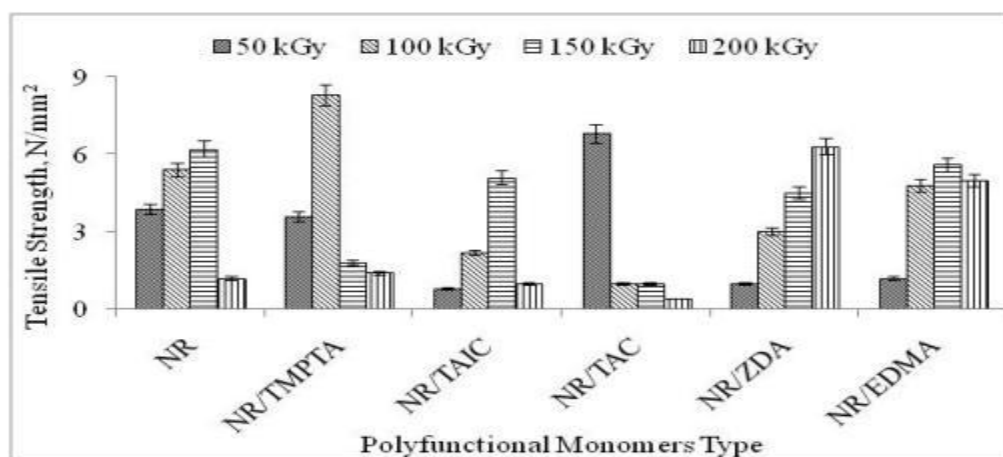


Figure 2.5: Tensile Strength versus Polyfunctional Monomers Type under Various EB-Irradiation (Manaila et al., 2014).

Mitra et al. (2010) have investigated the SEM micrographs of the NR containing butyl acrylate at 20 kGy doses cross-linked gel in the NR latex. The surface roughness on the 2.0 phr and 4.0 phr of cross-linked gel in the NR latex exhibited much lower than raw NR latex. However, 8.0 phr and 16.0 phr of cross-linked gel in the NR latex show a much smoother surface. SEM micrographs of the 80 % HEMA/20 % n-BA coated NR film surface roughness increase with higher irradiation dose (Ratnam et al., 1999). For the FTIR of NR/PFs mixture, absorption bands were observed to be higher than mixture without PFMs due to the double bonds present in the PFMs structure. A reduction in the intensities of absorption bands and move to the same extent ($3035.44 - 3038.35 \text{ cm}^{-1}$) due to the double bonds consume in NR and PFMs molecules undergo irradiation up to 50 - 200 kGy. There are two peaks at 1560 and 1326 cm^{-1} appear in NR/TAC cross-linking after EB-irradiation. The triazine ring with the benzene structure from TAC appears at the intensity of 1560 cm^{-1} and C-O stretching vibrations from TAC appear at the absorption of 1326 cm^{-1} . The intensities increase with higher irradiation dose (Manaila et al.,

2014). The MMA absorption bands for C=O stretching and –C-O- moiety of the ester functional group in the TMPTMA and EDMA had disappeared after irradiated at 50 and 200 kGy for the NR/PFMs mixture (Manaila et al., 2014, Stelescu and Manaila, 2007). The 3.0 phr of butyl acrylate-sensitized latex showed marginally higher in gel content at any radiation doses compared to the unmodified latex indicated that the presence of butyl acrylate enhances the cross-linking. The gel content increased marginally at relatively higher doses due to less number of sites available for cross-linking (Mitra et al., 2008). TMPTA exists in the compound could be induced at a lower dose because it required to achieve 70 % gel content with a lower dose. The addition of Irganox 1010 and TBLS inhibits irradiation-induced cross-linking in NR as both additives require a higher dose to achieve 70 % gel content (Ratnam et al., 2000 and Ratnam et al., 2001). However, the gel fraction of TBLS in NR compound is higher than the gel fraction of pure NR with the irradiation dosages above 100 kGy due to the consumption of stabilizer result in the oxidation chemistry ensuing during irradiation and the radical scavenging ability reduced at higher doses (Ratnam et al., 2001). The addition of TMPTMA has significantly increased the cross-link density when compared to the pure NR and other PFMs like EDMA, TAC, TAIC and ZDA. Thus, the increase in gel content and cross-link density of samples with higher irradiation dose due to the three-dimensional network structure formed (Manaila et al., 2014). A slowly increasing for NR/TMPTMA mixture when irradiation dose has increased from 100 kGy to 250 kgy. Even at a low dose of 100 kGy, the gel fraction for NR and NR/TMTPMA are 76.60 % and 87.57 % respectively (Jayasuriya et al., 2001).

2.12 Natural Rubber – Rubber Waste Blend

The addition of reclaimed rubber powder (RRP) had lowered the tensile strength of the NR/RRP blend at any irradiation dose due to the reclaimed rubber has lower molecular weight. The elongation at break of NR/RRP blend decreased with higher RRP loading due to reinforcing filler exists in the RRP has inhibited the molecular orientation. Irradiation dose increased with a lower elongation at break due to the effectiveness increasing in cross-linking at higher irradiation dose which unable to stretch upon deformation. However, the glass fiber (GF) added in the NR/RRP (50/50) blend could increase the tensile strength with higher irradiation dose due to the cross-linking formed in the rubber chains between the molecules by EB-irradiation. The elongation at break of NR/RRP/GF blend decreased with higher glass fiber content which the orientation of molecular chains is restricted. The hardness of NR/RRP blend exhibited similar trend with a tensile strength of NR/RRP/GF blend. The hardness for irradiated composites was increase at 30 kGy doses then started to decrease at 50 kGy doses owing to the high degradation level (Hassan et al., 2007). Markovic et al. (2015) have investigated the mechanical properties of chlorosulfonated polyethylene rubber (CSM)/chlorinated natural rubber (CNR)/waste rubber powder (WRP) blends undergo irradiation. The tensile strength of 25 phr CNR content was found to be similar with the pure CSM even after irradiation indicated that CSM plays an important role in tensile properties of the blend up to 25 phr CNR content. Tensile strength, modulus and hardness for the blends were significantly decreased with higher CNR content after 200 kGy doses.

There is a rough surface for unirradiated RRP with many holes or loose RRP but irradiated RRP exhibits smoother surface due to the occurrence of cross-linking between the components of RRP. Besides, the tensile fracture surface of the un-irradiated NR/RRP blends exhibits many tear lines and many holes or loose RRP present on the failure surface due to weak interaction between RRP and NR matrix. However, the irradiated NR/RRP (70/30) blend exhibits smoother fracture plane. The morphology of the surface on the un-irradiated NR/RRP/MA blend exhibits with many vacuoles and un-dispersed agglomerates with the smooth surface but unable to found in the irradiated blend. It can be seen that numerous voids associated with the debonding and pullout of fibers in the un-irradiated GF/NR/RRP/MA (50/50/50/5) blend but the irradiated blend has lower number voids associated with pullout of particles because the development of strong bonding between irradiated matrix and GF (Hassan et al., 2007). The SEM of CSM/CNR/WRP (75/25/50) reveals two-phase blend morphology while the CSM is continuous phase in the blends with CNR (Markovic et al., 2015).

2.13 Natural Rubber – Carbon Blend

Khalid et al. (2010) have studied the radiation dose and carbon nanotubes content influence on the mechanical properties natural rubber nanocomposites. Addition of CNT in the natural rubber enhanced tensile strength due to the surface area of the CNT highly contact with rubber molecules. Thus, the stress transfer between the rubber matrix and CNT

particles highly take place. The tensile strength of the NR/CNT nanocomposites increased with higher irradiation dose owing to the radiation-induced cross-linking in nanocomposites. However, the increasing trend became less remarkable at above 150 kGy due to the occurrence of degradation by radiation at higher doses. Oxidation cross-linking and chain scission are prevailing in the reactions at higher doses. The variation rate of M100 respect to irradiation dose had increased noticeably with the CNT loading level of 4.0 phr or more due to not only different interphase linking and radiation-induced cross-linking occurred but also the CNT nanofiller acts as a separate phase. Moreover, the elongation at break decreased with higher CNT loading due to the filler particles has stiffening the matrix. The hardness of the NR/CNT nanocomposites exhibits the similar trend with tensile strength and modulus. Atieh et al. (2010) have reported that the tensile strength of irradiated NR/CNT nanocomposites with 7.0 wt% CNTs is almost 1.8 times that of irradiated natural rubber. Elongation at break is expected to be a drop with higher irradiation doses. Wu et al. (2015) have investigated the EB-irradiation influence on the mechanical properties of NR filled with irradiated carbon black (CB). The tensile strength, M100, M300 and elongation at break increase firstly then decrease as the higher irradiation doses. Improvement of mechanical properties at low irradiation dosages is attributed to the oxygen-containing functional groups increased on the surface of the irradiated CBs and lead to the interaction between the CBs and rubber molecular chains further increased. However, the tensile strength, M100 and elongation at break decrease at higher than 500 kGy doses due to the CB particle size increase and particle size uniformity lower.

The morphologies of the irradiated CBs with bound rubber are studied by Wu et al. (2015) as shown in Figure 2.6. It can be seen that blurry edges around the CBs when the rubber molecular chains surrounded the CBs. The edges around the CBs irradiated at 600 kGy are much blurrier than un-irradiated CBs due to the bound rubber amount around the irradiated CBs are higher than those of un-irradiated CBs. Additionally, there are fewer holes between the irradiated CBs than un-irradiated CBs because of the stronger interaction between irradiated CBs with rubber molecules and bound rubber more than un-irradiated CBs. The gel fraction of the NR/CNTs rapidly increased with irradiation dose increasing up to 150 kGy attributed to the free radical mechanism could formed the radiation-induced cross-links. Thus, more cross-linking occurred by generation of free radicals in the polymer matrix as the irradiation dose increased. However, the gelation rate slowed down at above 150 kGy doses because the macromolecular chemical bonds are predominantly cross-linked between macromolecular networks at this stage. In the meanwhile, the gel fraction increased with higher loading level of CNT in the NR/CNT nanocomposite together with increasing in irradiation dose attributed to the presence of different grouping types such as carboxylic, phenolic, hydroxylic, aldehydic and ketonic on the CNT surfaces that would participate in physical and chemical bond formation as well as the free radical formation at the interface between the CNT and rubber matrix upon radiation (Khalid et al., 2010).

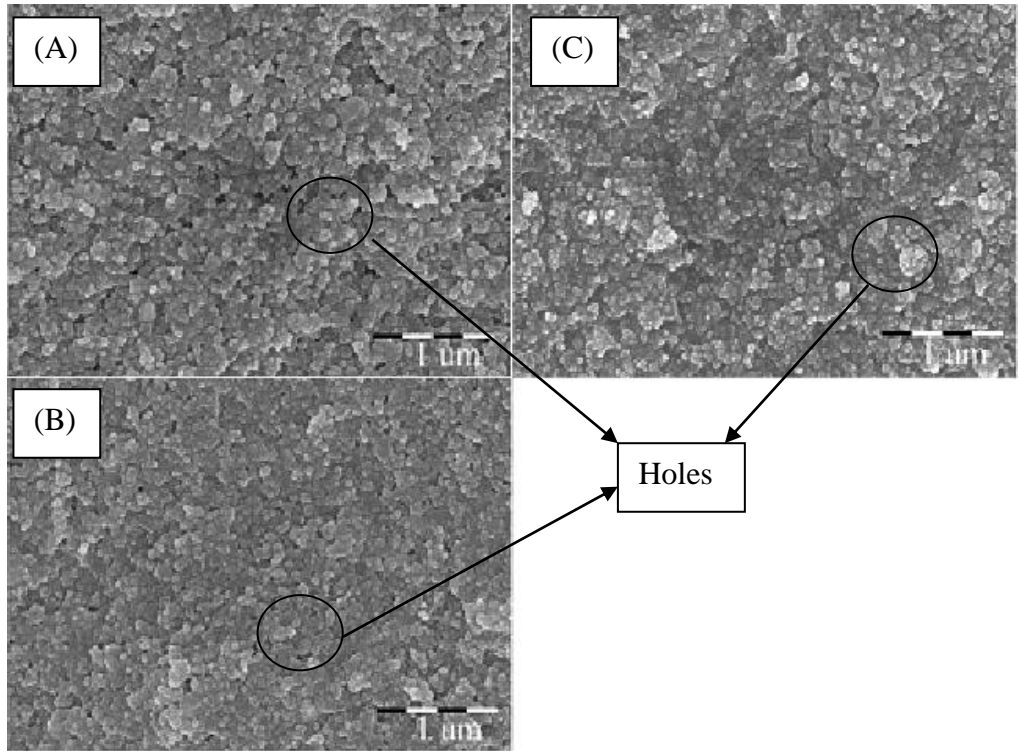


Figure 2.6: SEM Images of CBs Irradiated at (A) 0 kGy (B) 200 kGy (C) 600 kGy (Wu et al., 2015).

2.14 Natural Rubber – Natural Polymer Blend

Senna et al. (2012) have studied the mechanical properties of the NR/modified starch composites after EB-irradiation. The tensile strength of the NR improved by the addition of the 5.0 phr unmodified starch and further improved by using 5.0 phr starch modified with resorcinol-formaldehyde. The tensile strength of the composites increases up to 20.0 phr modified starch. On the contrary, the elongation at break decrease with higher starch content due to rigid starch chains incorporated in the matrix. Furthermore, the composites irradiated by EB-irradiation have decreased their mechanical properties but irradiated natural rubber not to the same extent. The addition of 10.0 phr starch

increased the hardness of un-irradiated natural rubber but the addition of starch up to 20.0 phr lead to further minor increase in hardness. Irradiation especially improves the hardness in the starch-filled samples for NR containing 10.0 phr modified starch. Sharif et al. (2005) have reported that the optimum tensile strength of irradiated NR/organoclay nanocomposites is irradiated at 250 kGy doses. The tensile strength of NR/Na-MMT decreased slightly up to 10.0 phr Na-MMT due to the poor compatibility and adhesion between Na-MMT clay aggregates and NR. Moreover, NR/DDA-MMT and NR/ODA-MMT with around 3.0 phr organoclay content exhibit the optimum tensile strength. The compatibility of the two materials improves by the intercalation of NR into clay silicate layers resulted in increasing of tensile strength. However, the tensile strength starts to decrease at more than 3.0 phr organoclay content and remain constant up to 10.0 phr organoclay content. There is a slight drop with higher concentration of DDA-MMT and ODA-MMT due to the clay aggregated in the matrix leads to a weak point formed in the NR matrix and reduction in elastomer strength. The elongation at breaks is expected to drop since the tensile strength for NR/DDA-MMT and NR/ODA-MMT nanocomposites increased. The M100 of NR/DDA-MMT and NR/ODA-MMT nanocomposites have higher value compared to NR/Na-MMT. The mechanical properties of NR/ODA-MMT are less superior than NR/DDA-MMT. Stelescu et al. (2014) have studied the mechanical properties of NR/hemp composites irradiated by EB-irradiation. The hardness of the composites was found to be increased with higher radiation dose and fiber composition. The optimum hardness obtained at 150 kGy doses and 20.0 phr hemp contents are much higher than without hemp due to the incorporation of

hemp into NR reduce the rubber chains elasticity and leads to rubber vulcanizates become more rigidity. M100 also exhibits the same trend as hardness. The optimum tensile strength of composites obtained at 300 kGy doses and 10.0 phr hemp contents. The elongation at break was observed to be decreased with higher absorbed radiation dose up to 150 kGy then raised back. The hardness of the NR/wood sawdust composites increased with higher radiation dose and wood sawdust content because the plasticity and flexibility of the rubber chains reduced with the wood sawdust incorporated into the NR matrix lead to the higher rigidity of composites. M100, M300 and tensile strength exhibit the similar trend with hardness attributed to the strong interface and close packing arrangement occurred in the composite. Elongation at break has reduced with higher radiation dose and wood sawdust content due to higher density of cross-link (Manaila et al., 2016).

The morphology of the fracture surfaces for NR/starch composites with different content of resorcinol-formaldehyde upon EB-irradiation has conducted by Senna et al. (2012). The surface of resorcinol-formaldehyde modification is very rough with no cavities indicated that the enhancement of interfacial strength. The phase morphology of the blends has significantly changed by irradiation. The roughness of blend increases and exhibit different textures with resorcinol-formaldehyde starch concentration at 20 kGy doses. The surface fracture appeared to be fewer cracks and rougher at 50 kGy doses. The fracture surface of NR/wood sawdust based on 10.0 phr and 20.0 phr of wood sawdust show the voids absent which indicates the interaction between the non-polar matrix and polar fillers is enhanced. Besides that, the presence

of filler particle is not restricted the blend deformation because of the adhesion between matrix and filler is improved. The XRD patterns of NR/Na-MMT, NR/DDA-MMT and NR/ODA-MMT are investigated as depicted in Table 2.2 by Sharif et al. (2005). It showed that the interlayer distances reduced with increasing of organoclay contents. There are several factors affect the extent of intercalation such as the elastomer chains diffuses within the silicate layers, the transportation of polymer processes via the agglomerate size and the nature of the elastomer itself. The interlayer distance of Na-MMT (1.22 nm) slightly expands to 1.25, 1.31, 1.32 and 1.38 nm for the NR that contains 1.0, 3.0, 5.0 and 10.0 phr Na-MMT respectively. As expected, the NR is hardly intercalated into the hydrophilic nature of Na-MMT. Three peaks were appeared at around 1.20 - 1.30, 1.50 - 1.70 and 3.29 - 3.90 nm for all concentration of DDA-MMT. The 1.20 – 1.30 nm peak attributed to the unmodified part of DDA-MMT and the 1.50 – 1.70 nm peak attributed to the silicate layers re-aggregated during the melt mixing process. In the meanwhile, the 3.29 – 3.90 nm peak shows the pronounced intercalation of NR into the hydrophobic silicate layers of DDA-MMT. In the 3.0 phr, 5.0 phr and 10.0 phr ODA-MMT, three peaks were appeared corresponding to basal spacing of 1.25 – 1.31, 1.80 – 1.90 and 3.6 – 4.0 nm. The higher order peak has caused two of them are below the initial basal spacing of ODA-MMT (2.90 nm) indicated that ODA-MMT can intercalated by NR without loss of layer structure. On the other hand, the 3.6 – 4.0 nm peak shows the pronounced intercalation of NR into the hydrophobic silicate layers.

Table 2.2: XRD Analysis of NR/modified MMT Nanocomposites (Sharif et al., 2005).

Organoclay composites/clay content	d ₀₀₁ spacing (nm)				
	0 phr	1 phr	3 phr	5 phr	10 phr
Na-MMT	1.22	-	-	-	-
DDA-MMT	1.73	-	-	-	-
ODA-MMT	2.90	-	-	-	-
NR/Na-MMT	-	1.38	1.32	1.31	1.25
NR/DDA-MMT	-	3.99, 1.74, 1.31	3.60, 1.70, 1.35	3.47, 1.64, 1.35	3.29, 1.50, 1.20
NR/ODA-MMT	-	1.87, 1.31	4.07, 1.94, 1.29	3.69, 1.89, 1.27	3.64, 1.86, 1.25

CHAPTER 3

METHODOLOGY

3.1 Formulation

There were 5 test samples used in this study with varies of devulcanized natural rubber quantity in a constant amount of PP. The amount of PP used 100 phr while devulcanized natural rubber was varied from 0, 5, 10, 15, and 20 phr. Table 3.1 shows the various content of devulcanized natural rubber adding to the fixed amount of PP.

Table 3.1: Various Content of Devulcanized Natural Rubber Adding to the Fixed Amount of PP.

Sample	PP (phr)	Devulcanized Natural Rubber (phr)
1	100	0
2	100	5
3	100	10
4	100	15
5	100	20

3.2 Sample Preparation

The various content of devulcanized natural rubber mix with 100 phr of PP was extruded by using twin screw extruder under 190 °C. The extruded compound cooled by chilled water and then pelletized using pelletizer before pressed it into a sheet form to ease for melting during the hot press. After that, the pelletized PP-DVC compound samples were pressed into sheet form of 3 cm x 15 cm x 15 cm dimension using 25 ton hot molding press at 170 °C. After finish compressed, the samples were cooled to room air temperature for 20 min. The sheet samples were irradiated under electron beam accelerator model NHV EPS-3000 at room temperature with a voltage of 3 MeV from 0 to 200 kGy irradiation dosages. The acceleration energy, beam current and dose rate were 2 MeV, 2 mA and 50 kGy per pass respectively.

3.3 Natural Weathering Test

The natural weathering test was conducted accordance to ASTM D1435. The samples were placed on the rack by adjusted to face the equator at an angle of 45°. The rack was located in an open area where it was free from overshadowed by other objects and exposed to all environmental effects such as rain, sunlight, wind and etc. The samples were collected after 2, 4 and 6 months to determine the degree of degradation by UV source. Moisture at the surface of the samples was removed with a clean towel and left in air for 24 h at room temperature before proceeding with further testing.

3.4 Gel Content Test

The gel content test was performed accordance to ASTM D2765. This test was investigated the cross-linking networks degree formed in the polypropylene matrix. The samples were weighed to obtain the initial weight (W_i) by using analytical balance. Then, the weighted samples were heated in xylene at 120 °C for 24 hours. After extraction process, the samples were washed and rinsed several times with clean xylene to remove soluble materials from the extracted samples. After that, the samples were rinsed twice with methanol and soaked in methanol for 20 min. The samples were dried to a constant weight in a vacuum oven at 70 °C for 4 hours. The weight of dried samples (W_f) was weighed by using analytical balance. The gel content percentage for each sample was obtained as the average of three specimens and calculated as below (3.1):

$$\text{Gel Content Percentage (\%)} = \frac{W_i - W_f}{W_i} \times 100\% \quad (3.1)$$

Where W_i = Initial weight of the samples before the extraction process (g), W_f = Final weight of the dried remaining samples after the extraction process (g)

3.5 Tensile Test

The tensile test was tested using Instron Universal Testing Machine 5582 series IX tensile tester with a crosshead speed of 50 mm/min to obtain tensile properties of the samples. The 3 mm thick sheets were cut into dumbbell shapes accordance to the ASTM D638 (Type IV) standard. The

tensile strength, elongation at break and Young's Modulus of the samples were obtained as the average of five specimens.

The Young's Modulus of the samples was calculated with the following equation (3.2):

$$\text{Young's Modulus} = \frac{\text{Stress}}{\text{Strain}} \quad (3.2)$$

The elongation at break of the samples can be determined from the following equation (3.3):

$$\text{Elongation at Break} = \frac{l_f - l_0}{l_0} \times 100\% \quad (3.3)$$

Where l_f = final length of specimen (mm), l_0 = initial length of specimen (mm)

3.6 Impact Test

Impact test was performed in accordance with ASTM D256 standard for the notched sample bars by using Izod Impact Tester. The pendulum-type of hammer connected to the impact tester was released to break the notched sample bars. The sample bars with a V-shape notch for notched Izod impact test were cut from sample sheets while each of the test bars has standard dimensions of $12.7 \times 63.5 \times 3$ mm (width \times length \times depth) following by making 2.54 ± 0.05 mm indentations. The obtained impact strength value of each sample was taken as the average of three specimens and calculated as below (3.4):

$$\text{Impact Strength} = \frac{W}{h \times b} \times 10 \text{ kJ/m}^2 \quad (3.4)$$

Where W = specimen impact broken energy (J), h = specimen thickness (mm),
b = specimen width (mm), from indented point to lateral surface

3.7 Hardness Test

Hardness test was conducted accordance to ASTM D2240. The sheet samples were cut into 7cm x 7cm dimension and obtained the average of five points on the sheet samples. Durometer Model 3000-D was used as testing equipment and the unit of hardness was expressed in (Shore D).

3.8 X-ray Diffraction (XRD) Analysis

The dispersion and crystallinity of the DVC in the PP matrix was tested by using Shimadzu XRD 6000 diffractometer with a Cu-K α radiation source ($\lambda=1.542 \text{ \AA}$) at 40 kV and 30 mA for a 2θ range of 3-40° at a scanning rate of 1.2°/min. The scanning pattern was recorded by using Rigaku software. The degree of crystallinity was calculated as a percentage by dividing the scattered intensity of the crystalline phase by the total scattered intensity of the crystalline and amorphous phases. The d-spacing (3.5) and interchain-separation (3.6) of the samples were calculated with the following formula (Bragg's formula):

$$d = \frac{\lambda}{2 \sin \theta} \quad (3.5)$$

$$R = \frac{5}{8} \left(\frac{\lambda}{\sin \theta} \right) \quad (3.6)$$

Where d = d-spacing, Å; λ = wavelength, nm; θ = Bragg angle, radian; R = interchain-separation, Å.

The crystallize size of the samples was calculated with the following formula (Scherrer formula) (3.7):

$$L = \frac{k\lambda}{\beta \cos \theta} \quad (3.7)$$

Where L = crystallize size, Å; k = Scherrer constant (0.9); β = full width of half maximum (FWHM), radian.

The percent of crystallinity of the samples can be determined from the following equation (3.8):

$$\% \text{ Crystallinity} = \frac{\text{Area under crystalline peaks}}{\text{Total area under all peaks}} \times 100\% \quad (3.8)$$

3.9 Scanning Electron Microscope (SEM)

The surface morphologies of the fractured surface for all the samples were scanned by using Hitachi Scanning Electron Microscope model BS 340 TESLA. The fractured surfaces of the samples were cut into 3mm height and placed on the copper stub with a fractured surface facing up. The samples were coated with a thin layer of gold before proceeding to SEM scanning. The SEM micrographs were recorded at a magnification of 1000x.

3.10 Fourier Transform Infrared Spectroscopy (FTIR)

The interaction of chemical functional group of the specimens was analyzed by using Perkin Elmer Spectrum EX1. The infrared spectra were recorded with 32 scans for each measurement over the wavelength range of 500 – 4000 cm^{-1} . The carbonyl index was calculated using the equation as below:

$$\text{Carbonyl Index} = \frac{I_{1715}}{I_{2912}} \quad (3.9)$$

Where I_{1715} = peak intensity at 1715 cm^{-1} , I_{2912} = peak intensity at 2912 cm^{-1}

CHAPTER 4

RESULTS AND DISCUSSIONS

4.1 Effect of Devulcanized Natural Rubber Composition on the PP-DVC Compound

4.1.1 Gel Content Test

Figure 4.1 shows the different DVC compositions influence on the gel content of PP-DVC compound with. The result shows that all the non-irradiated PP-DVC compounds did not dissolve completely in hot xylene after 24 hours extraction process. This might be owing to the crystallinity region exists in the DVC particles and PP matrix that resisted from hot xylene attack (Bee et al., 2012). Besides, it was found that the addition of DVC from 0 phr to 20 phr in the PP matrix gives higher gel content of the non-irradiated samples (i.e 16.25 % to 19.85 %). This effect could be as a result of the higher crystallinity degree in the DVC phase compare to the PP matrix which resisted the hot xylene attack (Bee et al., 2014).

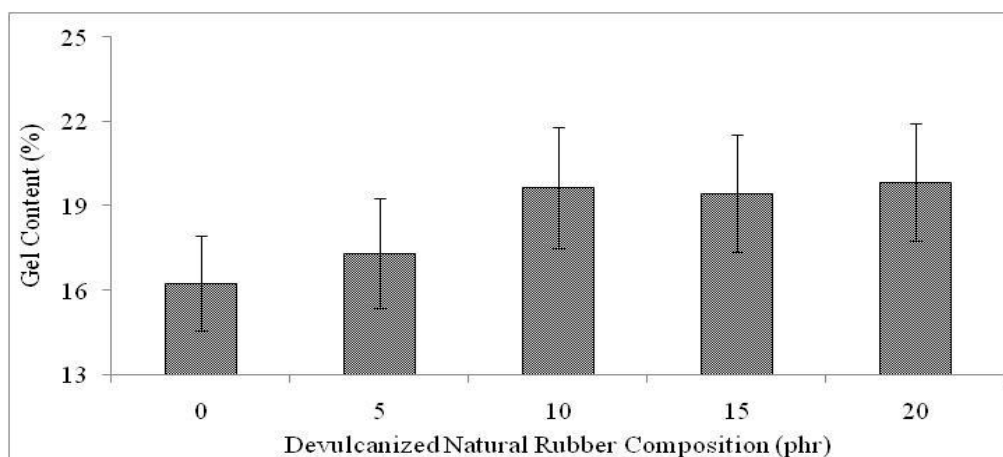


Figure 4.1: Gel Content for Different DVC Composition of PP-DVC Compound.

4.1.2 Tensile Test

Figure 4.2 (a) shows the different DVC compositions influence on the tensile strength of PP-DVC compounds. The tensile strength of the non-irradiated PP-DVC compounds has slightly increased when increasing the DVC composition from 0 phr to 5 phr. This was credited to the well distribution and dispersion of DVC particles in the PP matrix as a result of the least voids and enables to transfer stress effectively between the filler and matrix. (Kamalbabu and Kumar, 2014) Thus, low loading level of DVC could enhance the reinforcing effect between DVC particles and PP matrix in PP-DVC compound. However, the DVC composition further increase from 5 phr to 20 phr has marginally reduced the tensile strength of the PP-DVC compounds. This is due to DVC tend to promote a high particle-particle interaction among DVC particles and further lead to the DVC poorly distributed and dispersed at PP matrix at high loading level (Murray et al.,

2012). This effect caused the DVC particles inclined to form larger DVC agglomerated particles via agglomerate together and acts as a stress concentration point. Thus, the stress from tensile extension applied on the PP matrix unable to transfer effectively between DVC particles and PP matrix at a high loading level of DVC.

Figure 4.2 (b) shows that the Young's Modulus for the non-irradiated PP-DVC compounds decreased with higher DVC composition. This is because the addition of DVC imparts the elastic behavior to the PP-DVC compound as a result of more rubber-like properties in PP-DVC compounds. As the DVC content increases, the particle-particle interaction in the DVC phase increases and become more rubber behavior in the PP-DVC compounds (Mohamad et al., 2013). Thus, it reduced the rigidity of the PP-DVC compounds and resulted in a lower value of Young's Modulus.

By referring to Figure 4.2 (c), the incorporation of DVC into PP from 0 phr to 15 phr has significantly increased the value of elongation at break for the non-irradiated PP-DVC compound. The enhancement of the interaction between DVC particles and PP matrix has increased the mobility of the polymer chains in the PP matrix as the restriction effect reduced. Therefore, the existence of DVC particles in PP matrix tends to resist breaking under tensile stress. Conversely, further add in the DVC from 15 phr to 20 phr in PP-DVC compounds could reduce the elongation at break. This could be owing to the excessive of DVC particles in PP matrix tend to form larger DVC particles via agglomerate together and lead to poor intermolecular bonding between

DVC particles and PP matrix. Thus, it limits the flow and mobility of the PP matrix and reduces the extendibility of the PP-DVC compounds.

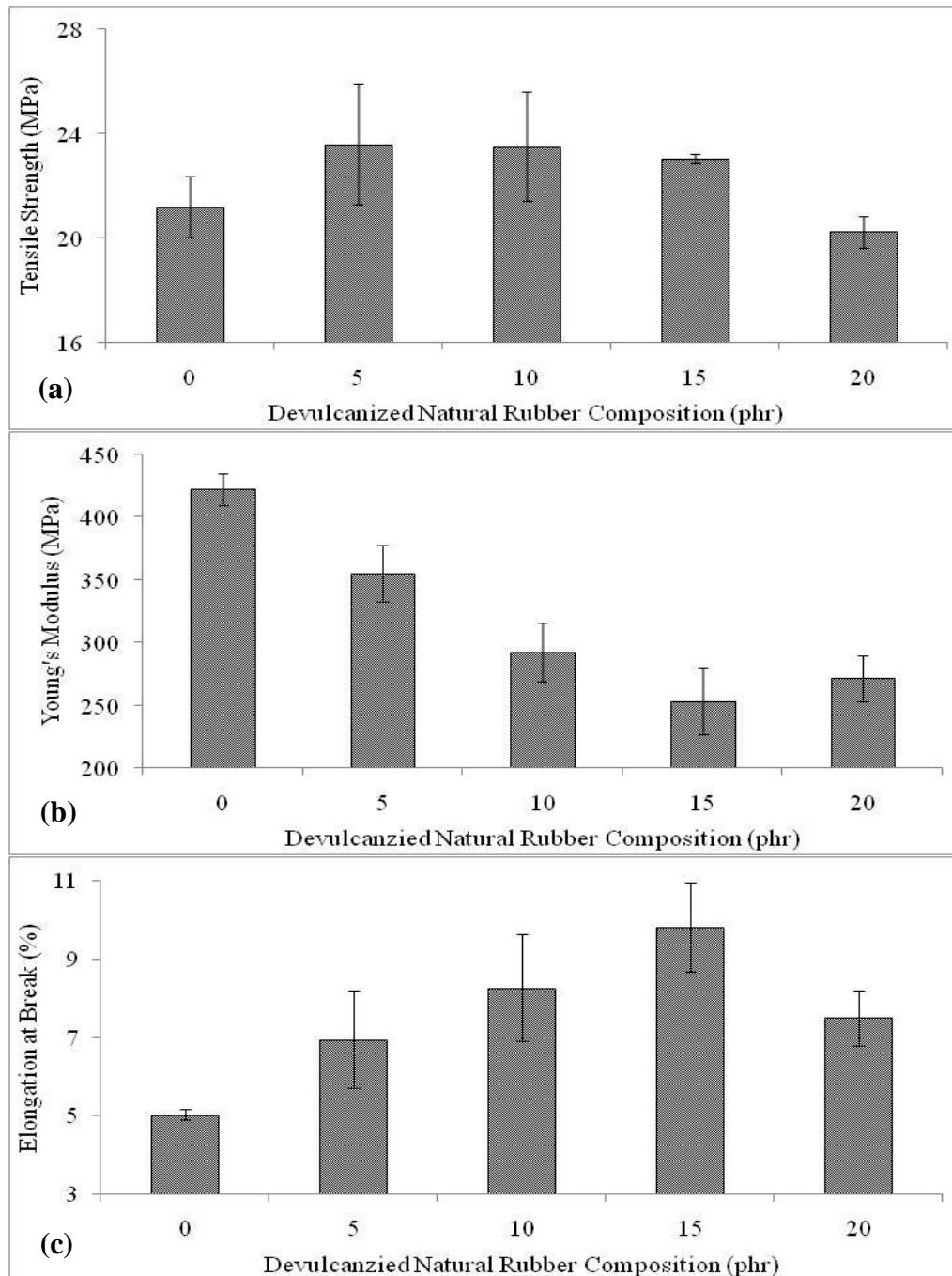


Figure 4.2: (a) Tensile Strength, (b) Young's Modulus and (c) Elongation at Break for Different DVC Composition of PP-DVC Compound.

4.1.3 Impact and Hardness Test

The impact strength for different composition of DVC added PP compounds subjected to various irradiation doses as shown in Figure 4.3 (a). The impact strength of the non-irradiated PP-DVC compounds was found to be slightly higher when the DVC composition increasing from 0 phr to 5 phr. The PP-DVC compounds tended to be arranged into more highly ordered structure in the polymer matrix at low DVC composition due to the strong interaction between PP matrix and DVC particles. Therefore, it enables to transfer stress effectively between the filler and matrix and increase the capability of the PP-DVC compound to withstand the sudden load applied. However, the impact strength of the non-irradiated PP-DVC compounds decreased marginally with the DVC composition increasing from 5 phr to 20 phr. The excessive of DVC particles in PP matrix has deteriorated the dispersion and distribution in PP matrix at high DVC composition. This phenomenon caused the DVC particles tend to form larger agglomerated DVC particles via agglomerate together in PP matrix and weaken the matrix uniformity. Thus, the force from the sudden load applied on the compounds was unable to transfer effectively between filler and matrix at high DVC composition.

Figure 4.3 (b) shows the different DVC compositions influence on the hardness value of PP-DVC compound under various irradiation dosages. The DVC composition at low loading level (≤ 5 phr) added into PP could slightly increase the hardness value of the PP-DVC compound. This is due to the

homogenous distribution of DVC particles into PP matrix enhanced the interaction between DVC particles and PP matrix. Thus, such enhancement resulted in more ability to resist from deformation. However, the DVC composition further add in up to 20 phr into PP has marginally reduced the hardness value of the PP-DVC compound. This could be due to the DVC particles tends to the interaction between particle-particle in the DVC phase at higher composition which eventually leads to poor distribution and dispersion in the PP matrix. Hence, the reinforcing effect of the DVC particles in the PP matrix could reduce and result in less ability to resist from deformation by the load applied.

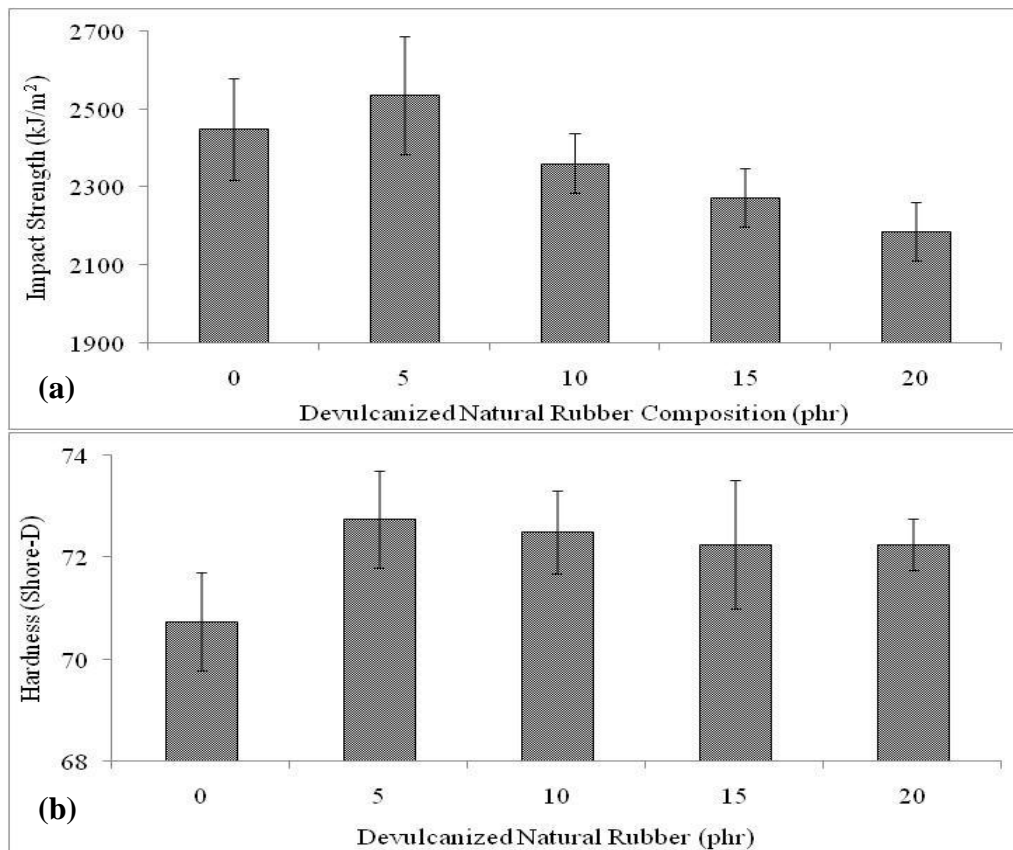


Figure 4.3: (a) Impact Strength and (b) Hardness for Different DVC Composition of PP-DVC Compound.

4.1.4 XRD Analysis

The XRD patterns of different DVC composition of PP-DVC compounds subject to electron beam irradiation under various irradiation dosages are shown in Figure 4.4. There are five significant sharp peaks can be observed on XRD curve at $2\theta = 14.29^\circ$, 17.14° , 18.88° , 21.83° and 37.68° which represented by peak A, peak B, peak C, peak D and peak E respectively. It can be noted that the intensity of the peaks decreased with higher DVC composition. This might be due to the incorporation of DVC in PP matrix caused the orientation of molecules changed and lower the crystallinity ratio in PP polymer. With reference to Table 4.1, the d-spacing and inter-chain separation of non-irradiated PP-DVC compound slightly increased when the DVC added up to 10 phr into PP. This is due to the increment of separation distance between DVC molecules chains in PP matrix. This effect could lead to DVC dispersed effectively and well distributed into PP matrix. Furthermore, the DVC composition further increasing from 10 phr to 20 phr has slightly decreased the value of d-spacing and inter-chain separation for PP-DVC compounds. This also indicated that further increasing of DVC composition could reduce the dispersion and distribution effectiveness of DVC into PP matrix. This is due to the DVC particles more tendency to coalesce together in PP matrix at higher composition. Therefore, the separation distance between DVC molecules chain in PP matrix reduced at higher loading level of DVC. Moreover, the DVC compositions increasing up to 15 phr has gradually reduced the crystallinity of non-irradiated PP-DVC compounds from 18.06 % to 15.41 % as shown in Table 4.1. This indicates that the DVC compositions

added up to 15 phr in PP matrix could disrupt the highly ordered structural arrangement of PP matrix into random chain arrangement structure. This can be further proved with the crystallize size for the samples as shown in Table 4.1. The crystallize size decreased from 70.05 nm to 55.91 nm when the increasing of DVC compositions up to 15 phr added in PP. This is due to the existence of DVC as rubber particles are present in the inter- and intra-spherulitic region of the crystalline phase plastic affected the crystallization behavior of the PP-DVC blends (Medhat et al., 2013). Therefore, the incorporation of 15 phr DVC has slightly re-structured the crystallize structure and resulted in lower crystallinity. However, when the DVC composition increased up to 20 phr added in PP matrix, the crystallinity increased up to 20.08 %. This is mostly contributed by the overdose of DVC particles in PP matrix could ruptured and disrupt the highly ordered structural arrangement inside PP matrix into random structural arrangement. As a result, the crystallinity of the PP-DVC compounds can be increased when 20 phr of DVC added in PP. This also shows in the crystallize size of 20 phr of PP-DVC compound had expanded to 62.61 nm indicated that the agglomerated DVC particles disrupt and rupture the crystalline structural arrangement in PP matrix into random chain arrangement structure (Bee et al., 2015). Thus, these agglomerated DVC particles would enlarge the crystallize sizes and in the PP matrix.

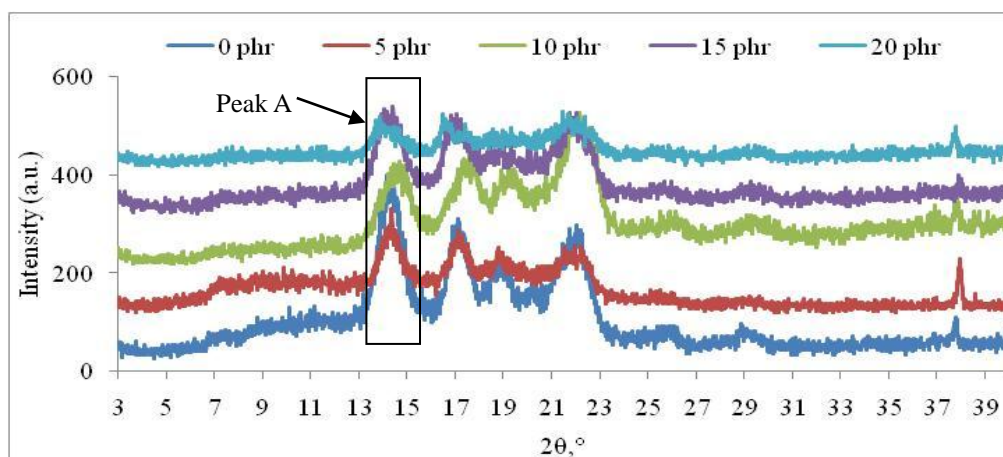


Figure 4.4: XRD Curve ($3^\circ \leq 2\theta \leq 40^\circ$) for Different DVC Composition of PP-DVC Compound.

Table 4.1: Inter-chain Separation, d-spacing, Crystallize Size and Crystallinity for Different DVC Composition of PP-DVC Compound at Peak A.

DVC Composition, phr	$2\theta, ^\circ$	d-spacing, Å	Inter-chain Separation, Å	Crystallize Size, nm	Crystallinity, %
0	14.29	6.19	7.75	70.05	18.06
5	14.30	6.19	7.74	64.15	16.47
10	14.25	6.21	7.77	60.79	15.63
15	14.30	6.19	7.74	55.91	15.41
20	14.35	6.17	7.72	62.61	20.08

4.1.5 SEM Analysis

Figure 4.5 illustrates the fractured surface morphologies of the pristine PP and PP-DVC compounds filled with various compositions of DVC at 1000x magnification. The formation of tear lines is observed in Figure 4.5 (a) which attributed by the ability of PP matrix resist from straining stress applied during the tensile test. This phenomenon caused by the tearing effect of polymer matrix when applied straining stress on it (Bee et al., 2012). With reference to the Figure 4.5 (b), the tear lines formation increased on the fractured surface when 5 phr DVC added into PP. This increment of tear lines formation indicated that the PP matrix has higher plastic deformation ability under applied straining stress. This effect leads to more tear lines formed and increased the tensile strength as discussed earlier. Besides, it is apparent that the presence of flake-like appearance on the fractured surface in Figure 4.5 (c) – Figure 4.5 (d) indicated that the dispersion of DVC phase in the PP matrix become poorer. With the higher DVC compositions could increase the average size of dispersed DVC phase increased and give rise to re-agglomeration or coalescence of the dispersed DVC particles due to the existence of the bigger particle size in the DVC phase. This flake-like appearance could lead to poor stress transfer across the interface as the poor interaction between DVC and PP has caused the tensile strength reduced (Medhat et al., 2013). In addition, there is an appearance of voids when the composition increased up to 20 phr as depicted in Figure 4.5 (e). These non-homogeneous distributions of the bigger agglomerated DVC particles in the PP matrix have reduced the interfacial adhesion forces between DVC and PP phase by restricting the effective

intermolecular bonding between them.

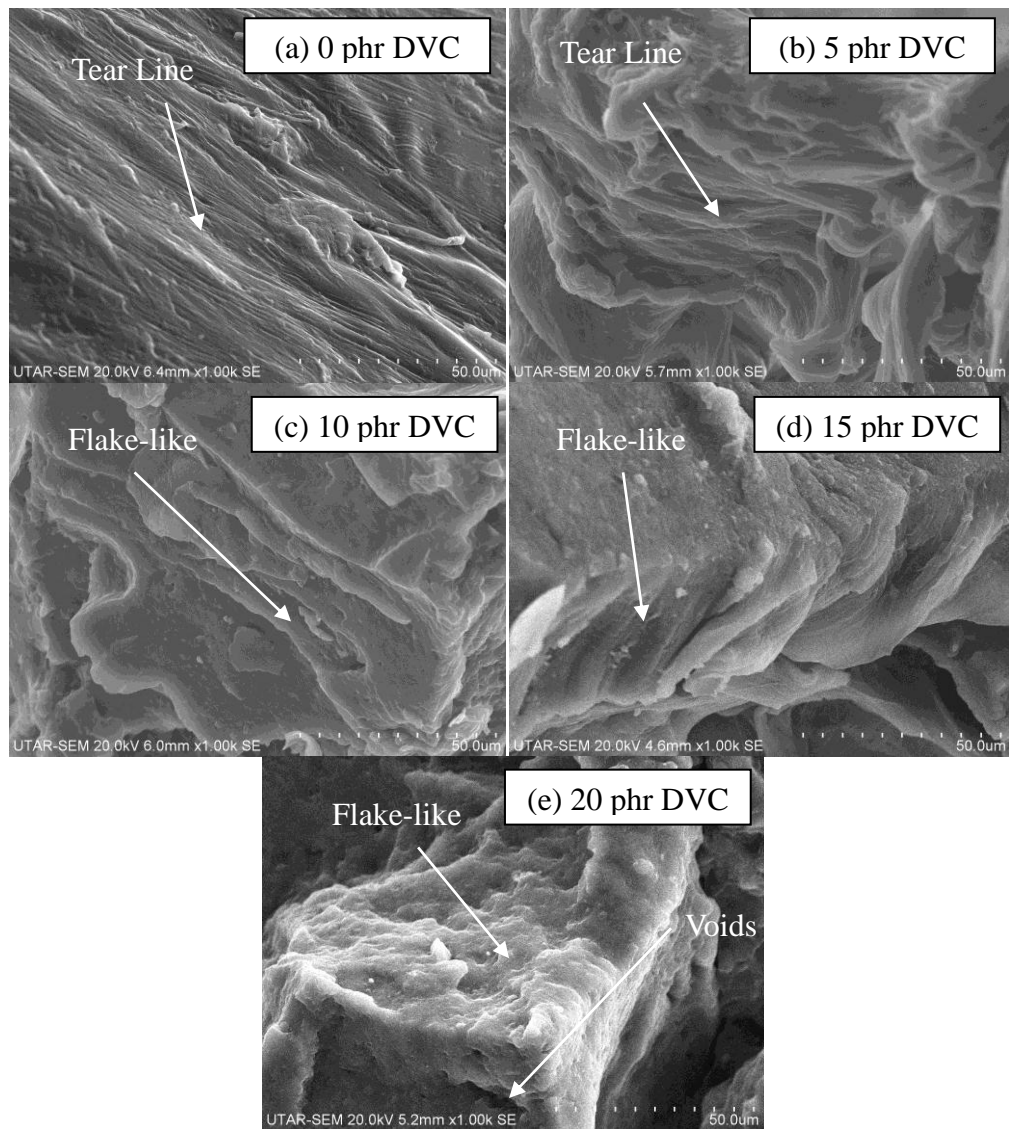


Figure 4.5: SEM Micrographs of Fractured Surface for Different DVC Composition of PP-DVC Compound under Magnification of 1000x.

4.1.6 FTIR Analysis

Figure 4.6 depicts the FTIR absorption spectra for the PP-DVC compound with different DVC compositions made in the range of 4000 - 650

cm^{-1} . According to Figure 4.6, it shows a strong absorption peak around 2915 cm^{-1} which assigned to asymmetric C-H stretching vibration. Besides that, there is a new peak appeared at 1537 cm^{-1} which assigned to C=C bending when increased the DVC composition. Furthermore, the higher DVC composition also increased the intensity of the peak at 1650 cm^{-1} representing C=C stretching as shown in Figure 4.6. This effect as a result of the addition of DVC in PP has increased the formation of C=C bonding. Other than that, the peak around 1454 cm^{-1} and 1372 cm^{-1} corresponding to CH_2 bending vibration and CH_3 bending vibration respectively (Medhat et al., 2013). Moreover, 3 small peaks visible at 1160 , 980 and 836 cm^{-1} were corresponding to $-\text{CH}_3$ symmetric deformation vibration, $-\text{CH}_3$ rocking vibration and $-\text{CH}_2$ rocking vibration of PP respectively (Wieslawa, 2012).

In order to further investigate the effect of different DVC composition in PP-DVC compound, the wavenumbers of asymmetric C-H stretching vibration and CH_2 bending vibration are summarized in Figure 4.7. It was found that the wavenumber of asymmetric C-H stretching vibration of the PP-DVC compound increase gradually with higher DVC composition as shown in Figure 4.7 (a). This effect owing to the vibrational effect of the asymmetric C-H stretching required more energy to enable at higher stiffness of the molecular structure (i.e. higher wavenumber). Moreover, this enhancement of stiffness of the matrix was also induced by the dispersion and distribution effect of DVC in the PP matrix (Tee et al., 2013). When investigation expanded to CH_2 bending vibration infrared absorption, the wavenumber of the respective group for the PP-DVC compound was found to be reduced with

higher DVC composition as shown in Figure 4.7 (b). Such reduction is caused by the existence of DVC has formed C=C bonding with the PP and lead to bonding strength of CH₂ bending vibration weaken in PP-DVC compound. The same agreement has been observed as in Figure 4.6 with the existence of C=C group when adding the DVC into PP.

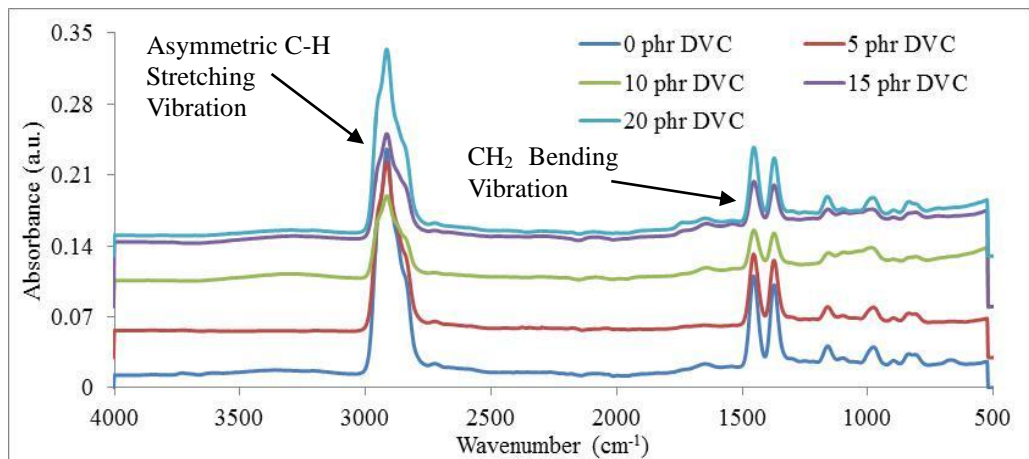
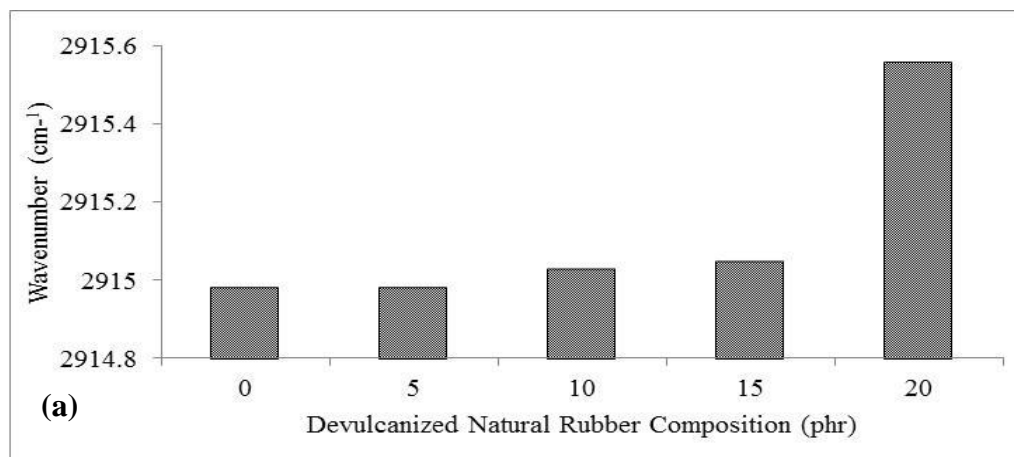


Figure 4.6: FTIR Absorption Spectra for Different DVC Composition of PP-DVC Compound.



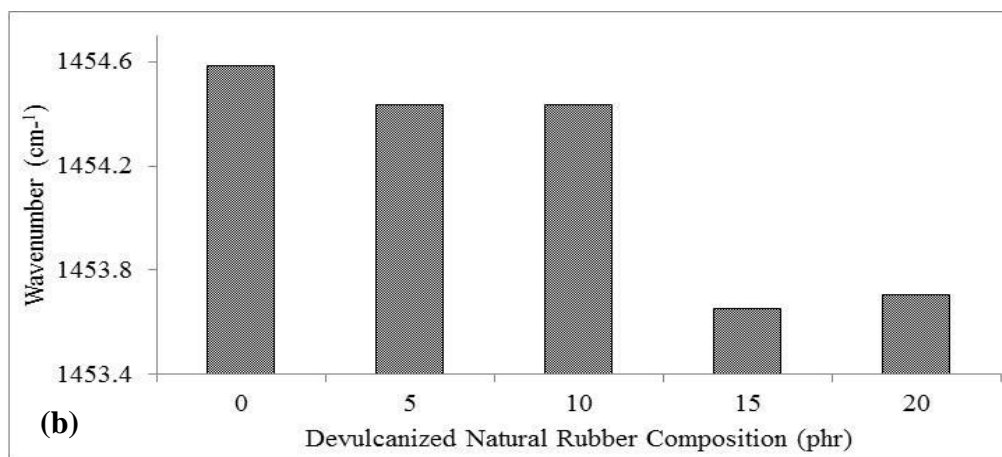


Figure 4.7: (a) Wavenumber of the Asymmetric C-H Stretching Vibration and (b) CH₂ Bending Vibration for Different DVC Composition of PP-DVC Compound.

4.2 Effect of Electron Beam Irradiation on the PP-DVC Compound

4.2.1 Gel Content Test

For the irradiated pristine PP as depicted in Figure 4.8, the irradiation doses increased from 0 kGy to 50 kGy was found to be slightly increasing the gel content from 16.24 % to 18.1 %. At the low irradiation dose, it could slightly induce the cross-linking networks formation in the PP. Therefore, the solubility of the pristine PP in the hot xylene reduced. As per contra, the gel content of irradiated pristine PP gradually reduced with a subsequent increasing of irradiation dosages up to 200 kGy. This result shows that cross-linking process is less favorable than chain scissioning process at higher irradiation dosage. It tends to break the bonds between atoms in the PP's main

chain at the high level of irradiation dosages. Therefore, the gel content of irradiated pristine PP has higher solubility against the hot xylene attack at high irradiation dosage. The irradiation dosages increasing from 0 kGy to 200 kGy has marginally increased the gel content for all the irradiated DVC added in PP compounds as shown in Figure 4.8. The increment of irradiation dosages could give rise to the number of accelerated electrons which generated by electron beam accelerator. (Murray et al., 2012) Then, these accelerated electrons have been shifted to DVC and PP matrix from electron beam accelerator and attack the DVC and PP macromolecule chains by the reactive free radicals formed in DVC and PP matrix as shown in Scheme 4.1. These reactive free radicals formation could further react together to form cross-linking networks between DVC and PP matrix by releasing hydrogen gas as shown in Scheme 4.2. This cross-linked chains formation in PP matrix has remarkably expanded the average macromolecular sizes of polymer chains. Subsequently, it could reduce the solubility of the irradiated PP-DVC compound in the hot xylene.

On the other hands, the results show that the increasing of DVC composition in PP matrix could give higher gel content of all irradiated PP-DVC compound. This indicated that the existence of DVC plays a key role in cross-linking enhancement in the PP matrix by promoting a more extensive three-dimensional network formation via a substantial reaction with the larger amount of free radicals (Bee et al., 2012). However, the existence of DVC particles in the PP matrix could rupture the cross-linking network formation between polymer chains which brings insignificant effect on the cross-linking

network formation. Furthermore, it could also limit the transportability of the polymeric free radicals inside PP matrix and lower the cross-linking networks formed in the PP matrix. Therefore, the gel content for all irradiated PP-DVC compound increased with higher DVC composition is generally contributed by the insolubility behavior of entrapped DVC particles increase in cross-linking networks. (Bee et al., 2015)

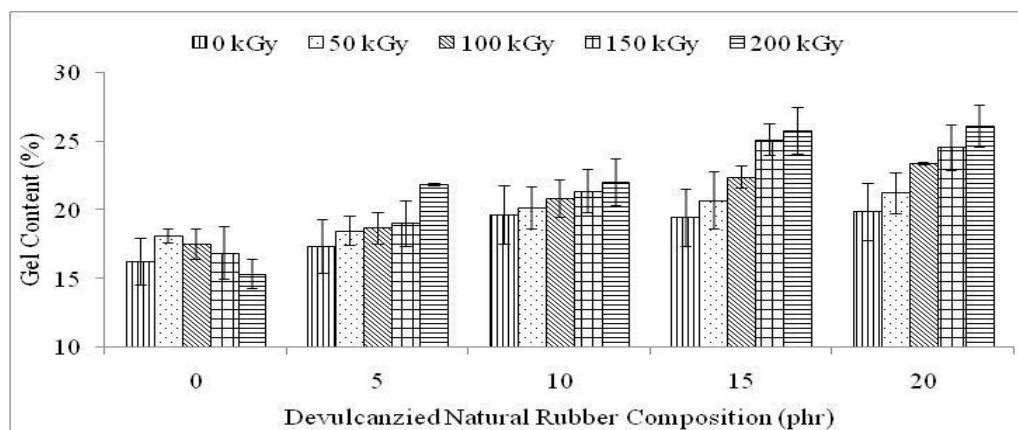
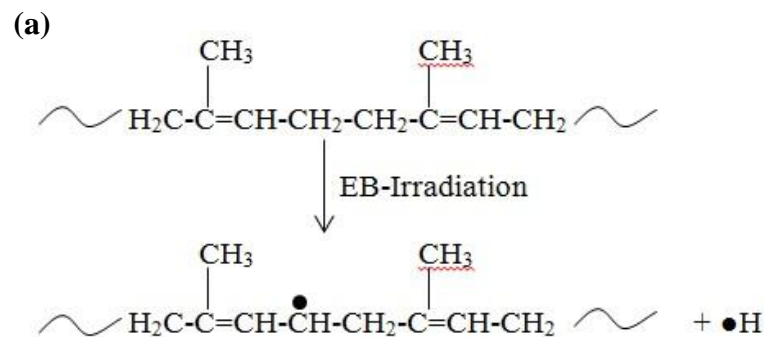
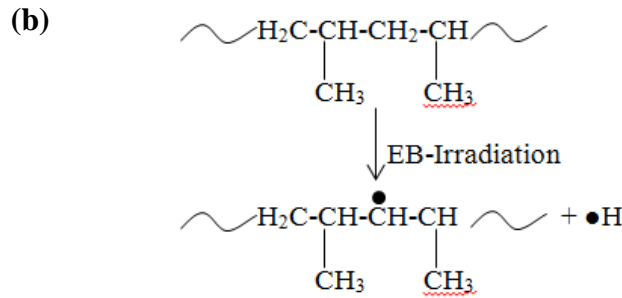
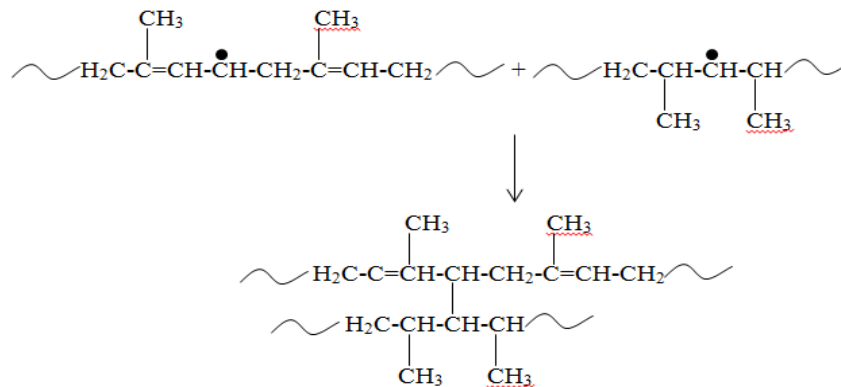


Figure 4.8: Gel Content for Different DVC Composition of PP-DVC Compound before and after EB-Irradiation.





Scheme 4.1: Possible Reaction Mechanism for Free Radical Generation by EB-Irradiation (a) Devulcanized Natural Rubber (b) Polypropylene.



Scheme 4.2: Possible Reaction Mechanism for Bond Formation between the Free Radical of Devulcanized Natural Rubber and Polypropylene.

4.2.2 Tensile Test

Refer to the Figure 4.9 (a), the tensile strength of pristine PP increased with the irradiation dosages increasing from 0 kGy to 50 kGy. The application of electron beam irradiation could release the free radicals by attack the macromolecular chains of the PP. Then, these free radicals combine to form the cross-linking networks in the PP matrix. This cross-linking network

formation could provide reinforcement effect to the PP matrix in applied stress against the tension extension by increasing the polymer macromolecular sizes and weight in PP matrix (Bee et al., 2015). However, the irradiation dosages further increasing from 50 kGy to 200 kGy has greatly decreased the tensile strength of irradiated pristine PP. The higher level of irradiation dosages might break the attractive forces between atoms in the PP chains due to the chain scissioning occurs in PP matrix. This phenomenon could remarkably bring down the ability of PP matrix to resist the tensile stress as the macromolecules size of PP chains reduced. Besides that, the tensile strength for all the irradiated PP-DVC compounds irradiated from 0 kGy to 50 kGy was found to be higher with the incorporation of DVC in PP matrix as shown in Figure 4.9 (a). The low level of irradiation dosages could promote the polymeric free radicals in PP matrix release by forming cross-linking networks in PP matrix. The interaction between DVC particles and PP matrix could be enhanced with the cross-linking networks formation in PP matrix. Hence, it improves the compatibility between DVC particles and PP matrix and enables the tensile stress applied transferred efficiently between filler and matrix. In contrast, the irradiation dosages further increasing from 50 kGy to 200 kGy could significantly reduce the tensile strength for all the irradiated PP-DVC compounds. As mention earlier, chain scissioning process is predominant in the higher energy of electron beam irradiation. Thus, it tends to break down the long macromolecular chains into shorter macromolecular chains for the DVC and PP as shown in Scheme 4.3. Thereafter, it weakens the ability of irradiated PP-DVC compounds to resist the tensile stress.

Refer to the Figure 4.9 (b), the irradiation dosages increasing from 0 kGy to 150 kGy was found to be gradually increase the Young's Modulus of the irradiated pristine PP. The implementation of electron beam irradiation could highly restrict the mobility of the PP chains from slippage each other. Thus, this cross-linking formation in PP matrix promotes the structure become more rigid. As per contra, further irradiated the pristine PP form 150 kGy to 200 kGy has reduced Young's Modulus value. The overdose of the electron beam irradiation could lead to chain scissioning process which breaks down the long polymer chains into shorter polymer chains and result in the cross-linking degree decreases (Bee et al., 2014). Consequently, the rigidity of the irradiated pristine PP reduced as the shorter polymer chains experience lower hindrance effects and higher mobility from the cross-linking networks. Moreover, with the incorporation of the DVC in PP matrix could marginally increase the Young's Modulus of the irradiated PP-DVC compounds when irradiated from 0 kGy to 150 kGy. The cross-linking formation in the PP matrix induced by electron beam irradiation could highly restrict the mobility of the PP chains and thus enhance the stiffness of PP-DVC compounds. Furthermore, it could also improve the interfacial adhesion between DVC particles and PP matrix by enhancing the reinforcement effect of DVC particles in PP matrix. Therefore, this highly restriction in the mobility of polymer chains by the cross-linking networks formed in the polymer matrix has improved the Young's Modulus of the irradiated PP-DVC compounds. On the other hands, the irradiation dosages further increasing from 150 kGy to 200 kGy was found to be lower the Young's Modulus of the irradiated PP-DVC compound. At a high level of irradiation dosages, chain scissioning

occurs with cross-linking networks degree reduction by break down the long chains into shorter chains. Subsequently, this phenomenon was reduced the rigidity of the irradiated PP-DVC matrix due to unable to enhance the reinforcement effect of DVC particles in PP matrix.

Refer to the Figure 4.9 (c), the elongation at break of the irradiated pristine PP was increased when irradiated from 0 kGy to 50 kGy. With the low level energy of electron beam irradiation could release a low amount of free radicals and form a low cross-linking networks degree in the PP matrix. Thus, this low cross-linking networks degree improves the elongation ability of the PP matrix by providing the reinforcement effect to the PP matrix. In contrast, the elongation at break of the irradiated pristine PP was found to be gradually reduced with the irradiation dosages increasing from 50 kGy to 200 kGy. The elevation of irradiation dosages could induce the chain scissioning process as it more favorable than cross-linking process at a higher energy of irradiation. This occurrence of chain scissioning could reduce the macromolecular sizes of PP chains by breaking the intermolecular bonding between atoms in the PP chains. As a result, the extendibility of the PP matrix reduces and escalates the breakage of the PP matrix by tensile stress applied. Furthermore, the addition of DVC in PP matrix has reduced the elongation at break of the irradiated PP-DVC compounds with the irradiation dosages increasing from 0 kGy to 200 kGy. The accelerated electrons induced by elevation of irradiation dosages have been transferred to DVC and PP from electron beam accelerator and attack the DVC PP macromolecule chains by the reactive free radicals formation. These reactive free radicals then react simultaneously between

DVC and PP to form cross-linking networks by releasing hydrogen gas and thus increase the average macromolecular sizes of polymer chains. Therefore, it could improve the intermolecular forces in PP matrix and reduced the elongation ability of the irradiated PP-DVC compounds.

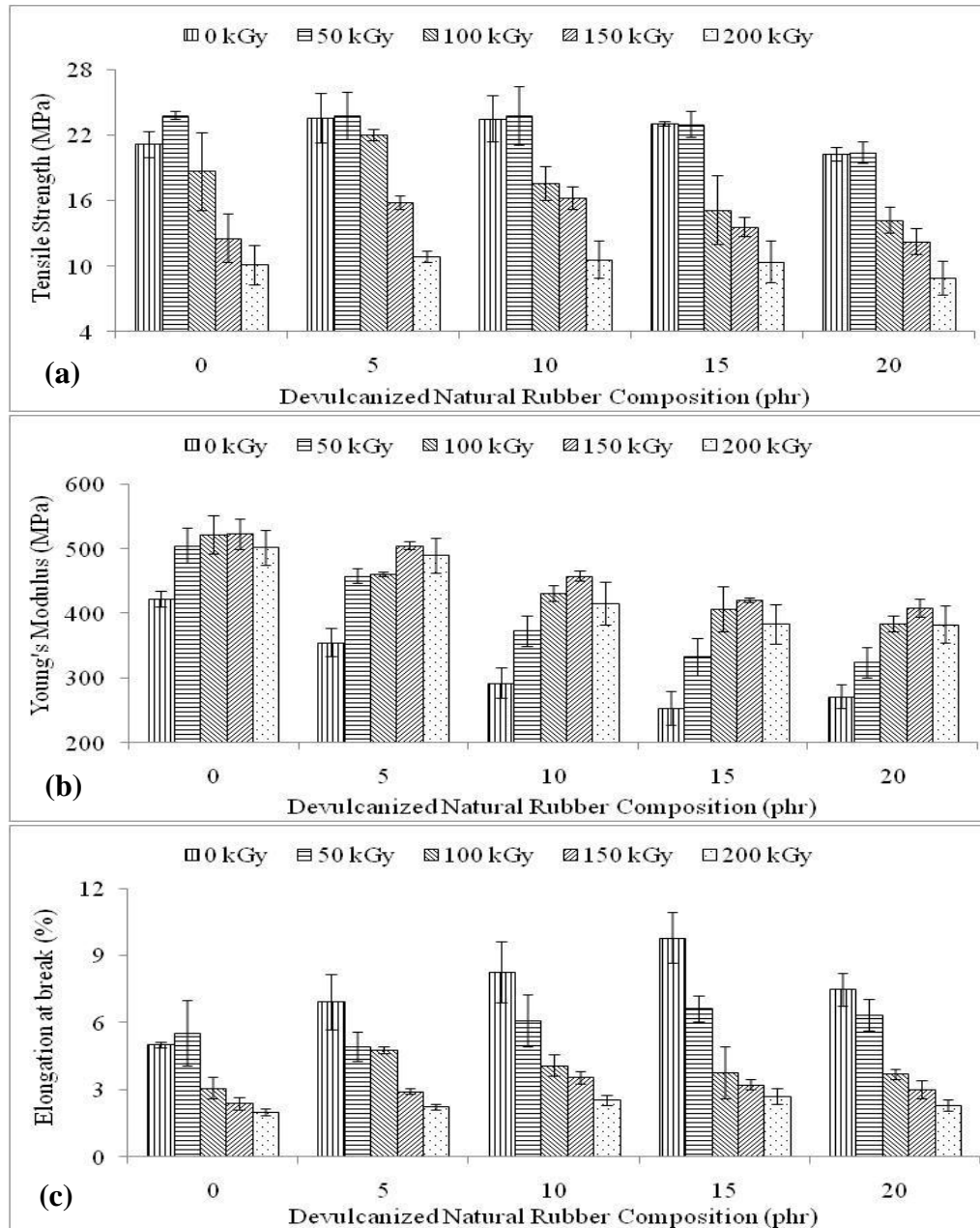
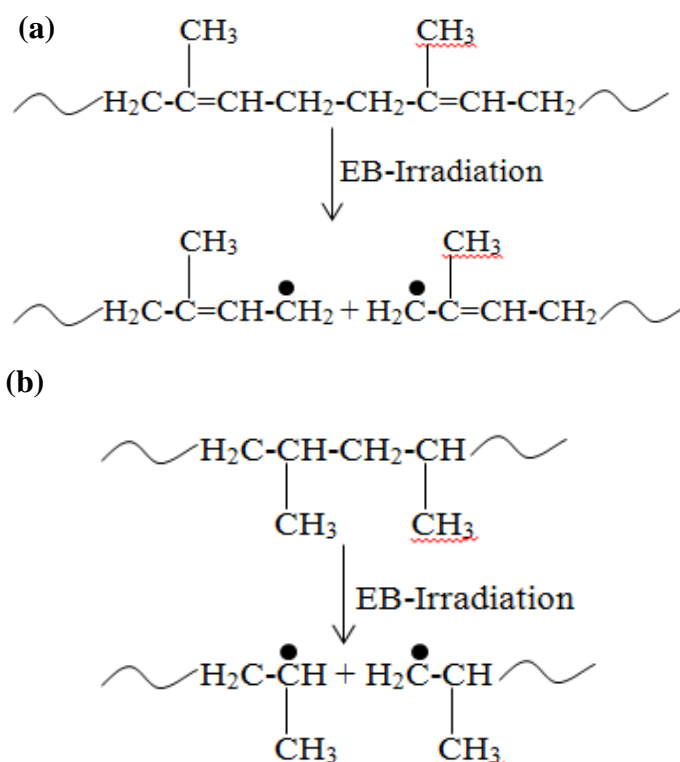


Figure 4.9: (a) Tensile Strength, (b) Young's Modulus and (c) Elongation at Break for Different DVC Composition of PP-DVC Compound before

and after EB-Irradiation.



Scheme 4.3: Possible Reaction Mechanism for Chain Scission by EB-Irradiation (a) Devulcanized Natural Rubber (b) Polypropylene.

4.2.3 Impact and Hardness Test

The various irradiation dosages influence on the impact strength of PP-DVC compounds has shown in Figure 4.10 (a). It was found that the impact strength of the irradiated pristine PP and PP-DVC compounds exhibits the same trend with the tensile strength when applying with electron beam irradiation. For the irradiated PP-DVC compounds irradiated at 50 kGy, the increasing of DVC compositions up to 10 phr could enhance the impact

strength of the samples. The low energy of the electron beam irradiation could generate a great number of free radicals in the PP matrix. Then, the cross-linking networks formed in the PP matrix with these free radicals attack the macromolecule chains of the PP matrix and remarkably expand the molecular weight of the polymer chains. Furthermore, this cross-linking networks formation could promote the low loading level of DVC disperse and distribute better in PP matrix to form stronger intermolecular bonding between DVC particles and PP matrix. Thus, it could transfer the force effectively between DVC particles and PP matrix when the sudden load applied. However, further increasing of the DVC composition up to 20 phr could marginally reduce the impact strength of the irradiated PP-DVC compounds. Although cross-linking networks formed at a low level of irradiation dosages, the overdose of DVC particles in PP matrix has diminished the interaction between DVC particles and PP matrix. Consequently, it ruptured the highly ordered chain arrangement structures in PP matrix into random chains arrangement and reduces the capability of the samples to withstand the sudden load applied. For the irradiated PP-DVC compounds irradiated at higher doses (i.e, 100 kGy, 150 kGy and 200 kGy), it was found that the impact strength of the samples gradually reduced with the DVC compositions increasing up to 20 phr. This is mainly caused by the chain scissioning process occurs at the high level of irradiation dosages on the PP matrix. The chain scissioning process in the PP matrix could reduce the molecular weight of PP resulted in a reduction of intermolecular forces of the PP (Bee et al., 2014). Therefore, it has weakened the interaction between DVC particles and PP matrix and reduced the impact resistance against the sudden load.

For irradiated samples, the Figure 4.10 (b) shows that with the aids of electron beam irradiation could increase the hardness value of the PP-DVC compounds up to 100 kGy. This is due to the polymer matrix exposed under irradiation could promote free radicals formation which in turn to form a higher cross-linking networks degree by the macromolecular chains of PP. Such cross-linking networks formation could strengthen the hardness of the samples in resisting deformation by the load applied. Besides, the cross-linking network formation also could enhance the interaction between DVC and PP. A good interaction between them could enable the load applied transferred more efficiently from the PP matrix to DVC particles and thus increased the hardness value of PP-DVC compounds. However, the hardness value of PP-DVC compounds was found to be decreased rapidly when further irradiated from 100 kGy to 200 kGy. This could be owing to the chain scissioning process occurred by the high level of irradiation dosages. This chain scissioning process could cause the attractive forces between atoms breaking in the PP chains. It could remarkably extend the happening of backbone main chain scissioning in the PP matrix and further reduced the molecular weight of PP (Loo et al., 2005). Therefore, the hardness value of PP-DVC compound decreased as the smaller macromolecular PP chains reduced the ability of the PP matrix to resist from deformation by the load applied.

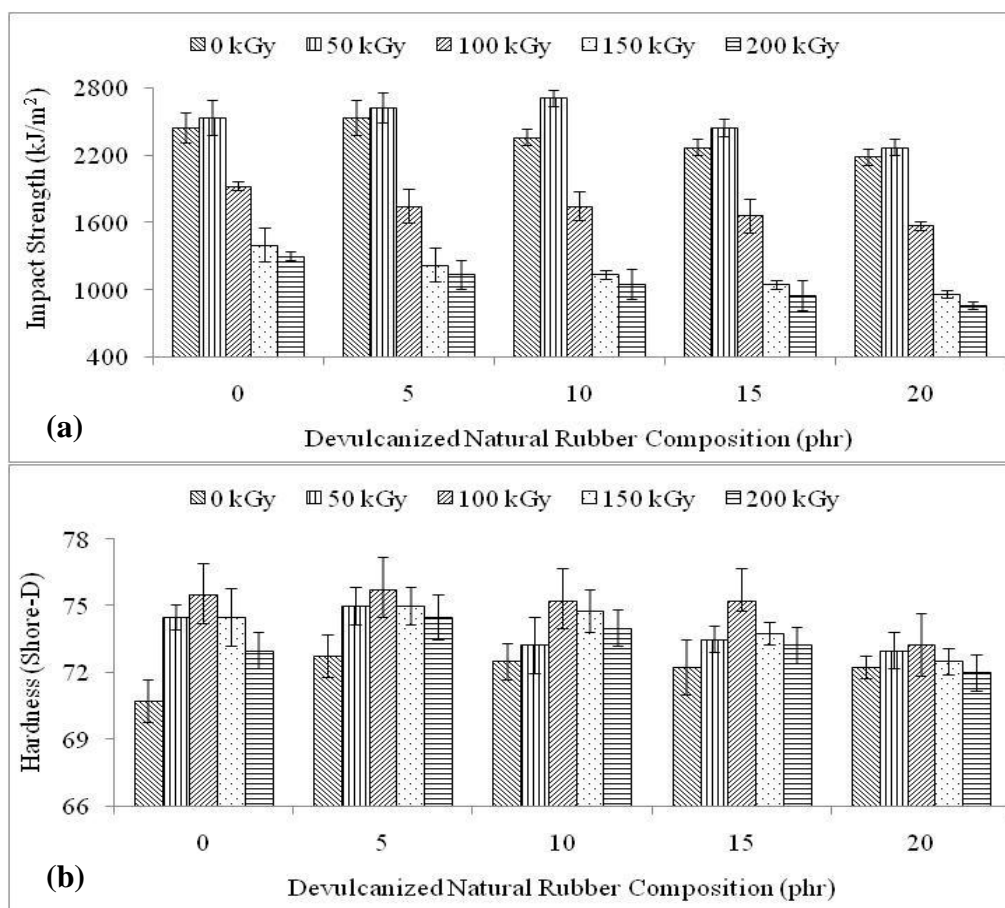


Figure 4.10: (a) Impact Strength and (b) Hardness for Different DVC Composition of PP-DVC Compound before and after EB-Irradiation.

4.2.4 XRD Analysis

Figure 4.11 presents the XRD patterns of irradiated pristine PP and PP-DVC compound subjected to 50 kGy and 200 kGy. It can be noticed that the intensity of the peaks decreased with higher irradiation dosages. This might be due to the chain scissioning process occurred at higher irradiation dosages and ruptured the crystallite structure of pristine PP and PP-DVC compounds. There is a new small sharp peak appear at $2\theta = 31.75^\circ$ when irradiated at 200

kGy indicated that the new crystalline structure formation in the PP matrix. From Table 4.2, the irradiation dosages increasing from 0 kGy to 50 kGy has slightly increased the d-spacing and inter-chain separation of the irradiated pristine PP and PP-DVC compounds indicated that the existing chain arrangement in the PP matrix able to transform into a highly ordered crystalline structure by the cross-linking networks formed in the PP matrix. Besides that, the crystallize size and crystallinity of the irradiated samples (≤ 10 phr) increased when irradiated from 0 kGy to 50 kGy as shown in Table 4.2 and Table 4.3. At low irradiation dosages and DVC composition, radiation-induced cross-linking could transform the PP matrix into a highly ordered crystalline structure as the interaction between DVC and PP matrix improved. In contrast, the crystallinity of the irradiated samples (> 10 phr) reduced while the crystallize size expanded when irradiated from 0 kGy to 50 kGy. Although with the low level of irradiation dosages could improve the interaction between DVC and PP matrix, DVC particles tend to agglomerate together at high composition. These agglomerated DVC particles align themselves around the original crystalline structure when the structural's chain arrangement re-orientated. Furthermore, with the irradiation dosages increasing from 50 kGy to 200 kGy has gradually reduced the d-spacing and inter-chain separation of irradiated samples. The chain scissioning process occurs in the PP matrix has caused the highly ordered crystalline structures started to break down. Besides that, the crystallinity of irradiated samples also decreased with the irradiation dosages further increased to 200 kGy because of the chain scissioning process occurs has ruptured the highly ordered crystalline structures in PP matrix. However, the crystallize size of the irradiated samples expanded with higher

irradiation dosages as shown in Table 4.2. The structural has re-orientated the chain arrangement around the crystalline structure and allowed the agglomerated DVC particles align themselves more easily around the original crystalline structure (Bee et al., 2014).

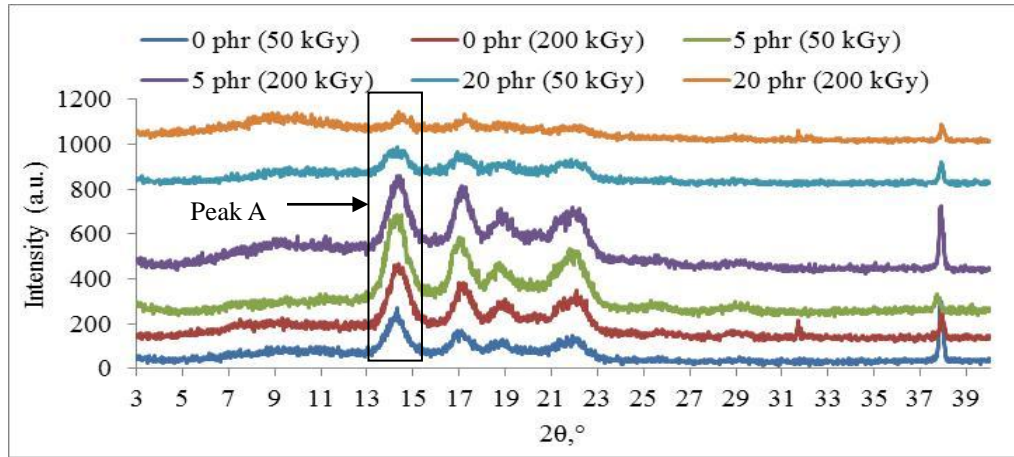


Figure 4.11: XRD Curve ($3^\circ \leq 2\theta \leq 40^\circ$) for 50 kGy and 200 kGy of Pristine PP and Different DVC Composition added in PP.

Table 4.2: Inter-chain Separation, d-spacing and Crystallize Size for Different DVC Composition of PP-DVC Compound at Various Irradiation Dosages at Peak A.

DVC Composition, phr	Irradiation Dosage, kGy	$2\theta, ^\circ$	d-spacing, Å	Inter-chain Separation, Å	Crystallize Size, nm
0	0	14.29	6.19	7.75	70.05
	50	14.24	6.21	7.78	74.20
	100	14.42	6.14	7.68	71.99
	150	14.29	6.19	7.75	68.22

	200	14.36	6.16	7.71	77.06
5	0	14.30	6.19	7.74	64.15
	50	14.27	6.20	7.76	75.32
	100	14.35	6.17	7.72	74.21
	150	14.36	6.16	7.71	75.27
	200	14.33	6.18	7.73	76.86
10	0	14.25	6.21	7.77	60.79
	50	14.33	6.18	7.73	71.88
	100	14.27	6.20	7.76	72.85
	150	14.40	6.15	7.69	77.06
	200	14.43	6.13	7.67	77.31
15	0	14.30	6.19	7.74	55.91
	50	14.34	6.17	7.72	68.30
	100	14.32	6.18	7.73	62.61
	150	14.33	6.18	7.73	77.81
	200	14.38	6.15	7.70	71.56
20	0	14.35	6.17	7.72	62.61
	50	14.25	6.21	7.77	66.60
	100	14.24	6.21	7.78	66.78
	150	14.32	6.18	7.73	74.67
	200	14.45	6.12	7.66	108.31

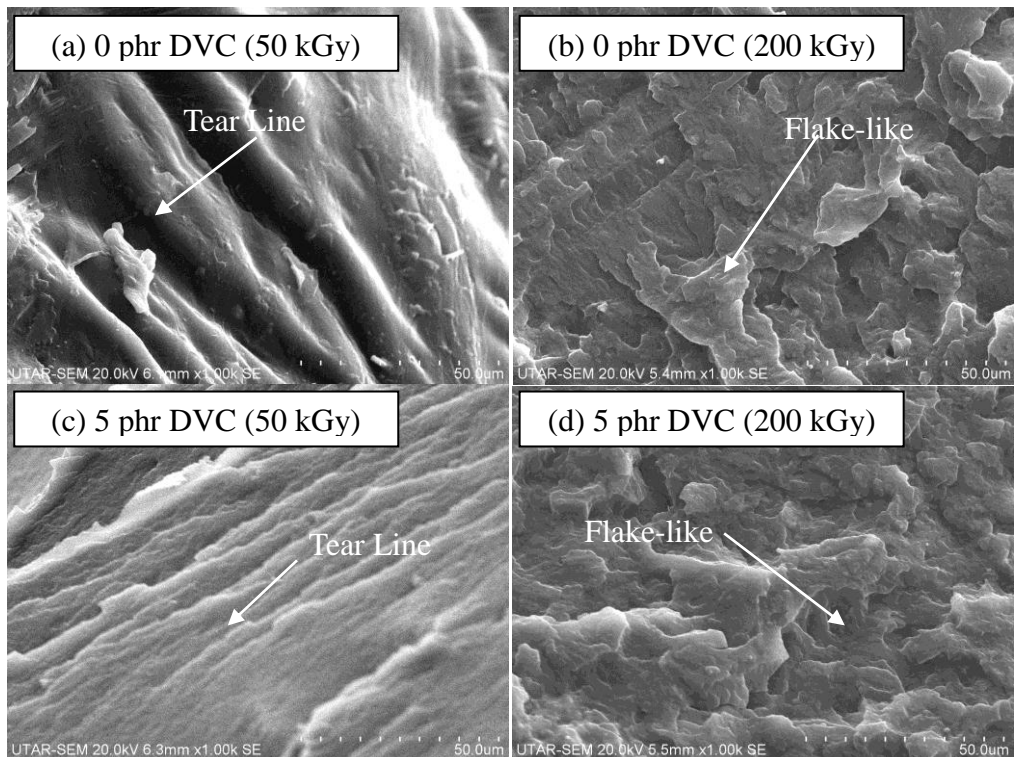
Table 4.3: Crystallinity for Different DVC Composition of PP-DVC Compound before and after EB-Irradiation.

DVC Composition, phr	Crystallinity, %				
	0 kGy	50 kGy	100 kGy	150 kGy	200 kGy
0	18.1	20.0	16.3	16.7	17.8
5	16.5	17.6	16.1	18.0	16.2
10	15.6	17.1	15.7	16.7	16.0
15	15.4	15.3	17.5	18.8	13.7
20	20.1	19.0	14.2	18.1	16.6

4.2.5 SEM Analysis

Figure 4.12 illustrates the fractured surface morphologies of irradiated PP-DVC compounds when applying with irradiation dose of 50 kGy and 200 kGy at 1000x magnification. According to the Figure 4.12 (a) and Figure 4.12 (b), it was found that with the aid of electron beam irradiation at higher irradiation dosages for the pristine PP significantly reduced the tear lines formation and more flake-like appearance formed on the fractured surface. This effect could be due to the chain scissioning process which reduces the continuities of the PP matrix resulted in lower plastic deformation of the PP matrix. The same observation can be seen on the Figure 4.12 (c) and Figure 4.12 (d), there is a reduction of tear lines amount and flake-like appearance formed on the fracture surface of 5 phr of DVC added in PP. The chain scissioning process occurs in the PP matrix has reduced the interaction

between DVC and PP while DVC tended to agglomerated together at high irradiation dosages. As a consequence, it degraded the polymer matrix and resulted in lower plastic deformation of the polymer matrix. The fractured surface of 20 phr of DVC added in PP shows an increasing number of voids on the flake-like appearance when irradiated from 50 kGy to 200 kGy as illustrated in Figure 4.12 (e) and Figure 4.12 (f). The overdose of EB-irradiation could cause the DVC degrades into particles aggregate and form isolated patches on the PP matrix (Chong et al., 2010). Thus, it increased the amount of agglomerated DVC particles and more non-homogeneous distribution of DVC particles in the PP matrix occurs.



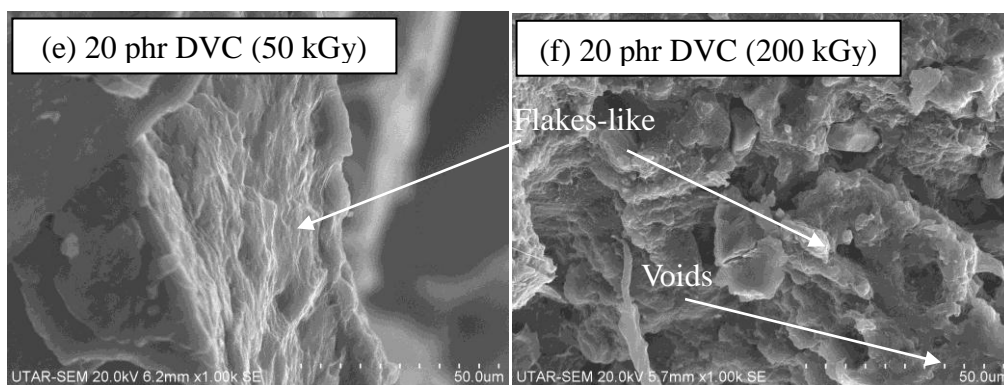


Figure 4.12: SEM Micrographs of Fractured Surface for Different PP-DVC Compound with Various Irradiation Dosages under Magnification of 1000x.

4.2.6 FTIR Analysis

Figure 4.13 depicted the FTIR absorption spectra of the PP-DVC compound with different composition of DVC subject to various irradiation dosages made in the range of 4000 - 650 cm^{-1} . It can be noted that new peak appearing at 1706 cm^{-1} which represents the C=O stretching when the irradiation dosages increasing up to 200 kGy. This result indicated that the oxidation process occurs by the formation of ketonic and aldehydic carbonyl groups. The intensity of the peak at 1650 cm^{-1} representing C=C stretching decreased when the irradiation dosages increasing up to 200 kGy. This phenomenon could be due to the implementation of electron beam irradiation has occurred the oxidation process and thus weakened the C=C stretching bonding. In order to further investigating the effect of electron beam irradiation in PP-DVC compound subject to different DVC compositions, the wavenumber of asymmetric C-H stretching vibration and CH_2 bending

vibration are summarized in Figure 4.14 (a) and Figure 4.14 (b).

With reference to Figure 4.14 (a), the wavenumber of asymmetric C-H stretching vibration of PP-DVC compounds gradually increased when irradiated up to 100 kGy with the incorporation of DVC in the PP matrix. The intermolecular bonding between DVC particles and PP matrix could enhance by the cross-linking network formed in the PP matrix and resulted in higher bonding strength of asymmetric C-H stretching vibration. Moreover, the wavenumber of asymmetric C-H stretching vibration decreased with further irradiation doses (> 100 kGy) regardless DVC compositions. The chain scissioning process occurs with the attractive forces between atoms breaking in the PP chains and further diminishes the intermolecular bonding of the PP-DVC compound and resulted in lower bonding strength of the asymmetric C-H stretching vibration. Moreover, it was found that the wavenumber CH_2 bending vibration for PP-DVC compound has gradually reduced with the irradiation dosages increasing from 0 kGy to 200 kGy as shown in Figure 4.14 (b). The formation of carbonyl (C=O) group has weakened the CH_2 bonding as the oxidation occurs when applying with the electron beam irradiation (Gorelik et al., 1993). This result shows agreement in Figure 4.13 as the intensity of carbonyl groups (C=O) increased when irradiation doses higher.

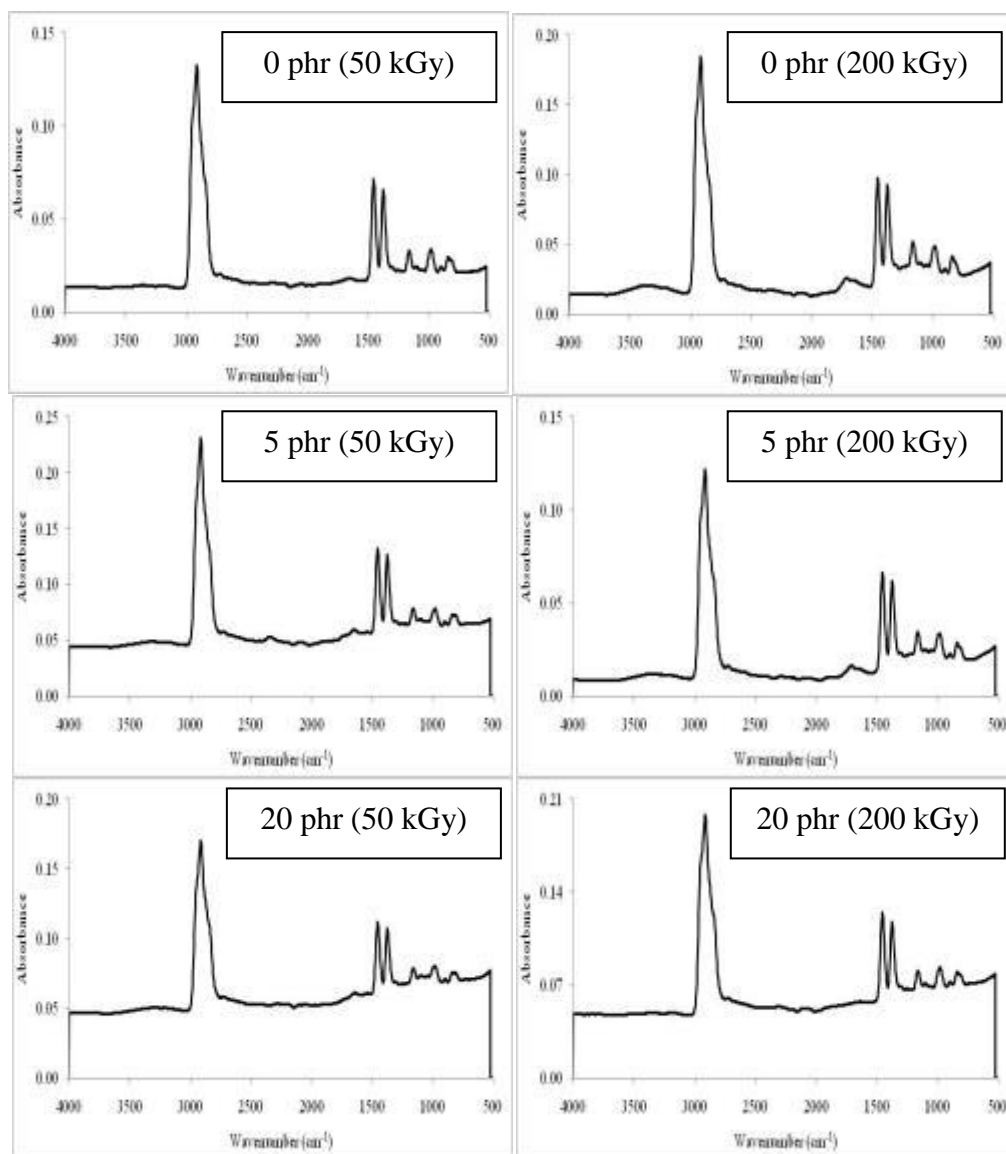


Figure 4.13: FTIR Absorption Spectra for Different DVC Composition of PP-DVC Compound before and after EB-Irradiation.

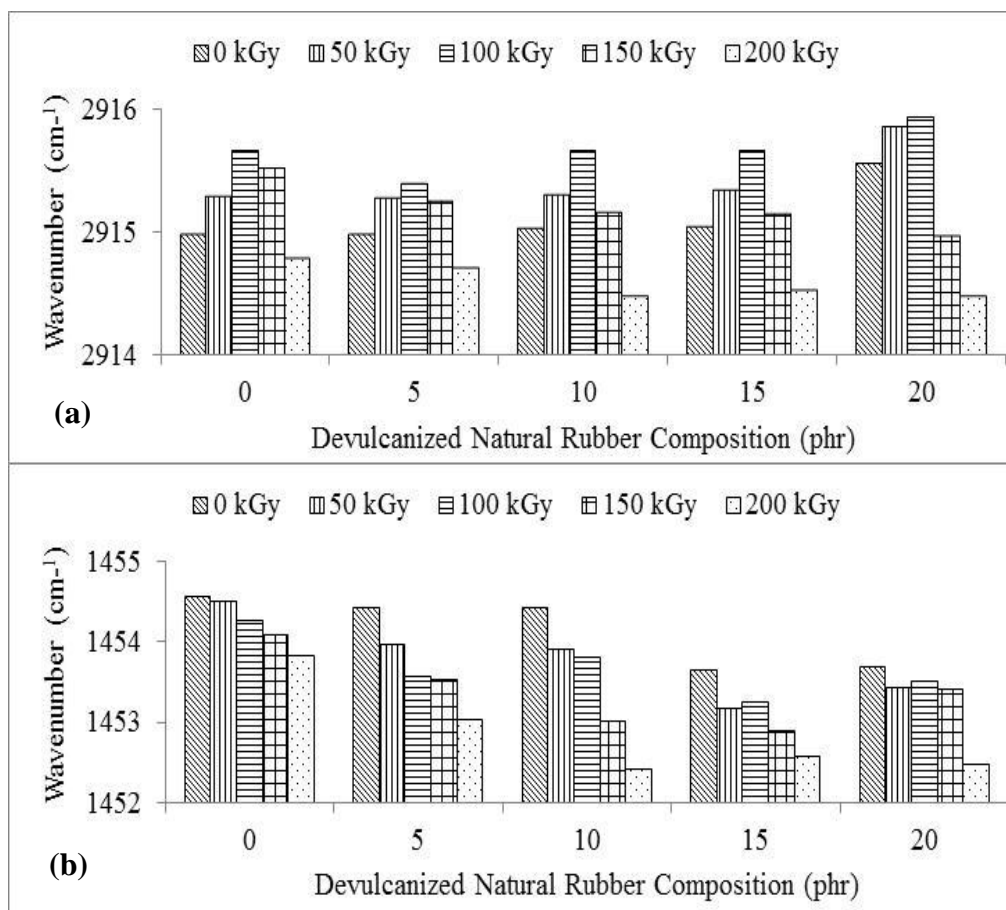


Figure 4.14: (a) Wavenumber of the Asymmetric C-H Stretching Vibration and (b) CH₂ Bending Vibration for Different DVC Composition of PP-DVC Compound before and after EB-Irradiation.

4.3 Effect of Devulcanized Natural Rubber Composition on the PP-DVC Compound upon Natural Weathering

4.3.1 Gel Content Test

With reference to the Figure 4.15, the gel content of the pristine PP gradually increased with longer exposure period. This result can be attributed to the increasing in cross-linking by photo-oxidation when exposed under sunlight caused the high rate of radical termination in the bulk of the polymer (Majid et al., 2010). As a result, the pristine PP has higher resistivity against the hot xylene attack when exposed to outdoor. Besides that, the post-weathering samples have higher gel content compared to pre-weathering samples. The exposure of UV radiation may give rise to the cross-linking networks formation in the PP matrix and reduced the solubility in hot xylene. Furthermore, it can be seen that with addition of DVC in PP could gradually increase the gel content when exposed to outdoor up to 4 months. The predominance of cross-linking under UV exposure has enhanced the interaction between DVC particles and PP matrix. However, the gel content of PP-DVC compounds reduced when further exposed to outdoor for 6 months. The predominance of chain scission by photo-oxidation has caused the DVC particles tend to agglomerated together in the PP matrix. This effect resulted in poor interaction between DVC particles and PP matrix and reduced the hot xylene attack resistance.

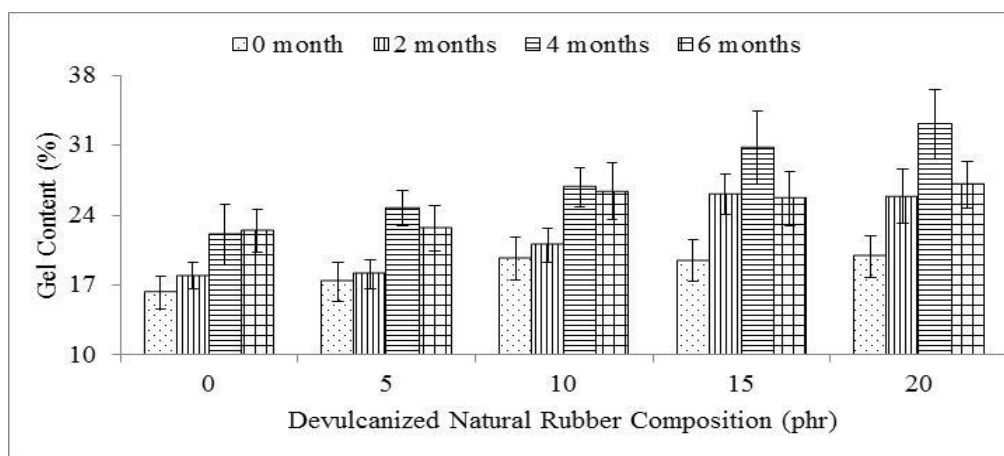


Figure 4.15: Gel Content for Different DVC Composition of PP-DVC Compound upon Natural Weathering.

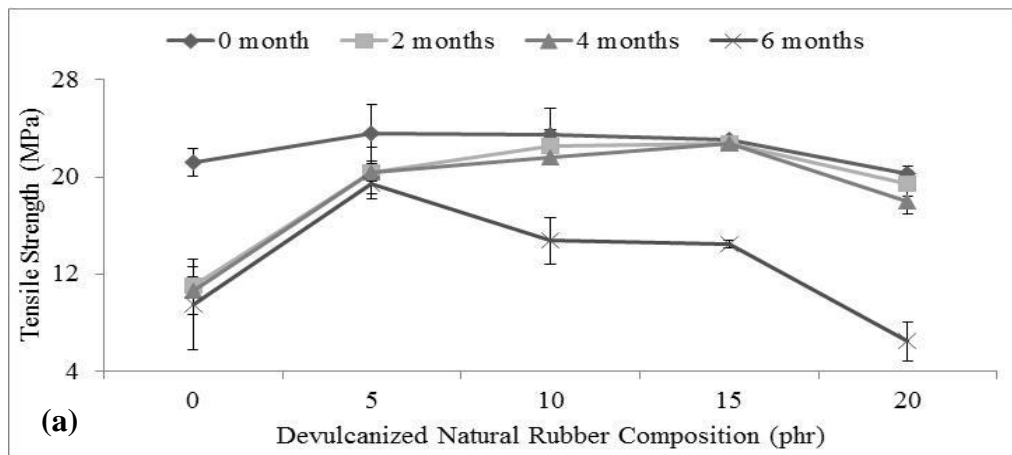
4.3.2 Tensile Test

With reference to Figure 4.16 (a), the tensile strength of pristine PP was reduced drastically with around 45 % after 6 months outdoor exposure. The photo-degradation process occurs by attacking the macromolecule and generated the free radicals at the tertiary C-atom of the PP chain under high energy of UV radiation from sunlight (Jose et al., 2014). This effect leads to chain scissioning process which molecular weight of the PP reduced. Thus, it reduced the tensile strength of the pristine PP. It is noteworthy that the addition of 5 phr DVC into PP matrix could give higher tensile strength than pristine PP after outdoor exposure. The existing of the carbon black particles in DVC acts as UV absorber and antioxidant by absorbing all the incident lights and inhibits photo-oxidation via its chemical properties (Amin, 2009). Therefore, it increased the ability of PP matrix to resist the straining stress. However,

further addition of DVC up to 20 phr into PP matrix could gradually reduce the tensile strength of the compounds after outdoor exposure. This is due to the DVC particles tend to agglomerate together at higher concentration and weaken the interaction between DVC and PP. Thus, this effect has deteriorated by the photo-degradation process and lower resistance against the straining stress.

With reference to Figure 4.16 (b), the Young's Modulus of the pristine PP reduced from 422.38 MPa to 337.53 MPa after 6 months outdoor exposure. The photo-degradation process could cause the chain scission of molecules by breaking down the tie chain molecules and entanglements in the amorphous region (Rabello and White, 1997). Thus, it has weakened the rigidity of pristine PP and induced it to change from ductile to the brittle material. Moreover, it can be noticed that the addition of DVC into PP could slightly increase the Young's Modulus of the compounds when exposed to outdoor for 2 months. This could be due to the photo-oxidation occurs with the increasing in cross-linking and the rate of radical termination increase in the bulk of the polymer where O₂ from photo-oxidation cannot gain access (Majid et al., 2010). Thus, it resulted in increasing the rigidity of the PP-DVC compound. In contrast, the Young's Modulus of the PP-DVC compounds gradually reduced with longer exposure period up to 6 months. This might be attributed to the predominance of the chain scission occurs during photo-oxidation process has caused the rate of radical termination reduced in the bulk of the polymer. Therefore, the rigidity of the PP-DVC compounds reduced as the chain scission leads to embrittlement of the materials.

With reference to Figure 4.16 (c), the elongation at break of the pristine PP and PP-DVC compounds reduced after exposed to outdoor for 6 months. The photo-degradation process caused the surface crack and defect as a result of disruption of crystalline order which in turn the crack become breakage concentrators (Jose et al., 2014). Therefore, it reduced the elongation ability of the PP matrix and accelerated the breakage of the PP matrix by straining stress applied. On the other hand, it is noteworthy that the addition of DVC up to 15 phr into PP exhibits a higher value of elongation at break compared to pristine PP. The incorporation of DVC into PP matrix could reduce resilience and toughness of the compounds because of its rubber-like properties (Mohamad et al., 2013). Thus, it increased the elongation ability of the PP- DVC compound under tensile stress. As per contra, 20 phr DVC added in PP after 6 months outdoor exposure exhibits the lowest elongation at break (2.39 %). The excessive of the DVC particles in PP matrix caused the uneven distribution of DVC particles in the compound. Hence, it limits the mobility and flow of the PP matrix when straining stress applied.



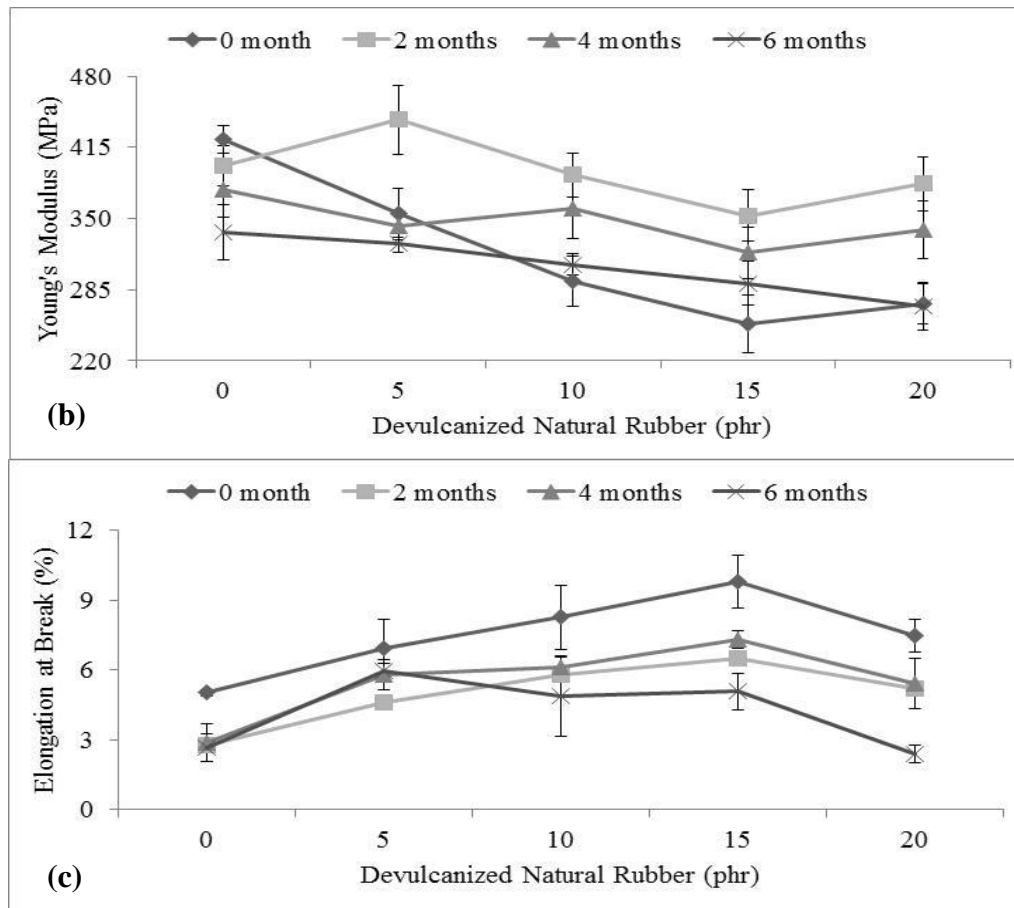


Figure 4.16: (a) Tensile Strength, (b) Young's Modulus and (c) Elongation at Break for Different DVC Composition of PP-DVC Compound Subject to Natural Weathering.

4.3.3 Impact and Hardness Test

With reference to the Figure 4.17 (a), the impact strength of the pristine PP reduced with around 60.7 % after exposed to outdoor for 6 months. The photo-oxidation process deteriorated the PP matrix by allowing a higher rate of oxygen penetration into the interior of PP. As a result, the deep crack surfaces formed and caused the polymer transforms from ductile to brittle

(Song et al., 2014). Thus, this effect leads to loss of its original toughness by embrittlement. Besides that, it was found that with the 5 phr of DVC added in PP exhibits the highest impact strength throughout the outdoor exposure. The incorporation of DVC in PP matrix at low composition level was able to enhance the DVC particles dispersed in PP matrix. It could delay the photo-degradation process by UV radiation towards the PP matrix where O₂ from photo-oxidation cannot gain access. As per contra, with further increase of DVC composition in PP up to 20 phr gradually reduced the impact strength of the compounds. The overdose of DVC particles in PP matrix could cause the poor dispersion and distribution of DVC particles in the matrix. Therefore, it has accelerated the photo-degradation process and weakens the ability to resist from the sudden load applied.

With reference to the Figure 4.17 (b), the hardness value of the pristine PP gradually reduced with longer exposure period. The predominance of chain scission caused the rate of radical termination reduced in the bulk of the polymer where O₂ able to gain access from photo-oxidation. As a result, it changes from ductile to brittle and losing its original toughness. Moreover, it can be noticed that the 5 phr DVC added in PP retains the highest hardness value. The addition of DVC in PP at low composition could enhance the distribution of DVC particles in PP matrix. Therefore, it could prolong the photo-degradation process by UV radiation from sunlight deteriorate the PP matrix. However, the hardness value of the PP-DVC compounds gradually reduced when further increases the DVC composition up to 20 phr. The DVC particles inclined to coalescence together in PP matrix at high composition.

Thus, this effect has accelerated the photo-degradation process by UV radiation towards the PP matrix and weakens the deformation resistance of the compound.

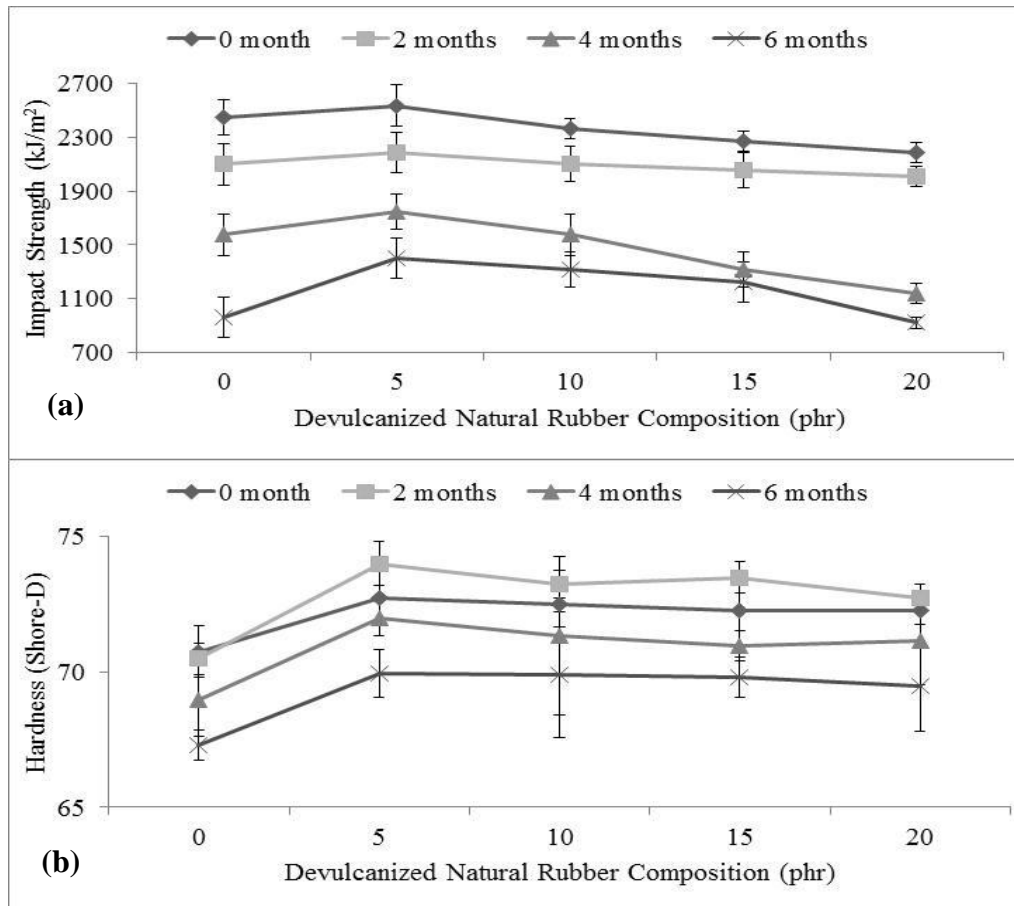


Figure 4.17: (a) Impact Strength and (b) Hardness for Different DVC Composition of PP-DVC Compound Subject to Natural Weathering.

4.3.4 XRD Analysis

XRD patterns for different DVC composition added in PP upon natural weathering are shown in Figure 4.18. It was found that the intensity of the five sharp peaks at $2\theta = 14.29^\circ$, 17.14° , 18.88° , 21.83° and 37.68° for all the PP-DVC compounds decreased after 6 months outdoor exposure. This might be due to the occurrence of chain scissioning by photo-oxidation caused the breakdown of the crystallite structure. For the 20 phr DVC added in PP, there is a new broad peak appears at $2\theta = 9.12^\circ$ (Peak B) after 6 months outdoor exposure. This might be attributed to the photo-oxidation caused the new crystallite structure establishment in the PP matrix at the high composition of DVC.

From Table 4.4, the d-spacing and inter-chain separation of pristine PP gradually expands with longer exposure period (≤ 4 months). This indicated that the predominance of cross-linking network occur by UV irradiation from sunlight in the PP matrix could transform the existing chains arrangement in PP matrix into the highly ordered crystalline structure. As per contra, the d-spacing and inter-chain separation of pristine PP slightly decreased when further exposed for 6 months. This could be due to the chain scission process occurs by photo-oxidation has caused the highly ordered crystalline structures in PP matrix break down into random crystalline structure. Other than that, the crystallize size and crystallinity of the pristine PP gradually increased with longer exposure period as shown in Table 4.4 and Figure 4.19 respectively. This might be caused by the molecular chains rupture along with the

segregation of entangled molecule segments and cross-link in the amorphous regions that were unable to crystallize during the original crystallization process. Then, these freed segments re-arranged in a crystalline phase to provide them enough mobility. This process is also known as chemi-crystallization (Rabello and White, 1997).

From Table 4.4, the d-spacing and inter-chain separation of the weathered PP-DVC compounds gradually increased when exposed to outdoor up to 4 months. This might be attributed to the photo-oxidation by UV exposure has caused the predominance of cross-linking network formed where O₂ cannot gain access in the PP matrix by enhancing the DVC particles dispersed in PP matrix. The d-spacing and inter-chain separation of the PP-DVC compound slightly reduced when further exposed to outdoor until 6 months. The longer UV exposure could reduce the effectiveness of DVC dispersed into PP matrix where the DVC particles inclined to agglomerate together in the PP matrix. Besides that, the crystallize size of all the PP-DVC compounds gradually increased with longer exposure period. The photo-oxidation under UV exposure has caused the re-orientation of the freed segments in the crystalline phase by chemi-crystallization and resulted in the expansion of the crystallize size for the PP-DVC compounds.

With reference to the Figure 4.19, it was found that the crystallinity of the PP-DVC compounds gradually increased when exposed to outdoor up to 4 months. This increment as a result of the photo-oxidation caused the re-arrangement of entangled molecule segments in the amorphous phase by

enhancing the regularity of PP (Ismail et al., 2008). However, when the PP-DVC compounds further outdoor exposed up to 6 months has reduced the crystallinity of the PP-DVC compounds. At longer exposure period, the chemical degradation of the PP takes place whereby the impurity groups formed such as carbonyls and hydroperoxides competes in the process of crystallinity change. These chemical groups then attached to the molecular segments and no longer fit into the crystal lattice. Therefore, it hindered the crystallization process and causing the crystallinity of the compounds reduced (Leong et al., 2004).

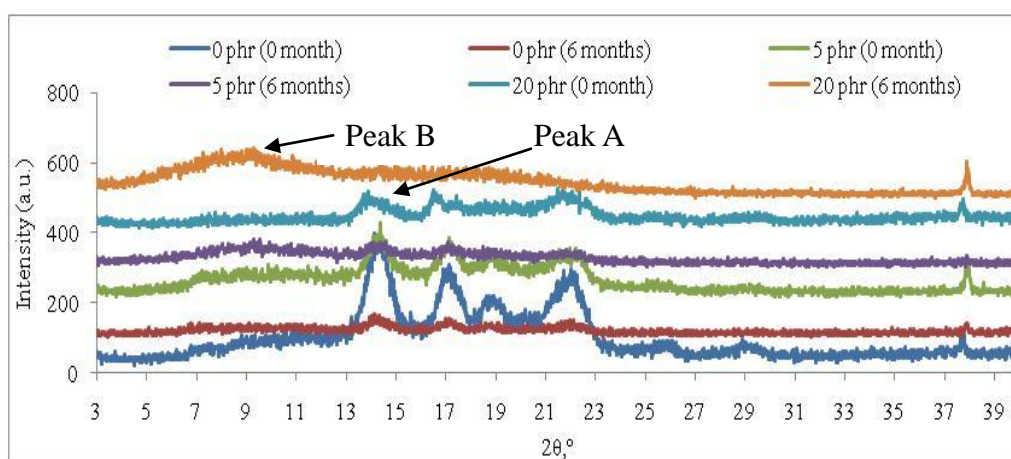


Figure 4.18: XRD Curve ($3^\circ \leq 2\theta \leq 40^\circ$) for Different DVC Composition of PP-DVC Compound before and after Natural Weathering.

Table 4.4: Inter-chain Separation, d-spacing and Crystallize Size for Different DVC Composition of PP-DVC Compound before and after Natural Weathering at Peak A.

DVC Composition, phr	Natural Weathering, month	$2\theta, ^\circ$	d- spacing, Å	Inter-chain Separation, Å	Crystallize Size, nm
0	0	14.29	6.19	7.75	70.05
	2	14.35	6.17	7.72	72.09
	4	14.28	6.20	7.75	83.48
	6	14.29	6.19	7.75	93.18
5	0	14.30	6.19	7.74	64.15
	2	14.33	6.18	7.73	81.78
	4	14.27	6.20	7.76	91.06
	6	14.30	6.19	7.74	100.17
10	0	14.25	6.21	7.77	60.79
	2	14.33	6.18	7.73	89.05
	4	14.26	6.21	7.76	97.73
	6	14.24	6.21	7.78	108.29
15	0	14.30	6.19	7.74	55.91
	2	14.32	6.18	7.73	83.48
	4	14.26	6.21	7.76	109.77
	6	14.26	6.21	7.76	112.87
20	0	14.35	6.17	7.72	62.61
	2	14.30	6.19	7.74	78.31

4	14.28	6.20	7.75	114.48
6	14.29	6.19	7.75	121.42

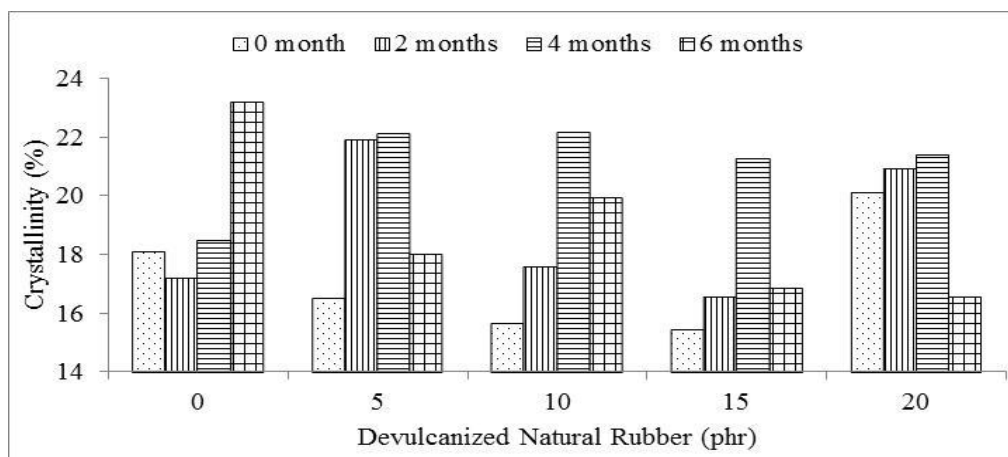
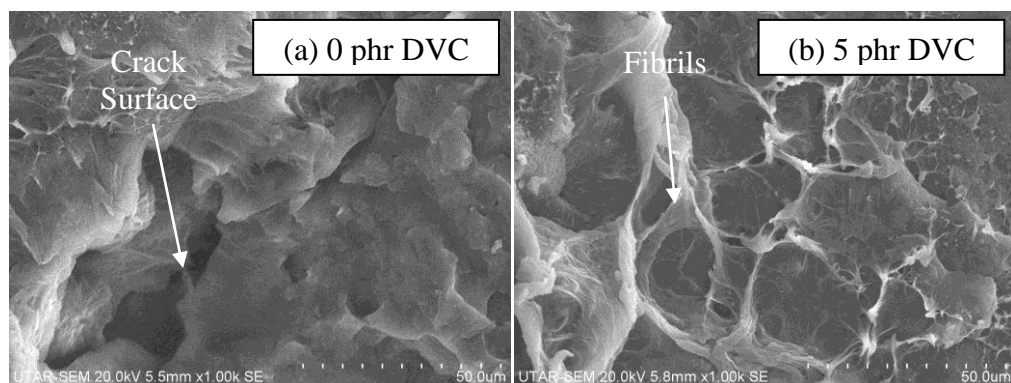


Figure 4.19: Crystallinity for Different Composition of PP-DVC Compound upon Natural Weathering.

4.3.5 SEM Analysis

Figure 4.20 represents SEM micrographs of the fractured surface for different DVC composition of PP-DVC compound after 6 months outdoor exposure. According to the Figure 4.20 (a), it can be noticed that the fractured surface of pristine PP exposed under sunlight for 6 months has severely deteriorated with large and long surface cracks formed. This might be due to the chemi-crystallization whereby the entangled segments and tie chain molecules release in the amorphous region that unable to crystallize during the original solidification process caused by molecular chain scission. Then, these freed segments re-arrange into a crystalline phase by providing them enough mobility resulted in a contraction of the surface layer by crack formation

(Rabello and White, 1997). With reference to Figure 4.20 (b), it can be seen that with the 5 phr of DVC added in the PP could improve the fractured surface with more fibrils formation as a better dispersion of DVC particles in PP. Moreover, the presence of carbon black particles in DVC caused the compound more resistant toward weathering as it acts as UV absorber and antioxidant by absorbing all the incident lights and inhibits photo-oxidation with its phenolic and quinoid groups (Ammala et al., 2002). However, the fractured surface of the PP-DVC compound become more flake-like appearance with further increasing of DVC up to 15 phr as depicted in Figure 4.20 (c) and Figure 4.20 (d). In fact, the photo-oxidation process has deteriorated the interaction between DVC and PP as the predominance of chain scission occurs. According to Figure 4.20 (e), it can be noticed that 20 phr DVC added in PP has a long crack surface formed after 6 months exposure. At the high concentration of DVC, it tends to agglomerate together and weakens the interaction between DVC and PP. Furthermore, photo-degradation process deteriorated the PP matrix and allowed a higher rate of oxygen penetration into the interior of the compound. As a result, long crack surface formed and weaken the structure of the compound.



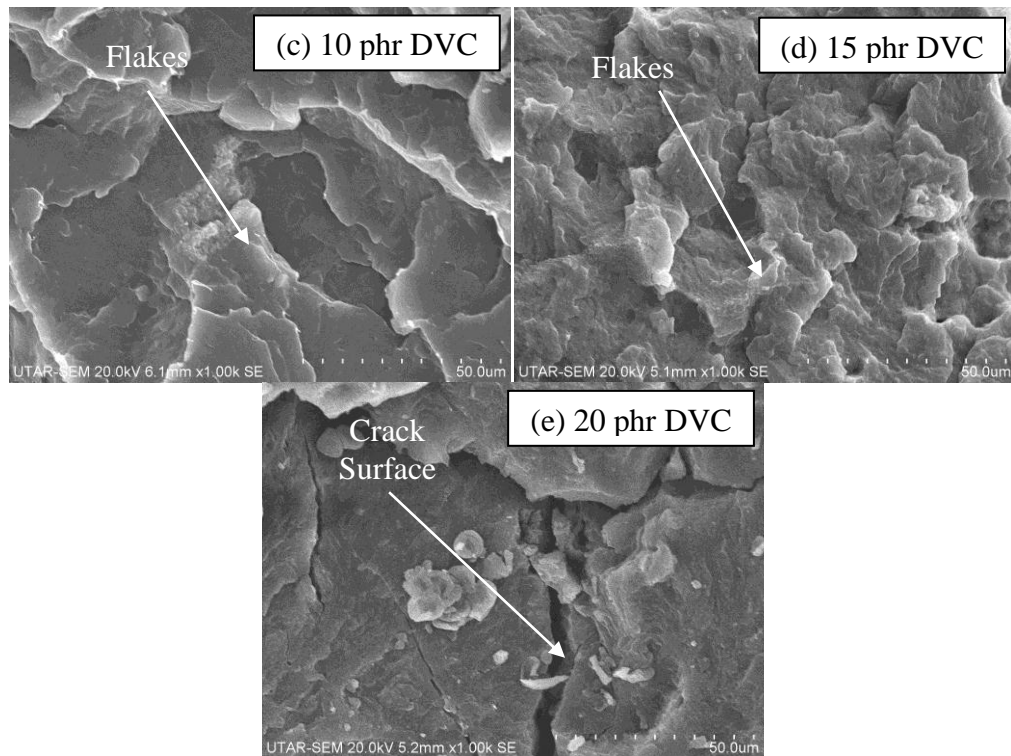


Figure 4.20: SEM Micrographs of Fractured Surface for Different DVC Composition of PP-DVC Compound after 6 Months Outdoor Exposure under Magnification of 1000x.

4.3.6 FTIR Analysis

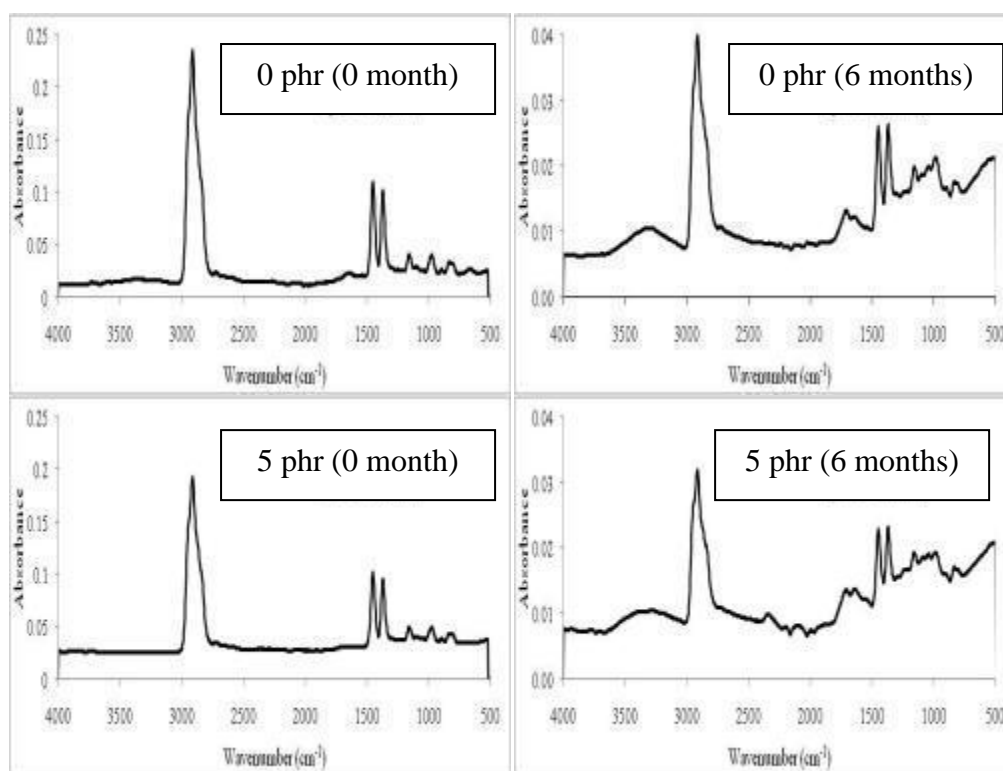
Figure 4.21 depicted the FTIR absorption spectra of the PP-DVC compound with different composition of DVC upon natural weathering made in the range of $4000 - 650 \text{ cm}^{-1}$. The appearance of the absorption peak at 3300 cm^{-1} and 1710 cm^{-1} corresponding to hydroxyl (O-H) and carbonyl (C=O) stretching vibration respectively represented that the photo-degradation occurs after 6 months outdoor exposure. It was found that the intensity of absorption peak around 2915 cm^{-1} assigned to asymmetric C-H stretching vibration reduced significantly after 6 months outdoor exposure due to the oxidation

occurs by photo-degradation lead to the formation of hydroxyl and carbonyl group. Furthermore, higher DVC composition could increase the intensity of the peak at 1640 cm^{-1} representing C=C stretching due to more C-C bonding formed by DVC particles with PP matrix.

With reference to Figure 4.22 (a), the wavenumber of asymmetric C-H stretching vibration for the addition of DVC composition up to 15 phr in PP gradually increased with longer exposure time. This result indicated that DVC particles dispersed and distribute better in the PP matrix has improved the stiffness of the matrix. Furthermore, carbon black particles in DVC absorb all the incident lights and inhibit photo-oxidation via its chemical properties. Therefore, photo-oxidation required higher energy to cause the vibrational effect of the asymmetric C-H stretching. However, the wavenumber for 20 phr DVC added in PP reduced upon natural weathering. This might be due to the DVC particles tend to agglomerate together at high concentration and weaken the interaction between DVC and PP. Thus, O_2 from photo-oxidation can easily gain access to PP matrix and weaken the C-H group bonding.

In order to further investigating the weathering effect to the different DVC composition of the PP-DVC compound, carbonyl index was used to indicate the amount of polymer chain scission in the compound as shown in Figure 4.22 (b). For the PP-DVC compound with less than 10 phr DVC composition, it can be noticed that the carbonyl index increase with longer exposure time. As expected, the polymer degradation takes place through the oxidation process due to the predominance of chain scission under UV

exposure. Moreover, the carbonyl formation for PP after weathering is proportional to the number of chain scissions that occur in the PP (Popa et al., 2013). In contrast, the carbonyl index for the 15 phr DVC added in PP and 20 phr DVC added in PP decreased after 6 months outdoor exposure. This might be caused by the overdose of the DVC particles in the PP matrix has reduced the carbonyl formation in PP. The carbon black particles in DVC can absorb all the incident lights and inhibit photo-oxidation via its chemical properties. Therefore, the number of chain scissions reduced as the excessive amount of DVC has delayed the degradation of the polymer.



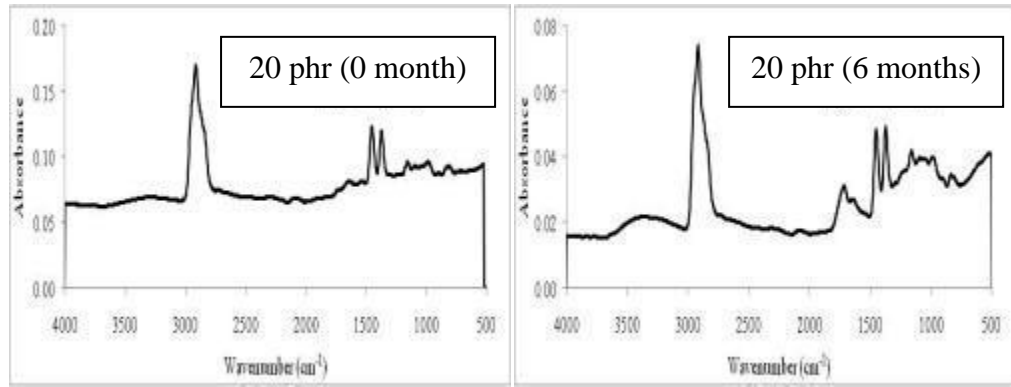


Figure 4.21: FTIR Absorption Spectra of PP-DVC Compound with Different Composition of DVC before and after Natural Weathering.

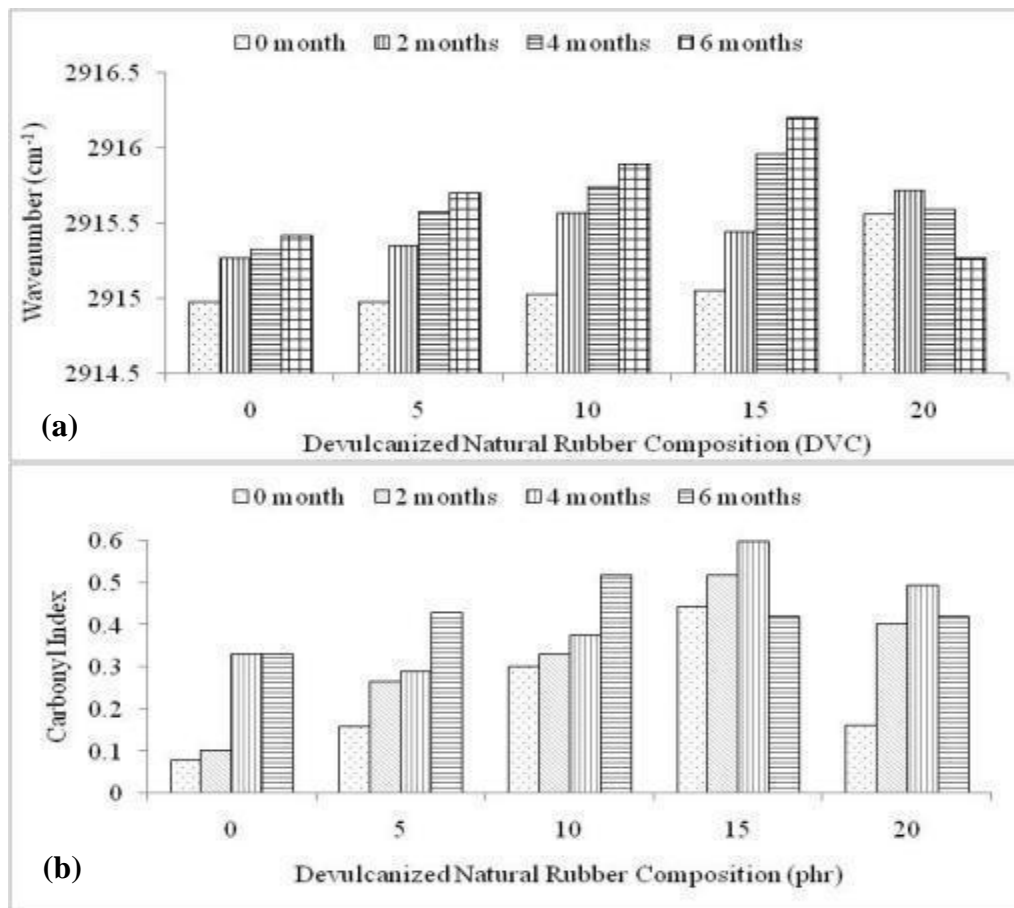


Figure 4.22: (a) Wavenumber of the Asymmetric C-H Stretching Vibration and (b) Carbonyl Index for Different DVC Composition of PP-DVC Compound before and after Natural Weathering.

4.4 Effect of Electron Beam Irradiation on the PP-DVC Compound upon Natural Weathering

4.4.1 Gel Content Test

Figure 4.23 shows the different irradiation dosages influence on the gel content of the 5 phr DVC added in PP compound subject to natural weathering. It was found that the gel content of 5 phr DVC added in PP irradiated at 50 kGy increased with longer exposure period. At low irradiation dosages, the predominance of cross-linking formation by photo-oxidation under UV exposure was promoting a more extensive three dimensional network formation via a substantial reaction with the larger amount of free radicals. In contrast, the gel content 5 phr DVC added in PP has decreased with the irradiation dosages increasing up to 200 kGy at 6 months outdoor exposure. This might be caused by the polymer degradation by the oxidation of the polymers under UV exposure. Thus, it could cause the chain scission on larger molecular chains which in turn the number of shorter chains increases in the polymer.

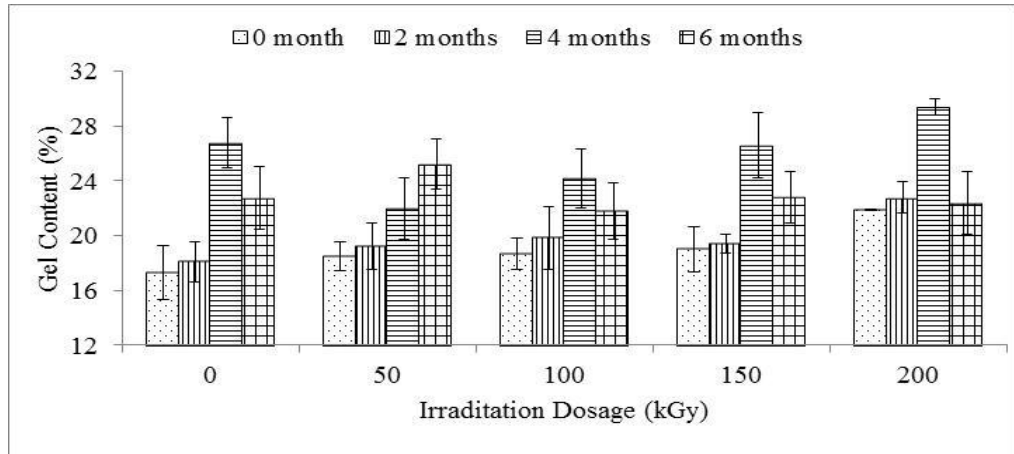


Figure 4.23: Gel Content for 5 phr DVC added in PP Compound with Various Irradiation Dosages Subject to Natural Weathering.

4.4.2 Tensile Test

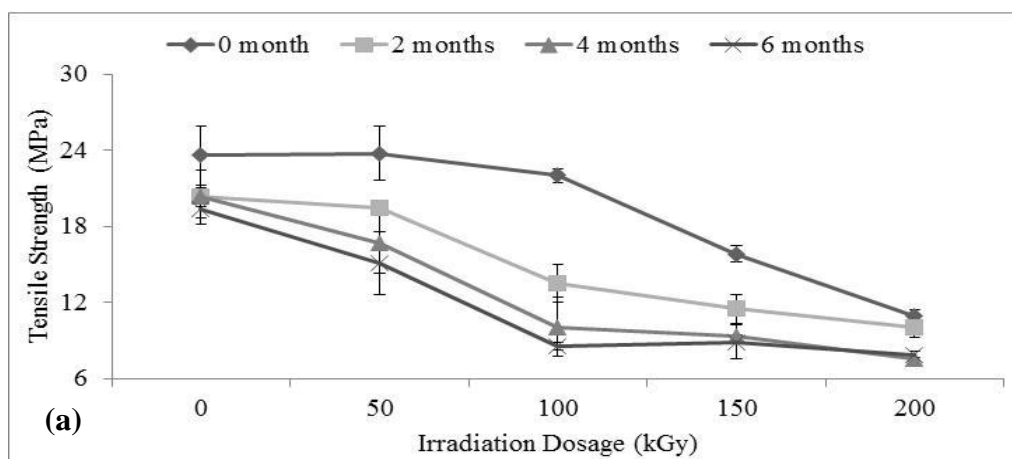
Figure 4.24 (a) shows the different irradiation dosages influence on the tensile strength of 5 phr DVC added in PP compound subject to natural weathering. The tensile strength of the non-irradiated PP-DVC compounds higher than the irradiated PP-DVC compounds when exposed to outdoor. This might be due to excessive cross-linking with the DVC particles together with the degradation in the PP phase occurred during outdoor exposure (Noriman and Ismail, 2011). Thus, it reduced the ability of PP matrix to resist the straining stress. Unlike the irradiated samples before weathering, the tensile strength of the irradiated samples after weathering reduced with higher irradiation dosages. This result is expected as the presence of surface microcracks induced by UV radiation exposure (Kumar et al., 2002). These microcracks only concentrated near the compound's surface and the process mainly occurs in the amorphous region as a result of high permeability to

oxygen (Majid et al., 2010). Eventually, these microcracks act as breakage concentrators and bring down the ability of the PP matrix to resist from straining stress.

Figure 4.24 (b) shows the Young's Modulus different irradiation dosages for 5 phr DVC added in PP compound subject to natural weathering. It was found that the Young's Modulus of the irradiated PP-DVC compounds higher than non-irradiated PP-DVC compounds after 6 months outdoor exposure. This was attributed to the photo-oxidation has caused the embrittlement effect in the compounds. Chemical degradation and water absorption could take place with longer exposure time by developing more surface cracks. Acidic rainwater and moisture can attack on the polymer bonds by seeping through the cavities of the surface cracks (Leong et al., 2004). With the surface cracks formed could deteriorate the rigidity of the compounds. Furthermore, it was found that Young's modulus of the irradiated samples before weathering higher than the irradiated samples after weathering. This might be due to the polymer degradation takes place with the predominance of chain scission under UV exposure through the oxidation of the polymers. Chain scission on the larger molecular chains could significantly increase the amount of shorter chains in the polymer which could give rise to few entanglements and caused an increase in brittleness of the compounds (Ismail et al., 2008).

Figure 4.24 (c) shows the elongation at break different irradiation dosages for 5 phr DVC added in PP compound subject to natural weathering.

For the irradiated samples after weathering, it was found that the elongation at break lower than non-irradiated samples after weathering. This result was caused by the photo-oxidation in which extensive chain scission occurs in the irradiated samples where the chain molecules and entanglements break down. It resulted in the ductility of the polymer reduce and lead to low breaking resistant (Al-Shabanat, 2011). Moreover, it was found that the elongation at break of the irradiated samples after weathering lower than the irradiated samples before weathering. The longer exposure period could accumulate the aromatic compounds on the surface of the samples by the pollution. These aromatic compounds then combined with hydroperoxides as well as carbonyl groups during photo-oxidation. This phenomenon could lead to the embrittlement of the compounds. Other than that, the formation of surface cracks caused the stress concentration points also favours in crack propagation rather than ductile yielding as the dominant failure mechanism (Leong et al., 2004).



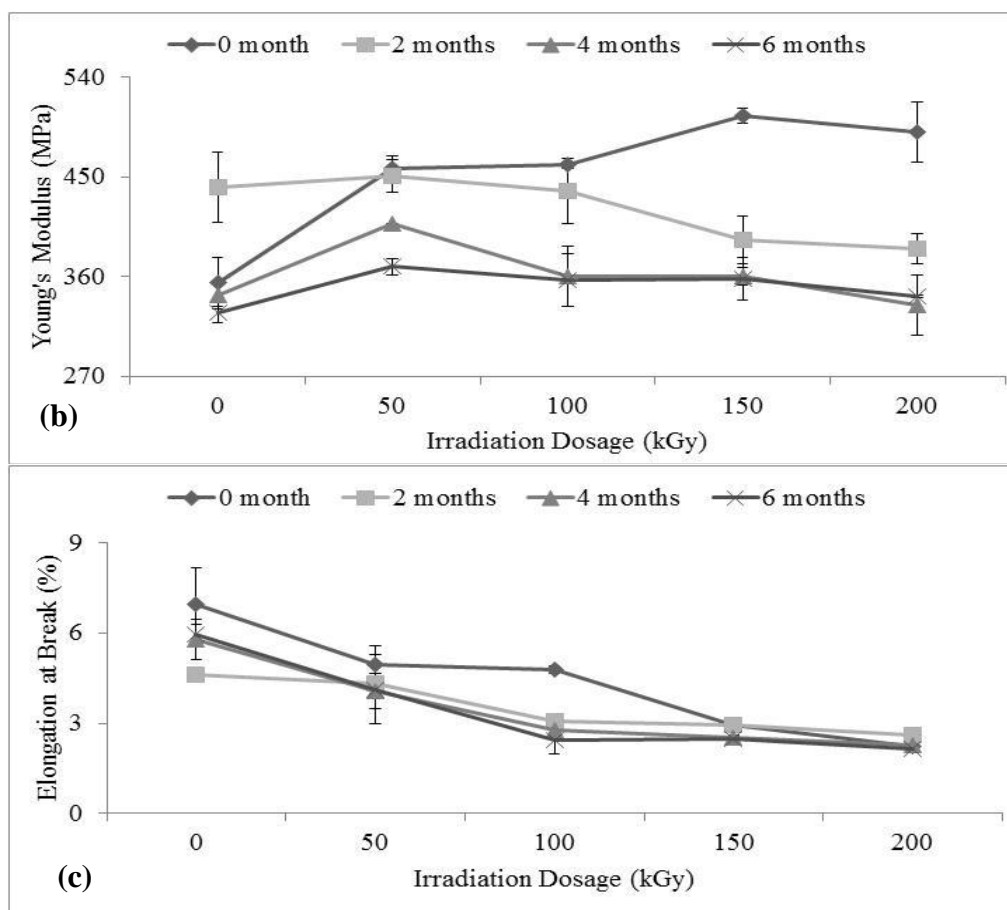


Figure 4.24: (a) Tensile Strength, (b) Young's Modulus and (c) Elongation at Break for 5 phr DVC added in PP Compound with Various Irradiation Dosages Subject to Natural Weathering.

4.4.3 Impact and Hardness Test

Figure 4.25 (a) shows the different irradiation dosages influence on the impact strength of 5 phr DVC added in PP compound subject to natural weathering. As seen in the figure, the impact strength of the non-irradiated and irradiated PP-DVC compounds gradually reduced with longer exposure time. As expected, the photo-oxidation under UV exposure could break down the

chain molecules and entanglements due to the extensive chain scission in the irradiated samples. Thus, it resulted in transition of the polymer from ductile to brittle and losing its original toughness. Moreover, the impact strength of PP-DVC compound slightly increased with irradiation dosage of 50 kGy after 6 months outdoor exposure. The preference of the cross-linking network in the PP matrix at low irradiation dosage under UV exposure has increased the toughness of the compounds. In contrast, the impact strength of PP-DVC compounds with further irradiation dosages up to 200 kGy gradually reduced when exposed to outdoor for 6 months. The predominance of chain scission at high irradiation dosages under UV exposure has caused the polymer degradation and resulted in toughness of the compounds reduced.

Figure 4.25 (b) shows the hardness of different irradiation dosages for 5 phr DVC added in PP compound subject to natural weathering. Generally, the hardness value of the PP-DVC compounds has the similar trend with impact strength. The hardness value of the non-irradiated and irradiated PP-DVC compounds gradually reduced with longer exposure time due to the photo-oxidation under UV exposure has changed the polymer from ductile to brittle and resulted in lower resistance to deform when a compressive force is applied. Besides that, the hardness value of the PP-DVC compound slightly higher with irradiation dosages up to 50 kGy after 6 months outdoor exposure. This might be caused by the predominance of the cross-linking network in the PP matrix at low level of irradiation dosage under UV irradiation has increased the deformation resistance of the compounds. In contrast, the hardness value of the PP-DVC compounds with further irradiation dosages up to 200 kGy

gradually reduced after 6 months outdoor exposure. The preference of chain scission at high irradiation dosages under UV exposure where O₂ gain access in the PP matrix has caused the polymer degradation and lead to lower deformation resistance when a compressive force is applied.

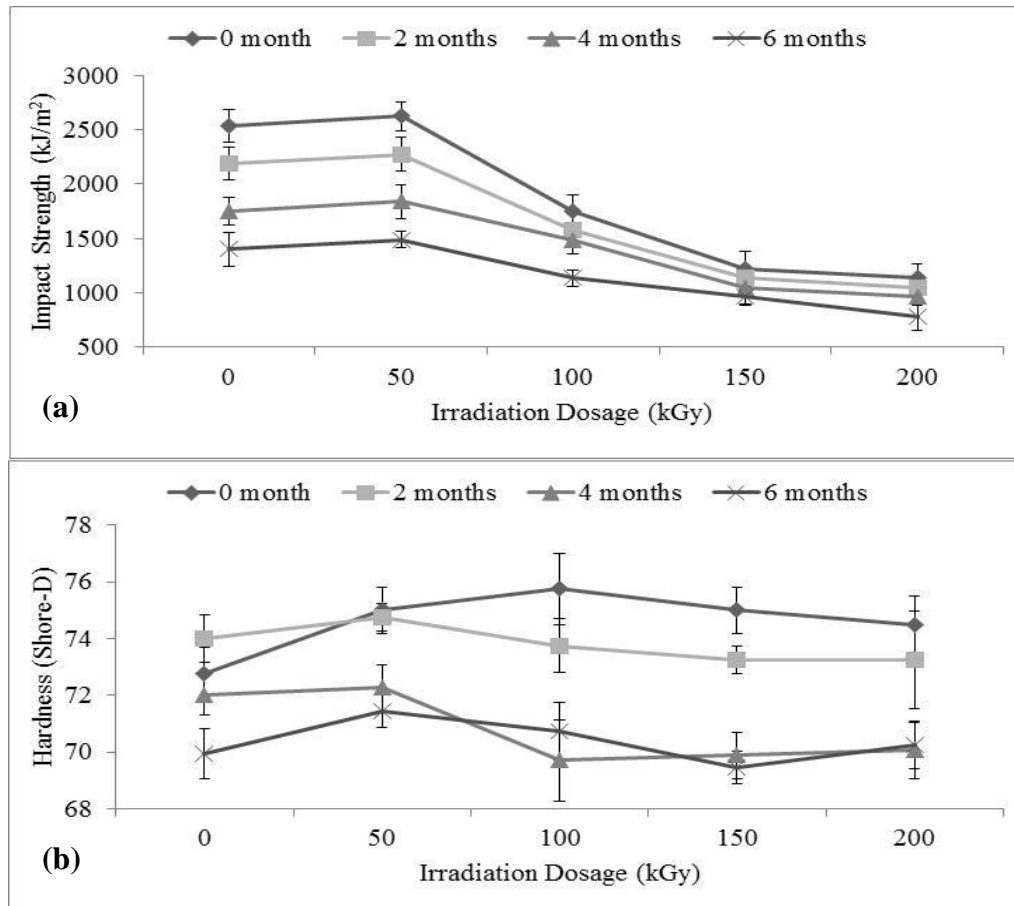


Figure 4.25: (a) Impact Strength and (b) Hardness for 5 phr DVC added in PP Compound with Various Irradiation Dosages Subject to Natural Weathering.

4.4.4 XRD Analysis

XRD patterns for 5 phr DVC added in PP subject to various irradiation dosages upon natural weathering are depicted in Figure 4.26. As seen in the figure, the intensity of the five sharp peaks at $2\theta = 14.29^\circ$, 17.14° , 18.88° , 21.83° and 37.68° for the PP-DVC compounds decreased after 6 months outdoor exposure. This might be due to the occurrence of chain scission by photo-oxidation caused the breakdown of the crystalline structure. The d-spacing and inter-chain separation of the irradiated 5 phr DVC added in PP gradually increased with longer exposure period (≤ 4 months) as shown in Table 4.5. This indicated that the predominance of cross-linking network occur by UV irradiation from sunlight where O_2 cannot gain access in the PP matrix lead to enhancement of DVC particles dispersion in PP matrix. However, further exposed to outdoor up to 6 months caused the d-spacing and inter-chain separation of irradiated 5 phr DVC added in PP slightly decreased. The preference of the chain scission by photo-oxidation where O_2 gain access in PP matrix caused the reduction of effectiveness of DVC distributed in PP lead to the highly ordered crystalline structures in PP matrix breakdown. Furthermore, the crystallize size gradually increased with longer exposure period as shown in Table 4.5. The photo-degradation by UV exposure caused the chain arrangement around crystalline structure re-orientated lead to an expansion of the crystallize size for the irradiated 5 phr DVC added in PP.

Besides, the crystallinity of the irradiated 5 phr DVC added in PP (≤ 150 kGy) gradually increased with outdoor exposure period up to 4 months as

shown in Figure 4.27. This might be due to the cross-linking networks formed by UV exposure dominate in the PP matrix resulted in the higher effectiveness of DVC dispersed into PP matrix to form highly ordered crystalline structure. In contrary, the crystallinity of the irradiated 5 phr added in PP (≤ 150 kGy) reduced when further exposed to outdoor for 6 months. This result indicated that photo-oxidation could cause the degradation of the PP matrix by chain scission and lead to poor dispersion of DVC particles in PP matrix when exposed to outdoor for a longer period. Therefore, it resulted in the DVC particles inclined to agglomerate together in the PP matrix and the highly ordered chain arrangement of crystalline structure breakdown. For the 5 phr DVC added in PP irradiated at 200 kGy, the crystallinity gradually increased with longer exposure period as depicted in Figure 4.27. The chemi-crystallization is the molecular chains rupture along with segregation of entangled molecule segments and cross-link in the amorphous regions that were unable to crystallize during the original crystallization process. Then, rearrangement of these freed segments in a crystalline phase which provided them enough mobility and give rise to the higher crystallinity in the compounds (Rabello and White, 1997).

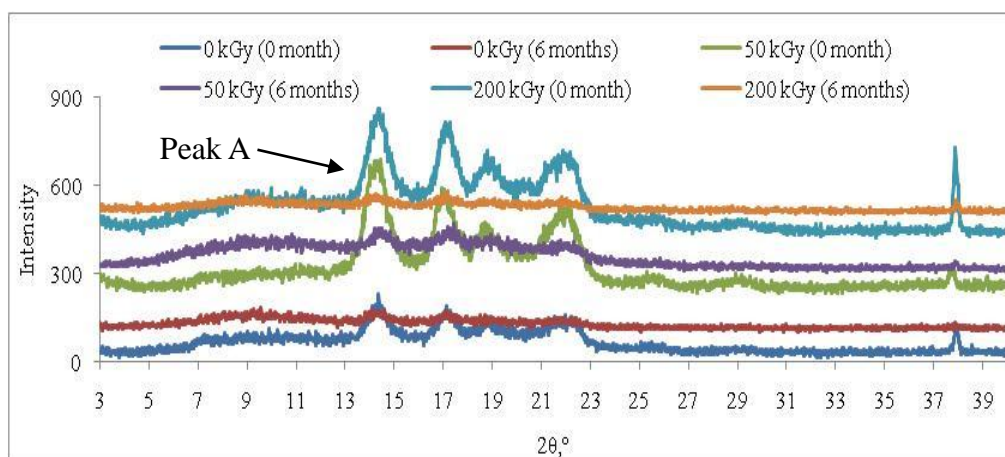


Figure 4.26: XRD Curve ($3^\circ \leq 2\theta \leq 40^\circ$) for 5 phr DVC added in PP at Various Irradiation Dosages before and after 6 Months Outdoor Exposure.

Table 4.5: Inter-chain Separation, d-spacing and Crystallize Size for 5 phr DVC added in PP at Various Irradiation Dosages before and after Natural Weathering at Peak A.

Irradiation Dosage, kGy	Natural Weathering, month	$2\theta, ^\circ$	d-spacing, Å	Interchain Separation, Å	Crystallize Size, nm
0	0	14.30	6.19	7.74	64.15
	2	14.33	6.18	7.73	81.78
	4	14.27	6.20	7.76	91.06
	6	14.30	6.19	7.74	100.17
50	0	14.27	6.20	7.76	64.14
	2	14.39	6.15	7.69	79.09
	4	14.36	6.16	7.71	95.41
	6	14.42	6.14	7.68	100.19
100	0	14.35	6.17	7.72	60.79

	2	14.38	6.15	7.70	78.45
	4	14.28	6.20	7.75	83.48
	6	14.55	6.08	7.61	95.43
150	0	14.36	6.16	7.71	55.92
	2	14.41	6.14	7.68	77.31
	4	14.32	6.18	7.73	83.48
	6	14.26	6.21	7.77	92.11
200	0	14.33	6.18	7.73	62.61
	2	14.42	6.14	7.68	74.91
	4	14.22	6.22	7.79	77.05
	6	14.29	6.19	7.75	85.25

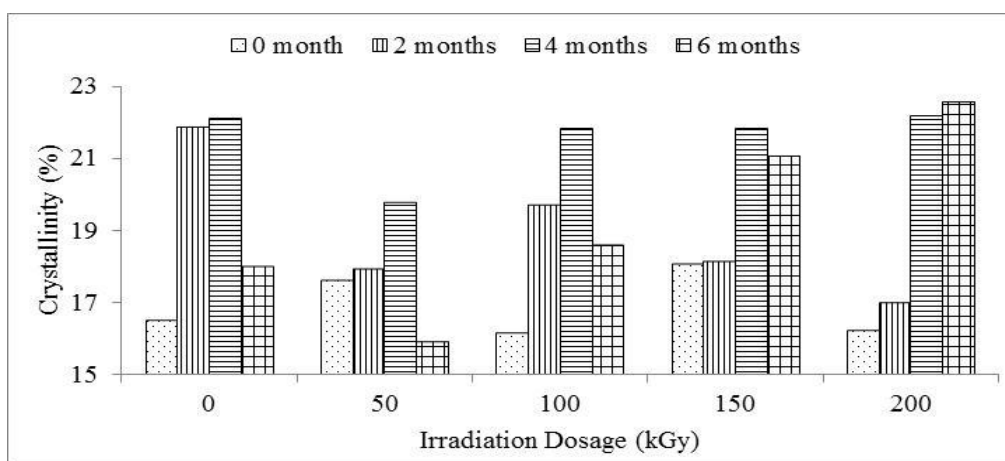


Figure 4.27: Crystallinity for 5 phr DVC added in PP at Various Irradiation Dosages upon Natural Weathering.

4.4.5 SEM Analysis

Figure 4.28 represents SEM micrographs of the fractured surface for different irradiation dosages of 5 phr DVC added in PP compound before and after natural weathering. Figure 4.28 (a) and Figure 4.28 (b) show with the addition of 5 phr DVC in the PP matrix exposed to outdoor 6 months has reduced the amount of tear lines formation on the fractured surface due to the photo-oxidation by UV exposure. The number of shorter chains in the polymer increase as the chain scission on the larger molecular chains and lead to few entanglements (Ismail et al., 2008). Thus, it reduced the plastic deformation ability of the PP matrix during straining stress applied on it. Besides that, the fractured surface of 5 phr DVC added in PP with 50 kGy doses has changed from tear lines appearance to flake-like appearance after exposed to outdoor for 6 months as shown in Figure 4.28 (c) and Figure 4.28 (d). In fact, the predominance of chain scission under UV exposure could cause the polymer degradation and reduced the filler-matrix interaction. The chain scissioning process has reduced the continuities of the PP matrix resulted in lower plastic deformation of the PP matrix. Therefore, the DVC particles inclined to agglomerate together in the PP matrix. The fractured surface of 5 phr DVC added in PP with 200 kGy doses has changed from the flake-like surface to a deep crack surface after 6 months weathering as depicted in Figure 4.28 (e) and Figure 4.28 (f). This result is expected due to the reduction of interaction between DVC and PP and DVC particles tend to agglomerate together at high irradiation dosages. Other than that, a high degree of photo-oxidation could form extensive microcracks on the surface and allowed high oxygen penetration into the interior of the compounds (Ismail et al., 2008). As a result,

weak interaction between DVC particles and PP matrix coupled with photo-oxidation and consequently deteriorates the mechanical properties of the compounds.

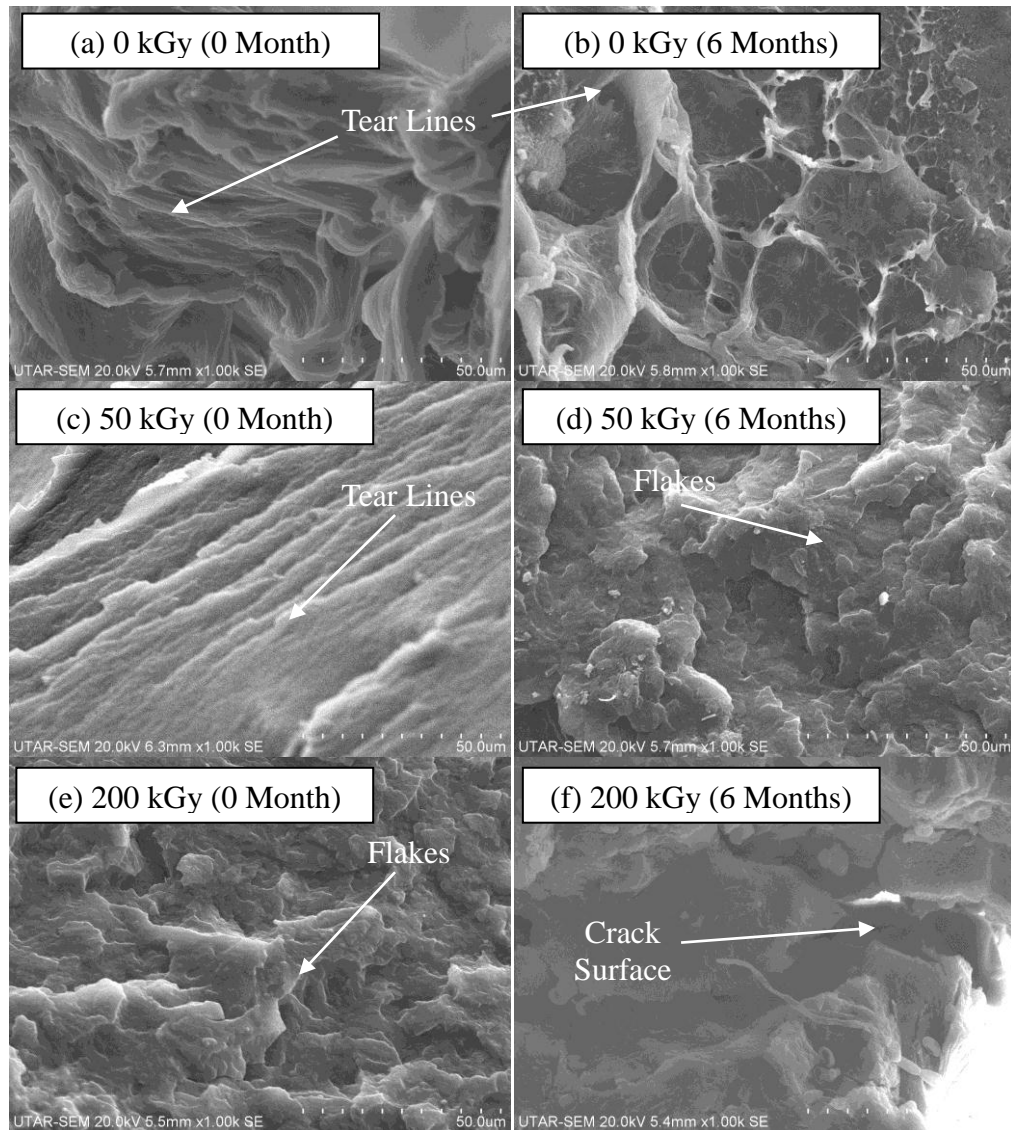


Figure 4.28: SEM Micrographs of Fractured Surface for Different Irradiation Dosages of 5 phr DVC added in PP before and after Natural Weathering under Magnification of 1000x.

4.4.6 FTIR Analysis

Figure 4.29 depicted the FTIR absorption spectra of the 5 phr DVC added in PP with different irradiation dosages before and after natural weathering made in the range of 4000 - 650 cm^{-1} . The appearance of new absorption broad peak at 3300 cm^{-1} which is O-H stretching vibration indicated that the oxidation process occurs by photo-oxidation after 6 months outdoor exposure. According to Figure 4.29, strong absorption peak around 2915 cm^{-1} assigned to asymmetric C-H stretching vibration. Besides, the intensity of the absorption peak at 1710 cm^{-1} which is C=O stretching vibration increased when exposed to outdoor for 6 months. This is due to the oxidation process from photo-oxidation occurs the formation of ketonic and aldehydic carbonyl groups. Moreover, the intensity of the peak at 1650 cm^{-1} representing C=C stretching increased after 6 months outdoor exposure as shown in Figure 4.29. This effect as a result of more DVC particles formed C=C bonding in the PP matrix when under UV exposure.

With reference to Figure 4.30 (a), the wavenumber of asymmetric C-H stretching vibration for irradiated PP-DVC compounds (≤ 50 kGy) gradually increased with longer exposure time. This might be caused by the preference of the cross-linking network in the PP matrix at low level of irradiation dosage under UV exposure. This effect enhanced the intermolecular bonding of the PP-DVC compounds and thus required higher energy to allow the vibrational effect of the C-H stretching (Tee et al., 2013). In contrast, the wavenumber of asymmetric C-H stretching vibration for irradiated PP-DVC compounds (> 50 kGy) increased up to 2 months exposure period. Then, the wavenumber begins

to decrease when further exposed to outdoor up to 6 months. The predominance of chain scission by photo-oxidation caused the attractive forces between atoms in the PP chains breakdown and further diminishes the intermolecular bonding of the PP-DVC compound. Thus, it required low energy to enabling the vibrational effect the C-H stretching.

In order to further investigating the weathering effect to the PP-DVC compounds, carbonyl index was used as an indicator of the polymer chain scission as depicted in Figure 4.30 (b). It was found that the carbonyl index increased with longer exposure period regardless irradiation dosages. As expected, the predominance of chain scission under UV exposure has caused the polymer degradation occurred through the oxidation of the polymers. The carbonyl formation for PP after weathering is increasing proportional to the number of chain scission that occurred in the PP (Stark and Matuana, 2004). The carbonyl index of the 5 phr DVC added in PP compound decreased up to 50 kGy when exposed to outdoor for 6 months. This might be caused by the predominance of the cross-linking network in the PP matrix at low level of irradiation dosage under UV exposure. Therefore, it reduced the number of chain scission in PP resulted in lower number of carbonyl index. As per contra, the carbonyl index increased with the irradiation dosages further increasing up to 200 kGy. This elevation of carbonyl index caused by the chain scission occurred at high irradiation dosages under UV exposure.

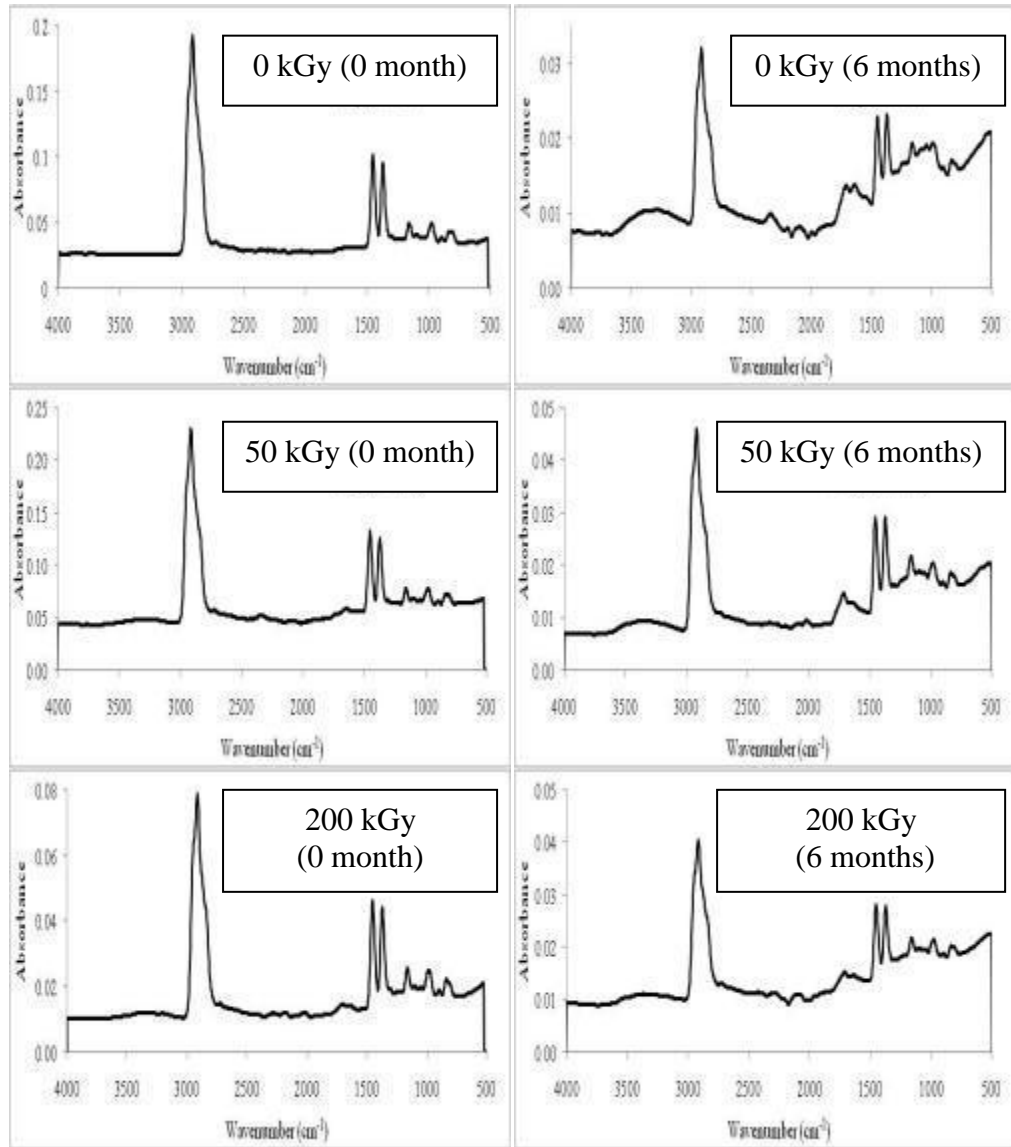
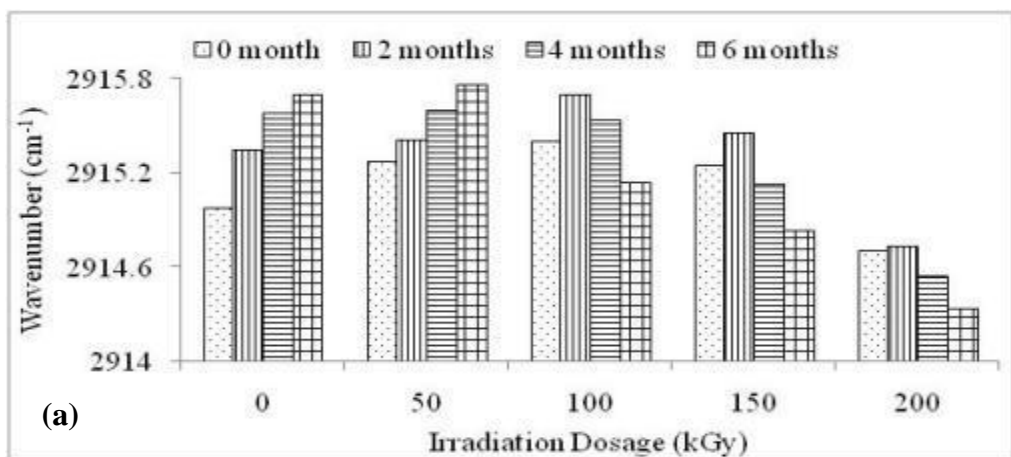


Figure 4.29: FTIR Absorption Spectra of 5 phr DVC added in PP at Various Irradiation Dosages before and after Natural Weathering.



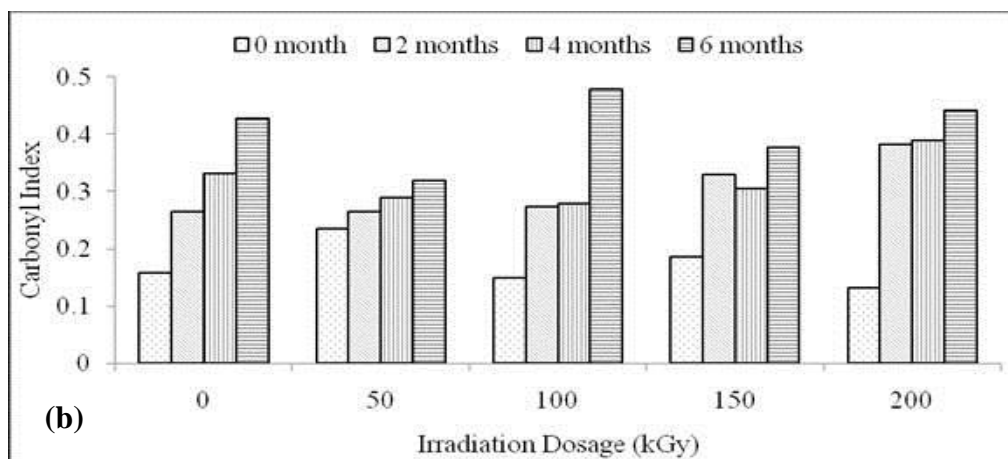


Figure 4.30: (a) Wavenumber of the Asymmetric C-H Stretching Vibration and (b) Carbonyl Index for 5 phr DVC added in PP Compound at Various Irradiation Dosages upon Natural Weathering.

CHAPTER 5

CONCLUSION

5.1 Conclusion

The performance of DVC composition, EB-irradiation and UV source degradation in relation to the performance of the PP-DVC compound were investigated. Various DVC compositions (0 phr – 20 phr) were compounded with PP and irradiated at several dosages (0 kGy – 200 kGy) under natural weathering condition (0 month – 6 months). It was found that with the addition of 5 phr DVC added in PP irradiated at 50 kGy has the optimum value of the mechanical properties after 6 months outdoor exposure. It could provide better tensile strength, impact strength and hardness value as the DVC particles dispersed better in PP matrix. The gel content increased with longer exposure period due to a more extensive three-dimensional network formation via a substantial reaction with the larger amount of free radicals promotes at low irradiation dosages. There is an expansion of crystallize size caused by the photo-oxidation where the chain arrangement around crystalline structure re-orientated. However, the intensity of the peaks and crystallinity reduced after outdoor exposure due to the photo-oxidation occurs has broken down the crystalline structure in the PP matrix. Furthermore, the fractured surface has changed from tear lines appearance to flake-like appearance because of the UV exposure has caused the polymer degradation and reduced the filler-matrix

interaction. Furthermore, the appearance of two new peaks at 1710 cm^{-1} and 3300 cm^{-1} which are C=O stretching vibration and O-H stretching vibration indicated that irradiation process occurs by electron beam irradiation and photo-oxidation under UV exposure.

5.2 Future Works

There are several additional works can be done in order to further investigate the performance of DVC composition, EB-irradiation and UV degradation on the PP-DVC compounds. Firstly, lower DVC compositions such as 0 – 5 phr can be used to blend with PP as lower composition give better dispersion and distribution effect in the PP matrix. Besides that, the PP-DVC compound can be irradiated at lower irradiation dosages such as 0 – 50 kGy to reduce the occurrence of chain scission process by EB-irradiation. Furthermore, with the addition of cross-linking agent such as TMPTMA in the PP-DVC compound to improve the mechanical properties. With the addition of an antioxidant agent such as HALS in the PP-DVC compound to improve the weather-resistant ability when exposed to natural weathering.

REFERENCES

- Adhikari, B. and Maiti, D. D. S., 2000. Reclamation and Recycling of Waste Rubber. *Progress in Polymer Science*, 25, pp. 909-948.
- Ahmad, A., Dahlan, H. M. and Abdullah, I., 2005. Electron Beam Cross-linking of NR/LLDPE Blends. *Iranian Polymer Journal*, 14(6), pp. 505-510.
- Ahmad, I., Chong, E. L., Dahlan, H. M. and Abdullah, I., 2012. Electron-Beam-Irradiated Rice Husk Powder as Reinforcing Filler in Natural Rubber / High-Density Polyethylene (NR / HDPE) Composites. *Composites: Part B*, 43, pp. 3069-3075.
- Akhtar, S., De, P. P. and De, S. K., 1986. Tensile Failure of γ -Ray Irradiated Blends of High-Density Polyethylene and Natural Rubber. *Journal of Applied Polymer Science*, 32, pp. 4169-4183.
- Amin, A., 2009. Synergistic Effect of TNPP and Carbon Black in Weathered XLPE Materials. *Journal of Polymers and the Environment*, 17, pp. 267-272.
- Ammala, A., Hill, A. J., Pas, S. J. and Turney, T. W., 2002. Degradation Studies of Polyolefins Incorporating Transparent Nanoparticulate Zinc Oxide UV Stabilizers. *Journal of Nanoparticle Research*, 4, pp. 167-174.
- Atieh, M. A., Nazir, N., Yusof, F., Fettouhi, M., Ratnam, C. T., Alharthi, M., Faraj, A. A., Khalid, M. and Adnan, A., 2010. Radiation Vulcanization of Natural Rubber Latex Loaded with Carbon Nanotubes. *Fullerenes, Nanotubes and Carbon Nanostructures*, 18, pp. 56-71.
- Bee, S. T., Hassan, A., Ratman, C. T., Tee, T. T. and Lee, T. S., 2012. Effects of Montmorillonite on the Electron Beam Irradiated Alumina Trihydrate Added Polyethylene and Ethylene Vinyl Acetate Nanocomposite. *Polymer Composites*, 33, pp. 1883-1892.

Bee, S. T., Ratnam, C. T., Lee, T. S., Tee, T. T., Hui, D., Kadhum, A. A. H., Rahmat, A. R. and Lau, J., 2014. Effects of Electron Beam Irradiation on Mechanical Properties and Nanostructural-morphology of Montmorillonite Added Polyvinyl Alcohol Composite. *Composites: Part B*, 63, pp. 141-153.

Bee, S. T., Ratnam, C. T., Lee, T. S., Tee, T. T., Wong, W. K., Lee, J. X. and Rahmat, A. R., 2014. Effects of Electron Beam Irradiation on the Structural Properties of Polylactic Acid/Polyethylene Blends. *Nuclear Instruments and Methods in Physics Research B*, 334, pp. 18-27.

Bee, S. T., Lee, T. S., Ratnam, C. T., Kavee-Raaz, R. R. D., Tee, T. T., Hui, D. and Rahmat, A. R., 2015. Electron Beam Irradiation Enhanced of Hibiscus Cannabinus Fiber Strengthen Polylactic Acid Composites. *Composites Part B: Engineering*, 79, pp. 35-46.

Bee, S. T., Lee, T. S., Ratnam, C. T., Haraveen, K. J. S., Tee, T. T. and Rahmat, A. R., 2015. Investigation of the Interaction of Copper (II) Oxide and Electron Beam Irradiation Cross-linkable Polyethylene. *Nuclear Instruments and Methods in Physics Research B*, 360, pp 36-45.

Bhagawan, S. S., Kuriakose, B. and De, S. K., 1987. Mechanical Properties and Failure Surfaces of Gamma-Ray Irradiated Systems Based on Thermoplastic 1, 2 Polybutadiene. *Radiation Physics and Chemistry*, 30(2), 95-104.

Chaudhari, C. V., Bhardwaj, Y. K., Patil, N. D., Dubey, K. A., Kumar, V. and Sabharwal, S., 2005. Radiation-Induced Vulcanisation of Natural Rubber Latex in Presence of Styrene-Butadiene Rubber Latex. *Radiation Physics and Chemistry*, 72, pp. 613-618.

Chirinos, H., Yoshii, F., Makuuchi, K. and Lugao, A., 2003. Radiation Vulcanization of Natural Rubber Latex Using 250 keV Electron Beam Machine. *Nuclear Instruments and Methods in Physics Research B*, 208, pp. 256-259.

Chong, E. L., Ahmad, I., Dahlan, H. M. and Abdullah, I., 2010. Reinforcement of Natural Rubber/High Density Polyethylene Blends with Electron Beam Irradiated Liquid Natural Rubber-coated Rice Husk. *Radiation Physics and Chemistry*, 79, pp. 906-911.

Chowdhury, R., 2007. Electron-Beam-Induced Cross-linking of Natural Rubber/Acrylonitrile-Butadiene Rubber Latex Blends in the Presence of Ethoxylated Pentaerythritol Tetraacrylate Used as a Cross-linking Promoter. *Journal of Applied Polymer Science*, 103, pp. 1206-1214.

Cockbain, E. G., Pendle, T. D. and Turner, D. T., 1959. Formation of Graft Polymer by γ -Irradiation of Natural Rubber Latex and Methyl Methacrylate. *Journal of Polymer Science*, 39, pp. 419-426.

Dahlan, H. M., Zaman, M. D. K. and Ibrahim, A., 2002. Liquid Natural Rubber (LNR) As a Compatibiliser in NR / LLDPE Blends – II: The Effects of Electron-Beam (EB) Irradiation. *Radiation Physics and Chemistry*, 64, 429-436.

De, D., Adhikari, B. and Maiti, S., 1997. Reclaiming of Rubber by a Renewable Resource Material. Part 1. Reclaiming of Natural Rubber Vulcanizates. *Journal of Polymer Materials*, 14(4), pp. 333–342.

De, D., Panda, P. K., Roy, M. and Bhunia, S., 2013. Reinforcing Effect of Reclaim Rubber on Natural Rubber/Polybutadiene Rubber Blends. *Materials and Design*, 46, pp. 142-150.

Drobny, J. G., 2013. *Ionizing Radiation and Polymers*. Massachusetts: William Andrew, 1-10.

El-Nahas, H. H., Heba, R. A. and Magida, M. M., 2010. Effect of Ionizing Irradiation and Blending of Natural Rubber Latex on Polyvinylalcohol Gelation by Using Chemical and Freezing-Thawing Processes for Use in the Field of Construction Engineering. *Journal of Applied Polymer Science*, 115, pp. 1073-1080.

El-Nahas, H. H. and Magida, M. M., 2012. The Use of Interfacial Blend to Increase the Adhesion Properties of Natural Rubber/Polyvinylalcohol Multilayer Using Electron Beam Irradiation. *Journal of Polymers and the Environment*, 20, pp. 70-79.

Fukumori, K., Matsushita, M., Okamoto, H., Sato, N., Suzuki, Y. and Takeuchi, K., 2001. Recycling Technology of Tire Rubber. *JSAE Review*, 23, pp. 259-264.

Ghazali, Z., Johnson, A. F., Dahlan, K. Z., 1999. Radiation Cross-linked Thermoplastics Natural Rubber (TPNR) Foams. *Radiation Physics and Chemistry*, 55, pp. 73-79.

Gorelik, B. A., Kolganova, I. V., Matisova-Rychla., L., Listvojb, G. I., Drabkina, A. M. and Golnik, A. G., 1993. Effect of Oxygen on the Degradation of Polypropylene Initiated by Ionizing Radiation. *Polymer Degradation and Stability*, 42, pp. 263-266.

Hafezi, M., Khorasani, S. N., Ziaei, F. and Azim, H. R., 2007. Comparison of Physicomechanical Properties of NBR-PVC Blend Cured by Sulfur and Electron Beam. *Journal of Elastomers and Plastics*, 39, pp. 151-163.

Haque, M. E., Dafader, N. C., Akhtar, F. and Ahmad, M. U., 1996. Radiation Dose Required for the Vulcanization of Natural Rubber Latex. *Radiation Physics and Chemistry*, 48(4), pp. 505-510.

Hassan, M. M., Mahmoud, G. A., Nahas, H. H. E. and Hegazy, E. S. A., 2007. Reinforced Material from Reclaimed Rubber/Natural Rubber, Using Electron Beam and Thermal Treatment. *Journal of Applied Polymer Science*, 104, pp. 2569-2578.

Holst, O., Stenberg, B. and Christiansson, M., 1998. Biotechnological Possibilities for Waste Tyre-rubber Treatment. *Biodegradation*, 9(3), pp. 301-310.

Hossain, A. K. M. Z. and Chowdhury, M. S., 2010. Grafting of N-Butyl Acrylate with Natural Rubber Film by Gamma Radiation: A Reaction Mechanism. *Journal of Science and Technology*, 5(1), pp. 81-88.

Hunt, L. K. and Kovalak, R. R., 1999. *Devulcanization of Cured Rubber*. US Patent 5891926.

Isayev, A. and Chen, J., 1994. *Continuous Ultrasonic Devulcanization of Vulcanized Elastomers*. US Patent 5284625.

Ismail, H., Munusamy, Y., Mariatti, M. and Ratnam, C. T., 2010. The Effect of Trimethylol Propane Tetraacrylate (TMPTA) and Organoclay Loading on the Properties of Electron Beam Irradiated Ethylene Vinyl Acetate (EVA)/Natural Rubber (SMR L)/Organoclay Nanocomposites. *Journal of Applied Polymer Science*, 117, pp. 865-874.

Ismail, H., Osman, H. and Jaafar, M., 2008. Hybrid-Filler Filled Polypropylene/ (Natural Rubber) Composites: Effects of Natural Weathering on Mechanical and Thermal Properties and Morphology. *Journal of Vinyl & Additive Technology*, 14, pp. 142-151.

Jayasuriya, M. M. and Makuuchi, K., Yoshi, F., 2001. Radiation Vulcanization of Natural Rubber Latex Using TMPTMA and PEA. *European Polymer Journal*, 37, pp. 93-98.

Jose, J., Nag, A. and Nando, G. B., 2014. Environmental Ageing Studies of Impact Modified Waste Polypropylene. *Iranian Polymer Journal*, 23(8), pp. 619-636.

Kamalbabu. P. and Kumar, G. C. M., 2014. Effects of Particle Size on Tensile Properties of Marine Coral Reinforced Polymer Composites. *Procedia Material Science*, 5, pp. 802-808.

Khalid, M., Ismail, A. F., Ratnam, C. T., Faridah, Y., Rashmi, W. and Al-Khatib, M. F., 2010. Effect of Radiation Dose on the Properties of Natural Rubber Nanocomposite. *Radiation Physics and Chemistry*, 79, pp. 1279-1285.

Khamplod, T., Loykulnant, S., Kongkaew, C. and Prapainainar, P., 2014. Preparation of Graft Copolymer of Natural Rubber and Polystyrene by Electron Beam Irradiation. *Advanced Materials Research*, 931, pp. 73-77.

Khamplod, T., Loykulnant, S., Kongkaew, C., Sureeyatanapas, P. and Prapainainar, P., 2015. Electron Beam Radiation Grafting of Styrene on Natural Rubber Using Taguchi's Design. *Polymer*, 79, pp. 135-145.

Kleps, T., Piaskiewicz, M. and Parasiewicz, W., 2000. The Use of Thermogravimetry in the Study of Rubber Devulcanization. *Journal of Thermal Analysis Calorimetry*, 60(1), pp. 271-277.

Kondo, Y., Miyazaki, K., Takayanagi, K. and Sakurai, K., 2008. Surface Treatment of PET Fiber by EB-Irradiation-Induced Graft Polymerization and Its Effect on Adhesion in Natural Rubber Matrix. *European Polymer Journal*, 44, pp. 1567-1576.

Kondo, Y., Miyazaki, K., Takayanagi, K. and Sakurai, K., 2009. Mechanical Properties of Fiber-Reinforced Natural Rubbers Using Surface-Modified PET Fibers under EB Irradiation. *Journal of Applied Polymer Science*, 114, pp. 2584-2590.

Kumar, V., Ali, Y., Sonkawade, R. G. and Dhaliwal, A. S., 2012. Effect of Gamma Irradiation on the Properties of Plastic Bottle Sheet. *Nuclear Instruments and Methods in Physics Research B*, 287, pp. 10-14.

Levin, Y. V., Kim, S. H. and Isayev, A. I., 1997. Effect of Cross-link Type on the Ultrasound Devulcanization of SBR Vulcanizates. *Rubber Chemistry & Technology*, 70(4), pp. 641–649.

Leyden, J. J., 1991. Cryogenic Processing and Recycling. *Rubber World*, 203(6), pp. 28-29.

Loo, J. S. C., Ooi, C. P. and Boey, F. Y.C., 2005. Degradation of Poly(Lactide-co-glycolide) (PLGA) and Poly(L-lactide) (PLLA) by Electron Beam Radiation. *Biomaterials*, 26, pp. 1359-1367.

Majid R. A., Ismail, H. and Taib, R. M., 2010. The Effects of Natural Weathering on the Properties of Linear Density Polyethylene (LDPE)/Thermoplastic Sago Starch (TPSS) Blends. *Polymer-Plastics Technology and Engineering*, 49, pp. 1142-1149.

Makuuchi, K. and Hagiwara, M., 1984. Radiation Vulcanization of Natural Rubber Latex with Polyfunctional Monomers – II. *Radiation Physics and Chemistry*, 24(2), pp. 203-207.

Manaila, E., Craciun, G., Stelescu, M. D., Ighigeanu, D. and Ficai, M., 2014. Radiation Vulcanization of Natural Rubber with Polyfunctional Monomers. *Polymer Bulletin*, 71, pp. 57-82.

Manaila, E., Martin, D., Zuga, D., Craciun, G., Ighigeanu, D. and Matei, C., 2008. Radiation processing of rubber mixtures with polyfunctional monomers. Proceedings of the 11th International Conference on Optimization of Electrical and Electronic Equipment, IEEE, Brasov, pp. 125-130.

Manaila, E., Stelescu, M. D., Craciun, G. and Ighigeanu, D., 2016. Wood Sawdust/Natural Rubber Ecocomposites Cross-Linked by Electron Beam Irradiation. *Materials*, 9(7), pp. 503-524.

Manshaie, R., Khorasani, S. N., Veshare, S. J. and Abadchi, M. R., 2011. Effect of Electron Beam Irradiation on the Properties of Natural Rubber (NR)/Styrene-Butadiene Rubber (SBR) Blend. *Radiation Physics and Chemistry*, 80, pp. 100-106.

Markovic, G., Marinovic-Cincovic, M., Jovanovic, V., Samarzija-Jovanovic, S. and Budinski-Simendic, J., 2015. Characterization of Composite Based on Chlorosulfonated Polyethylene Rubber/Chlorinated Natural Rubber/Waste Rubber Powder Rubber Blends. *Journal of Thermoplastic Composite Materials*, 28(2), pp. 241-256.

Medhat, M. H., Nagwa, A. B., Mona, Y. E. and El-Sayed, A. H., 2013. Thermo-mechanical Properties of Devulcanized Rubber/High Crystalline Polypropylene Blends Modified by Ionizing Radiation. *Journal of Industrial and Engineering Chemistry*, 19, pp. 1241-1250.

Mitra, S., Chattopadhyay, S., Bharadwaj, Y. K., Sabharwal, S and Bhowmick, A. K., 2008. Effect of Electron Beam-Cross-Linked Gels on the Rheological Properties of Raw Natural Rubber. *Radiation Physics and Chemistry*, 77, pp. 630-642.

Mitra, S., Chattopadhyay, S., Sabharwal, S. and Bhowmick, A. K., 2010. Electron Beam Cross-linked Gels – Preparation, Characterization and Their Effect on the Mechanical, Dynamic Mechanical and Rheological Properties of Rubbers. *Radiation Physics and Chemistry*, 79, pp. 289-296.

Mohamad, N., Zainol, N. S., Rahim, F. F., Hairul, E. A. M., Toibah, A. R., Siti, R. S., Azam, M.A., Yaakub, M.Y., Mohd, F. B. A. and Mohd, E. A. M., 2013. Mechanical and Morphological Properties of Polypropylene/Epoxidized Natural Rubber Blends at Various Mixing Ratio. *Procedia Engineering*, 68, pp. 439-445.

Mondal, M., Gohs, U., Wagenknecht, U. and Heinrich, G., 2012. Efficiency of High Energy Electrons to Produce Polypropylene/Natural Rubber-Based Thermoplastic Elastomer. *Polymer Engineering and Science*, 53(8), pp. 1696-1705.

Mondal, M., Gohs, U., Wagenknecht, U. and Heinrich, G., 2013. Additive Free Thermoplastic Vulcanizates Based on Natural Rubber. *Materials Chemistry and Physics*, 143, pp. 360-366.

Mondal, M., Gohs, U., Wagenknecht, U. and Heinrich, G., 2013. Polypropylene/Natural Rubber Thermoplastic Vulcanizates by Eco-Friendly and Sustainable Electron Induced Reactive Processing. *Radiation Physics and Chemistry*, 88, pp. 74-81.

Muhammad, N. H., Abdullah, I. and Dahlan, H. M., 2002. Effects of Electron-Beam (EB) - Irradiation on 60/40 Natural Rubber/Polystyrene Blends in the Presence of m-Phenylenebismaleimide (HVA-2). *Jurnal Sains Nuklear Malaysia*, 20, pp. 85-101.

Muhammad, N. H., Abdullah, I. and Dahlan, H. M., 2011. Effect of Electron Beam Irradiation on Natural Rubber / Linear Low Density Polyethylene Blends with m-Phenylenebismaleimide. *Sains Malaysiana*, 40(7), pp. 685-689.

Munusamy, Y., Ismail, H., Mariatti, M. M. and Ratnam, C. T., 2009. Effect of Electron Beam Irradiation on the Properties of Ethylene-(Vinyl Acetate) Copolymer/Natural Rubber/Organoclay Composites. *Journal of Vinyl & Additive Technology*, 15(1), pp. 39-46.

Munusamy, Y., Ismail, H. and Ratnam, C. T., 2013. Investigation on the Influence of Cross-link Promoter on the Irradiation Cross-linking, Dynamic Mechanical Property and Thermal Stability of Ethylene Vinyl Acetate (EVA)/Natural Rubber (SMR L)/Organoclay Nanocomposites. *International Journal of Materials Engineering Innovation*, 4, pp. 325-342.

Murray, K. A., Kennedy, J. E., McEvoy, B., Vrain, O., Ryan, D., Higginbotham, C. L., 2012. The Effects of High Energy Electron Beam Irradiation on the Thermal and Structural Properties of Low Density Polyethylene. *Radiation Physics and Chemistry*, 81, pp. 962-966.

Myers, R. D., Nicholson, P., MacLoed, J. B. and Moir, M. E., 1997. *Rubber Devulcanization Process*. US Patent 5602186.

Nabil, H. and Ismail, H., 2014. Enhancing the Thermal Stability of Natural Rubber/Recycled Ethylene-Propylene-Diene Rubber Blends by Means of Introducing Pre-vulcanised Ethylene-Propylene-Diene Rubber and Electron Beam Irradiation. *Materials and Design*, 56, pp. 1057-1067.

Nabil, H., Ismail, H. and Ratnam, C. T., 2014. Simultaneous Enhancement of Mechanical and Dynamic Mechanical Properties of Natural Rubber/Recycled Ethylene-Propylene-Diene Rubber Blends by Electron Beam Irradiation. *International Journal of Polymer Analysis and Characterization*, 19, pp. 272-285.

Noriman, N. Z. and Ismail, H., 2011. The Effects of Electron Beam Irradiation on the Thermal Properties, Fatigue Life and Natural Weathering of Styrene Butadiene Rubber/Recycled Acrylonitrile-Butadiene Rubber Blends. *Materials and Design*, 32, pp. 3336-3346.

Novotny, D. S., Marsh, R. L., Masters, F. C. and Tally, D. N., 1978. Microwave Devulcanization of Rubber. US Patent 4104205.

Oo, M. M., Zaman, K. and Hlaing, T., 2000. The Effects of Gamma Radiation and Electron Beam on the Mechanical Properties of Polypropylene Dominant Natural Rubber Blend. *Instrumentation Related to Nuclear Science and Technology*, 33(1), pp. 1-8.

Peng, P. L., Cheng, S. and Hu, F. M., 1993. The Sensitizing Effect of Acrylates on Radiation Vulcanization of Natural Rubber Latex. *Radiation Physics and Chemistry*, 42, pp. 121-124.

Popa, M. I., Pernevan, S., Sirghie, C., Spiridon, I., Chambre, D., Copolovici, D. M. and Popa, N., 2013. Mechanical Properties and Weathering Behavior of Polypropylene-Hemp Shives Composites. *Journal of Chemistry*, 2013, pp. 1-8.

Rabek, J. F., 1990. *Photostabilization of Polymers: Principles and Application*. London: Elsevier Science Publishers LTD.

Rabek, J. F., 1995. *Polymer Photodegradation: Mechanisms and Experimental Methods*. London: Chapman and Hill.

Rabello, M. S. and White, J. R., 1997. Crystallization and Melting Behaviour of Photodegraded Polypropylene - 1. Chemi-crystallization. *Polymer*, 38(26), pp. 6379-6387.

Rahman, W., Alam, J. and Khan, M. R., 2015. Effect of Manganese on Radiation Vulcanization of Natural Rubber. *International Journal of Polymer and Characteristics*, 20, pp. 406-413.

Ramlee, N. A., Hanapiah, S. S. M., Suhaimi, F. N., Ratnam, C. T. and Appadu, S., 2015. Effect of Blend Compositions on Mechanical Properties of Irradiated Titanium Dioxide (TiO₂)/Polyvinyl Chloride (PVC)/Epoxidized Natural Rubber (ENR) Nanocomposites. *Advanced Materials Research*, 1113, pp. 43-49.

Ramlee, N. A., Ratnam, C. T., Alias, N. H. and Rahman, M. F. A., 2014. Dynamic Mechanical and Gel Content Properties of Irradiated ENR/PVC Blends with TiO₂ Nanofillers. *International Journal of Science and Engineering*, 6(1), pp. 16-23.

Ratnam, C. T., 2002. Enhancement of PVC/ENR Blend Properties by Electron Beam Irradiation: Effect of Stabilizer Content and Mixing Time. *Polymer Testing*, 21, pp. 93-100.

Ratnam, C. T., 2002. Irradiation Modification of PVC/ENR Blend: Effect of TBLS Content. *Polymer-Plastic Technology Engineering*, 41(3), pp. 407-418.

Ratnam, C. T., Abdullah, Z., 2006. Electron Beam Irradiation of EVA/ENR Blend. *Polymer-Plastics Technology and Engineering*, 45, pp. 555-559.

Ratnam, C. T., Sabariah, K., Sivachalam, Y., Marina, T. and Norzawani, Y., 2006. Radiation Cross-linking of Rubber Phase in Poly (Vinyl Chloride)/Epoxidized Natural Rubber Blend: Effect on Mechanical Properties. *Polymer Testing*, 25, pp. 475-480.

Ratnam, C. T., Nasir, M., Baharin, A. and Zaman, K., 2000. Electron Beam Irradiation of Epoxidized Natural Rubber. *Nuclear Instruments and Methods in Physics Research B*, 171, pp. 455-464.

Ratnam, C. T., Nasir, M., Baharin, A. and Zaman, K., 2001. Effect of Blending Parameters on Electron Beam Enhancement of PVR/ENR Blends. *Polymer-Plastic Technology Engineering*, 40(4), pp. 561-575.

Ratnam, C. T., Nasir, M., Baharin, A. and Zaman, K., 2001. Effect of Electron-Beam Irradiation on Poly (Vinyl Chloride)/Epoxidized Natural Rubber Blend: Dynamic Mechanical Analysis. *Polymer Instrument*, 50, pp. 503-508.

Ratnam, C. T., Nasir, M., Baharin, A. and Zaman, K., 2001. Electron-Beam Irradiation of Poly (Vinyl Chloride)/Epoxidized Natural Rubber Blends in Presence of Trimethylolpropane Triacrylate. *Journal of Applied Polymer Science*, 81, pp. 1926-1935.

Ratnam, C. T., Nasir, M., Baharin, A. and Zaman, K., 2001. Electron-Beam Irradiation of Poly (Vinyl Chloride)/Epoxidized Natural Rubber Blends in Presence of Irganox 1010. *Polymer Degradation and Stability*, 72, pp. 147-155.

Ratnam, C. T., Nasir, M., Baharin, A. and Zaman, K., 2001. Evidence of Irradiated-Induced Cross-linking in Miscible Blends of Poly (Vinyl Chloride)/Epoxidized Natural Rubber in Presence of Trimethylolpropane Triacrylate. *Journal of Applied Polymer Science*, 81, pp. 1914-1925.

Ratnam, C. T., Nasir, M., Baharin, A. and Zaman, K., 2001. The Effect of Electron Beam Irradiation on the Tensile and Dynamic Mechanical Properties of Epoxidized Natural Rubber. *European Polymer Journal*, 37, pp. 1667-1676.

Ratnam, C. T., Raju, G. and Yunus, W. M. Z. W., 2007. Oil Palm Empty Fruit Bunch (OPEFB) Fiber Reinforced PVR/ENR Blend-Electron Beam Irradiation. *Nuclear Instruments and Methods in Physics Research B*, 265, pp. 510-514.

Ratnam, C. T., Ramlee, N. A., Appadu, S., Manshor, S. T. and Ismail, H., 2015. Preparation and Electron Beam Irradiation of PVC/ENR/CNTs Nanocomposites. *Polymer-Plastics Technology and Engineering*, 54, pp. 184-191.

Ratnam, C. T., Yoshii, F., Makuuchi, K. and Zaman, K., 1999. Hydrogel Coating of RVNRL Film by Electron-Beam Irradiation. *Journal of Applied Polymer Science*, 72, pp. 1421-1428.

Ratnam, C. T. and Zaman, K., 1999. Enhancement of Polyvinyl Chloride (PVC)/Epoxidized Natural Rubber (ENR) Blend Properties by Electron Beam Irradiation: Effect of Antioxidants. *Polymer Degradation and Stability*, 65, pp. 481-490.

Ratnam, C. T. and Zaman, K., 1999. Modification of PVR/ENR Blend by Electron Beam Irradiation: Effect of Cross-linking Agents. *Nuclear Instruments and Methods in Physics Research B*, 152, pp. 335-342.

Romine, R. A. and Snowden-Swan, L. J., 1997. *Method for the Addition of Vulcanized Waste Rubber to Virgin Rubber Products*. US Patent 5597851.

Roop, S., Thakur, V., Gohs, U., Wagenknecht, U., Bhowmick, A. K. and Heinrich, G., 2011. In Situ Reactive Compatibilization of Polypropylene/Epoxidized Natural Rubber Blends by Electron Induced Reactive Processing: Novel In-line Mixing Technology. *Polymers Advanced Technologies*, 22, pp. 2257-2263.

Rudin, A. K., Mohamad, Z., Ratnam C. T. and Bakar A. A., 2014. Electron Beam Cross-linking of EVA/ENR-50/HNTS Nanocomposites in the Presence of Trimethylol Propane Triacrylate, TMPTA. *Advanced Materials Research*, 970, pp. 84-87.

Sabharwal, S., Chaudhari, C. V., Bhardwaj, Y. K. and Majali, A. B., 1998. Mechanism of N-Butyl Acrylate Sensitization Action in Radiation Vulcanization of Natural Rubber Latex. *Radiation Physics and Chemistry*, 51(3), pp. 309-315.

Sam, S. T., Ismail, H. and Ahmad, Z., 2012. Study on Electron-Beam-Irradiated (Linear Low-Density Polyethylene) / (Soya Powder) Blends Under Outdoor Exposure. *Journal of Vinyl & Additive Technology*, 18, pp. 241-249.

Sekhar, B. C., Kormer, V. A., Sotnikova, E. N., Mironyuk, V. P., Trunova, L. N., Nikitina, N. A., 1998. *Reclaiming of Elastomeric Materials*. US Patent 5770632.

- Senna, M. M. H., Fattah, A. A. A. and Monem, Y. K. A., 2008. Spectroscopic Analysis and Mechanical Properties of Electron Beam Irradiated Polypropylene/Epoxidized Natural Rubber (PP/ENR) Polymer Blends. *Nuclear Instruments and Methods in Physics Research B*, 266, pp. 2599-2606.
- Senna, M. M. H., Mohamed, R. M., Eldin, A. N. S. and Hamouly, S. E., 2012. Characterization of Electron Beam Irradiated Natural Rubber/Modified Starch Composites. *Journal of Industrial and Engineering Chemistry*, 18, pp. 1654-1661.
- Senna, M. M. H. and Monem, Y. K. A., 2010. Effect of Beam Irradiation and Reactive Compatibilizers on Some Properties of Polypropylene and Epoxidized Natural Rubber Blends. *Journal of Elastomers and Plastics*, 42, pp. 275-295.
- Sharif, J., Bakar, N. A., Rusli, A. F. and Zaman, M. D. K., 2010. Radiation Effect on Polypropylene/Natural Rubber/Clay Nanocomposites. *2010 International Conference on Enabling Science and Nanotechnology*, IEEE, Kuala Lumpur, pp. 1-2.
- Sharif, J., Yunus, W. M. Z. W., Zaman, M. D. K. and Mansor, H. A., 2005. Preparation and Properties of Radiation Cross-linked Natural Rubber/Clay Nanocomposites. *Polymer Testing*, 24, pp. 211-217.
- Sharif, J., Zaman, M. D. K. and Yunus, W. M. Z. W., 2008. Radiation Cross-linked Natural Rubber/Ethylene Vinyl Acetate/Clay Nanocomposites – Effect of Organoclay Concentration. *Journal of Nuclear and Related Technologies*, 5(1), pp. 65-80.
- Shen, J., Wen, S., Du, Y., Li, N., Zhang, L., Yang, Y. and Liu, L., 2013. The Network and Properties of the NR/SBR Vulcanizate Modified by Electron Beam Irradiation. *Radiation Physics and Chemistry*, 92, pp. 99-104.

Song, D., Gao, J., Li, X. and Lu, L., 2014. Evaluation of Aging Behavior of Polypropylene in Natural Environment by Principal Component Analysis. *Polymer Testing*, 33, pp. 131-137.

Steleescu, M. D. and Manaila, E., 2007. Cross-linking and Grafting the Natural Rubber by Means of Accelerated Electrons in the Presence of Trimethylol-Propane Trimethacrylate (TMPA). *UPB Scientific Bulletin*, 69(4), pp. 33-38.

Steleescu, M. D., Manaila, E., Craciun, G. and Dumitrascu, M., 2014. New green polymeric composites based on hemp and natural rubber processed by electron beam irradiation. *Scientific World Journal* 2014, 684047, pp. 1-13.

Tee, T. T., Lee, T. S., Gobinath, R., Bee, S. T., Hui, D., Rahmat, A. R., Kong, I. and Fang, Q. H., 2013. Investigation of Nano-size Montmorillonite on Enhancing Polyvinyl Alcohol-Starch Blends Prepared via Solution Cast Approach. *Composites: Part B*, 47, pp. 238-247.

Verbruggen, M. A. L., Does, L. V. D., Noordermeer, J. W. M., Duin, M. V. and Manuel, H. J., 1999. Mechanisms Involved in the Recycling of NR and EPDM. *Rubber Chemistry and Technology*, 72(4), pp. 731-740.

White, J. R. and Turnbull, A., 1994. Review Weathering of Polymers: Mechanisms of Degradation and Stabilization, Testing Strategies and Modelling. *Journal of Materials Science*, 29, pp. 584-613.

Wieslawa, U. D., 2012. *The Use of the Spectrometric Technique FTIR-ATR to Examine the Polymers Surface*. Rijeka: InTech, pp. 90.

Wu, Y. P., Wen, S., Jing, S., Jian, J., Shui, H., Zhang, L. and Li, L., 2015. Improved Dynamic Properties of Natural Rubber Filled with Irradiation-Modified Carbon Black. *Radiation Physics and Chemistry*, 111, pp. 91-97.

Xu, Y. S., Siswono, H., Yoshii, F. and Makuuchi, K., 1997. Cross-linking of Cis-1, 4-Polyisoprene Rubber by Electron Beam Irradiation. *Journal of Applied Polymer Science*, 66, pp. 113-116.

Yatim, N. M., Yusof, F., Ratnam, C. T. and Sopyan, L., 2012. Irradiation Modification of Epoxidized Natural Rubber/Ethylene Vinyl Acetate/Carbon Nanotubes Nanocomposites. *Advanced Materials Research*, 364, pp. 196-201.

Yun, J., Oh, J. S., Isayev, A. I., 2001. Ultrasonic Devulcanization Reactors for Recycling of GRT: Comparative Study. *Rubber Chemistry and Technology*, 74(2), pp. 317-330.

Zurina, M., Ismail, H. and Ratnam, C. T., 2006. Characterization of Irradiation-Induced Cross-link of Epoxidised Natural Rubber/Ethylene Vinyl Acetate (ENR-50/EVA) Blend. *Polymer Degradation and Stability*, 91, pp. 2723-2730.

Zurina, M., Ismail, H. and Ratnam, C. T., 2008. The Effect of HVA-2 on Properties of Irradiated Epoxidized Natural Rubber (ENR-50), Ethylene Vinyl Acetate (EVA), and ENR-50/EVA Blend. *Polymer Testing*, 27, pp. 480-490.